

MSU-IFW-ILTPE Joint Workshop

**Synthesis, Theoretical Examination
and Experimental Investigation
of Emergent Materials**

Book Of Abstracts

Edited by

Igor V. Morozov, Alexander I. Boltalin and Andrei V. Shevelkov

Desktop publishing by

Pavel A. Kotin

Cover design by

Pavel A. Kotin and Maxim S. Likhanov

ISBN 978-5-9909981-3-1

<http://www.msu-ifw-ilt.ru/>

Moscow 2017

About conference

Synthesis, Theoretical Examination and Experimental Investigation of Emergent Materials

The Workshop will focus on the actual experimental and theoretic problems of Solid State Chemistry and Physics:

- iron-based superconductors
- topological insulators
- semimetals
- other relevant and emergent quantum materials

The workshop is organized in the frame of a trilateral research program supported by the Volkswagen foundation. The aim of the workshop is to bring together chemists and physicists from Russia, Ukraine, and Germany. The Workshop will focus on the problems of chemistry and physics of iron-based superconductors, topological insulators, semimetals, and other relevant and emergent quantum materials.



MSU-IFW-ILTPE Joint Workshop

supported by



VolkswagenStiftung

Organizing Committee

International Organizing Committee

| | |
|-----------------------------|--|
| Bernd Büchner | Professor, Director of the Institute for Solid State Research, IFW, Dresden |
| Jeroen van den Brink | Professor, Director of the Institute for Theoretical Solid State Physics, IFW, Dresden |
| Dmitri Efremov | Institute for Theoretical Solid State Physics, IFW, Dresden |
| Andrei Shevelkov | Professor, Head of Inorganic Chemistry Division Department of Chemistry, MSU, Moscow |
| Igor Morozov | Leading researcher, Inorganic Chemistry Division Department of Chemistry, MSU, Moscow |

Local Organizers

Inorganic Chemistry Division, Department of Chemistry, MSU, Moscow

Andrei Shevelkov

Alexander Boltalin

Igor Morozov

Maxim Likhanov

Pavel Kotin

Elena Kuznetsova

Anna Fedorova

Secretary of Local Organizing Committee

Mariia Volodina

Grigory Shipunov

e-mail: msu_ifw_ilt@inorg.chem.msu.ru



Conference Agenda

Tuesday, June 13, 2017

Arrival

Wednesday, June 14, 2017

| Time | Event | Page |
|--|---|------|
| 9:45 to 10:00 | Opening | |
| Chairman: Alexander N. Vasiliev | | |
| 10.00 to 10.30 | Prof. Dr. Bernd Büchner (IFW, Dresden) Orbitals and Polarons in Fe based superconductors | 7 |
| 10.30 to 10:50 | Dr. Daniil Evtushinskii (EPFL Lausanne) Primary Electronic Interactions in Iron-Based Superconductors as seen by ARPES | 8 |
| 10:50 to 11:10 | Dr. Igor V. Morozov (Chem. Dep. MSU, Moscow) An unusual type of substitution of lithium by a 3d-element in LiFeAs: the effect on physical properties | 9 |
| 11.10 to 11:30 | Prof. Dr. Alexander Sinchenko (Kotel'nikov IRE RAS, Moscow) Possible inhomogeneous high temperature superconductivity in FeSe at ambient pressure | 10 |
| 11:30 to 12:00 | Break | |
| Chairman: Andrei V. Shevelkov | | |
| 12:00 to 12:30 | Dr. Evgeny V. Antipov (Chem. Dep. MSU, Moscow) T_c -enhancement in $Fe_{1+\delta}Se$ by electrochemical lithium intercalation | 11 |
| 12:30 to 12:50 | Dr. Saicharan Aswartham (IFW, Dresden) Crystal growth and characterization of Fe-based superconductors | 12 |
| 12:50 to 13:10 | Dr. Alexey V. Sobolev (Chem. Dep. MSU, Moscow) ^{57}Fe Mössbauer spectroscopy of 11 and 111 iron pnictides | 13 |
| 13:10 to 13:30 | The winner of the Prof. B. A. Popovkin Prize-2017 To be announced | |
| 13:30 to 15:00 | Lunch | |
| Chairman: Bernd Büchner | | |
| 15:00 to 15:30 | Prof. Dr. Yurii Naidyuk (ILTPE NAS, Kharkiv) Yanson and Andreev-reflection point-contact spectroscopy of iron-based superconductors | 14 |
| 15:30 to 15:50 | Dr. Svetoslav Kuzmichev (Phys Dep. MSU, Moscow) Observation of boson resonance in oxypnictide superconductors by means of IMARE spectroscopy | 15 |
| 15:50 to 16:10 | Dr. Alexei N. Kuznetsov (Chem. Dep. MSU, Moscow) Iron Incorporation into Layered Nickel-rich Tellurides as a Way to Materials with Controlled Magnetic Anisotropy | 16 |
| 16:10 to 16:30 | Dr. Peter S. Berdonosov (Chem. Dep. MSU, Moscow) Selenite and tellurite halides of 3-d metals as possible low-dimensional magnets: synthesis, crystal structures and properties | 17 |
| 18:00 | Get together party | |

Conference Agenda

Thursday, June 15, 2017

| Time | Event | Page |
|------------------------------------|--|------|
| Chairman: Jochen Geck | | |
| 9.30 to 10.00 | Prof. Dr. Jeroen van den Brink (IFW, Dresden) Iridates: from Heisenberg antiferromagnets to potential Kitaev spin liquids | 18 |
| 10.00 to 10:20 | Dr. Stefan Drechsler (IFW, Dresden) Constraints on the coupling to low-energy bosons in Fe based superconductors | 19 |
| 10:20 to 10:40 | Dr. Dmitrii Bashlakov (ILTPE NAS, Kharkiv) Superconducting State in $\text{LaFe}_{1-x}\text{Co}_x\text{AsO}$ Studied by S-N Point Contacts | 20 |
| 10.40 to 11:00 | Dr. Tatjana E. Kuzmicheva (LPI RAS Moscow) Anisotropic superconducting gaps in optimally doped $\text{Ba}_{1-x}\text{K}_x\text{Fe}_2\text{As}_2$ and $\text{BaFe}_{2-x}\text{Ni}_x\text{As}_2$ | 21 |
| 11:00 to 11:30 | Break | |
| Chairman: Yurii Naidyuk | | |
| 11:30 to 12:00 | Prof. Dr. Andrey R. Kaul (Chem. Dep. MSU, Moscow) R&D of 2G HTS wire in joint work of SuperOx Company and MSU | 22 |
| 12:00 to 12:20 | Valeriy Yu. Verchenko (Chem. Dep. MSU, Moscow) Strong-Coupling Two-Ggap Superconductivity in $\text{Mo}_8\text{Ga}_{41}$ | 23 |
| 12:20 to 12:40 | Prof. Dr. Andrei A. Gippius (Phys Dep. MSU, Moscow) Evolution of magnetism in Co and Ni substituted FeGa_3 as probed by Ga NQR spectroscopy | 24 |
| 12:40 to 13:00 | Dr. Flavio Nogueira (IFW, Dresden) Axion electrodynamics of topological insulators-type II superconductor structures | 25 |
| 13:00 to 14:30 | Lunch | |
| Chairman: Andrei A. Gippius | | |
| 14:30 to 15:00 | Prof. Dr. Vladimir Pudalov (LPI RAS Moscow) Fe-based superconductors: complementary research and potential applications | 26 |
| 15:00 to 15:20 | Prof. Dr. Marina N. Rumyantseva (Chem. Dep. MSU, Moscow) Photosensitive semiconductor materials for gas sensors | 27 |
| 15:20 to 15:40 | Prof. Dr. Pavel E. Kazin (Chem. Dep. MSU, Moscow) Alkaline-earth apatites with cobalt ions in the trigonal channels as molecular magnets | 28 |
| 15:40 to 16:30 | Break | |
| 16:30 to 18:30 | Posters | |

Conference Agenda

Friday, June 16, 2017

| Time | Event | Page |
|--------------------------------------|---|------|
| Chairman: Dmitri Efremov | | |
| 9.30 to 10.00 | Prof. Dr. Jochen Geck (TU Dresden) Charge density wave, orbital order and superconductivity in 1T-TaS ₂ | 29 |
| 10.00 to 10:20 | Dr. Lada V. Yashina (Chem. Dep. MSU, Moscow) Gap opening in topological surface state | 30 |
| 10:20 to 10:40 | Dr. Joseph Dufouleur (IFW, Dresden) Transport properties of spin-helical Dirac fermions in disordered quantum confined systems | 31 |
| 10.40 to 11:00 | Dr. Roman B. Vasiliev (Chem. Dep. MSU, Moscow) Ultrathin heterostructures based on quasi-2D CdSe and CdTe nanoplatelets: synthesis, structure and optical properties | 32 |
| 11:00 to 11:30 | Break | |
| Chairman: Svetoslav Kuzmichev | | |
| 11:30 to 12:00 | Prof. Dr. Hans-Henning Klauss (TU Dresden) Complex electronic order and time reversal symmetry breaking in Fe-based superconductors studied by nuclear probe spectroscopy | 33 |
| 12:00 to 12:20 | Dr. Dmitri Efremov (IFW, Dresden) Superconductivity vs bound state formation in a two band superconductor | 34 |
| 12:20 to 12:40 | Dr. Seung-Ho Baek (IFW, Dresden) New spin gapped phase above the superconducting state in Na _{1-x} Li _x FeAs single crystals | 35 |
| 12:40 to 13:00 | Dr. Yuriy Yerin (ILTPE NAS, Kharkiv, Institute for Physics of Microstructures of RAS, Nizhny Novgorod) Soliton states in a three-band superconductor with broken time-reversal symmetry | 36 |
| 13:00 to 14:00 | Lunch | |

Oral session



MSU-IFW-ILTPE
Joint Workshop



Volkswagen **Stiftung**



Wednesday, June 14, 2017

Orbitals and Polarons in Fe based superconductors

B. Büchner

Institute for Solid State Physics, TU Dresden, 01062 Dresden, Germany

While there is broad consensus that superconductivity in Fe based superconductors is due to an unconventional, most likely purely electronic pairing, many important aspects of both, normal and superconducting state are still unexplored. For example the role of orbital degrees of freedom for the normal state electronic properties, nematicity, and pairing is discussed very controversial. It is not clear whether nesting or the proximity to Lifshitz points are crucial for superconductivity. Moreover, the broad variety of properties found for different systems raises the question about the generic phase diagram of these systems. In my talk I will focus on anomalous state properties of Fe based superconductors. Based on new NMR data I will discuss the origin of nematic order addressing again the apparent differences in FeSe and BaFe_2As_2 . The role of orbitals will be emphasized including the possibility of formation of “orbital polarons”. Moreover, highly unusual temperature dependencies of the electronic structure as revealed from our recent ARPES measurements will be presented. A possible connection to well-known anomalous T dependencies of both, magnetic and structural properties will be discussed.



Wednesday, June 14, 2017

Primary Electronic Interactions in Iron-Based Superconductors as seen by ARPES

D.V.Evtushinsky

Institute of Physics, Ecole Polytechnique Federale de Lausanne (EPFL), CH-1015 Lausanne, Switzerland

Owing to the possibility of preparing in a form of different and yet related compounds, iron superconductors, already provided an important insight into the complex problem of unconventional superconductivity---in particular it is becoming clear that the strong electron interaction with other electrons and with the magnetic excitation spectrum is the feature that unifies all relevant compounds from empirical point of view. At the same time even isostructural materials, exhibiting low level of the electronic interactions, never show high critical temperatures. I will review the electronic self energy, determined for the entire $3d$ band from the angle-resolved photoemission spectroscopy (ARPES) measurements of the iron pnictides and chalcogenides of 11, 111, 122, and 1111 families, and will compare it to the situation in the compounds with iron substituted by other d metals. Matching ARPES data with the results of calculations for correlated systems, shows detailed agreement as for the large-scale structure of the spectral function, implying that major deviations from the single-electron model are to be attributed to the electronic correlations of the moderate strength.

Wednesday, June 14, 2017

An unusual type of substitution of lithium by a 3d-element in LiFeAs: the effect on physical properties

*I.V. Morozov¹⁾²⁾, A.I. Boltalin¹⁾, M. Liu¹⁾²⁾, R. Kappenberger²⁾³⁾, Y.A. Ovchenkov¹⁾, S.M. Kazakov¹⁾, I.A. Presniakov¹⁾, A.V. Sobolev¹⁾, A.N. Vasiliev¹⁾, S. Wurmehl²⁾³⁾, B. Büchner²⁾³⁾.

¹⁾Lomonosov Moscow State University, Moscow, Russia ²⁾Leibniz Institute for Solid State and Materials Research 01069 Dresden, Germany ³⁾Institute for Solid State Physics, TU Dresden, 01062 Dresden, Germany

*morozov@inorg.chem.msu.ru

In our work we show that Mn or Cu atoms may be incorporated in the tetragonal-pyramidal polyhedra [LiAs₅] of the LiFeAs structure instead of lithium. In the case of Li_{1-x}Mn_xFeAs a continuous series of solid solutions (0 < x < 1) is formed, and in the case of Li_{1-x}Cu_xFeAs the maximum level of substitution x was found to be about 0.3.

The study of the isothermal magnetization curves and the T-dependence of the magnetic susceptibility curves for Li_{1-x}Cu_xFeAs samples (x ≤ 0.3) showed that they exhibit paramagnetic properties. Treatment of the $\chi(T)$ curves on the basis of the Curie-Weiss model allows us to conclude that the samples contain only diamagnetic Cu⁺ cations. Thus, the magnetic properties of Li_{1-x}Cu_xFeAs samples can be described within the model of non-interacting magnetic moments, which may be impurity iron cations in the lithium positions.

The features of the electronic and magnetic state of iron cations of the Li_{1-x}TM_xFeAs samples were studied by Mössbauer spectroscopy on ⁵⁷Fe. The main spectral component over the entire temperature range is a slightly enlarged broadened, quadrupole doublet, which corresponds to the localisation of iron in a tetrahedral environment of arsenic atoms within conducting layers. In addition to the main component, the second signal is present in the spectra, which corresponds to the FeAs impurity. In contrast to TM=Cu, Li_{1-x}Mn_xFeAs samples exhibited complex magnetic behavior and spontaneous magnetization observed up to room temperature.

The authors would like to acknowledge the financial support by the Volkswagen Foundation and the Russian Foundation for Basic Research (grant # 15-03-99628).

Wednesday, June 14, 2017

Possible inhomogeneous high temperature superconductivity in FeSe at ambient pressure

*A.A. Sinchenko¹⁾, P.D. Grigoriev^{2,3)}, A.P. Orlov¹⁾, A.V. Frolov¹⁾, A. Shakin³⁾,
D.A. Chareev^{4,5)}, O.S. Volkova^{3,5)} and A.N. Vasiliev^{3,5)}.

¹⁾Kotel'nikov Institute of Radioengineering and Electronics of RAS, Moscow, Russia ²⁾L.D. Landau Institute for Theoretical Physics, Chernogolovka, Russia ³⁾National University of Science and Technology "MISiS", Moscow, Russia ⁴⁾Institute of Experimental Mineralogy, RAS, Chernogolovka, Russia ⁵⁾Department of Physics, Lomonosov Moscow State University, Moscow, Russia

*sinchenko@cplire.ru

Based on high quality FeSe single-crystals the micro-bridges oriented parallel and transverse to the layer direction have been fabricated by the focused ion beam (FIB) technique and the measurements of electrical resistance and of current-voltage (IV) characteristics have been done in the conventional 4-probe configuration. The intralayer electronic transport demonstrates conventional behavior: at high current the differential resistance is a square function of voltage because of small Joule heating at all measured temperatures, but close to $T_c=8$ K we observed excess conductivity (deviation from square law) at low current corresponding the superconducting fluctuations which disappear rapidly and completely absent above $T\approx 13$ K. Quite different behavior is observed in the interlayer electronic transport: at high current IV curves follow square dependence but the excess conductivity observed at low current is much more pronounced and, more importantly, observed up to $T\approx 40$ K which is near 5 times higher than its zero-resistance superconducting transition temperature.

The temperature dependence of the real part of magnetic susceptibility demonstrates appearance additional diamagnetic contribution below the same temperature. Both magnetic and transport measurements indicate the existing inhomogeneous superconductivity in FeSe, most probably in the form of small superconducting inclusions.

To explain this effect the theoretical model has been proposed. We show that in a layered conductor with the anisotropy parameter $\eta = \sigma_{zz}/\sigma_{xx} \ll 1$ and small superconducting islands of volume ratio $\varphi \ll 1$ there are two parallel ways of interlayer current: $j_z \approx j_1 + j_2$ (see Fig. 1), so that the total conductivity $\sigma_{zz}^{tot} \approx \sigma_{zz}^{(1)} + \sigma_{zz}^{(2)}$. The first, standard way is with almost uniform current density and direction $j_1(\mathbf{r})$ perpendicular to the conducting layers. The rare superconducting inclusions then only slightly increase corresponding interlayer conductivity $\sigma_{zz}^{(1)}$ proportionally to their volume ratio, and $\sigma_{zz}^{(1)} \sim \eta \sigma_{xx}$. The second way of interlayer current is via superconducting islands. Since these islands are rare, the major part of the current path goes in the normal phase. But instead of flowing along the external field E_z , the current j_2 between the superconducting islands flows along the highly conducting layers until it comes to another island which allows next lift in the interlayer direction. Using Maxwell approximation the expression for interlayer conductivity has been obtained. We show that if inhomogeneous superconductivity in an anisotropic conductor first appears in the form of isolated superconducting islands, it reduces electric resistivity anisotropically with maximal effect along the least conducting axis [1]. This property provides a simple and very general tool to detect inhomogeneous superconductivity in various anisotropic compounds and this method may be applicable to almost all high-temperature superconductors, which have layered anisotropic crystal structure.

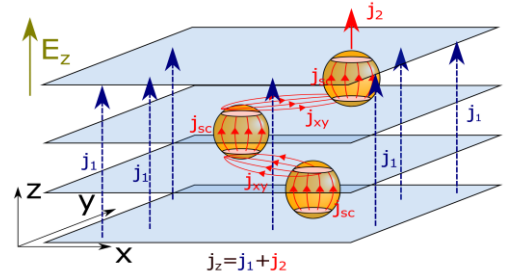


Fig.1 Illustration of two ways of interlayer current in a heterogeneous media with superconducting inclusions.

References:

1) A. A. Sinchenko, P. D. Grigoriev, A. P. Orlov, A. V. Frolov, A. Shakin, D. A. Chareev, O. S. Volkova and A. N. Vasiliev, Phys.Rev.B 95, 165120 (2017).

Wednesday, June 14, 2017

T_c-enhancement in Fe_{1+δ}Se by electrochemical lithium intercalation

E.V. Antipov¹⁾, A.M. Alekseeva^{1),2)}, O.A. Drozhzhin^{1),2)}, K.V. Zakharov³⁾, O.S. Volkova³⁾,
D.A.Chareev⁴⁾, A.N. Vasiliev³⁾, C. Koz⁵⁾, U. Schwarz⁵⁾, H. Rosner⁵⁾, Yu. Grin⁵⁾

¹⁾Department of Chemistry, Lomonosov Moscow State University, 119991 Moscow, Russia, ²⁾MPG-MSU Partner Group, Department of Chemistry, Lomonosov Moscow State University, 119991 Moscow, Russia, ³⁾Department of Physics, Lomonosov Moscow State University, 119991 Moscow, Russia, ⁴⁾Institute of Experimental Mineralogy, Russian Academy of Sciences, 142432 Chernogolovka, Russia, ⁵⁾Max-Planck-Institut für Chemische Physik fester Stoffe, 01187 Dresden, Germany

evgeny.antipov@gmail.com

The superconducting transition temperature (T_c) of tetragonal Fe_{1+δ}Se can be enhanced from 8.5 K to 44 K by chemical structure modification resulting in significant increase of [Fe₂Se₂]-interlayer separation: from 5.5 Å in native Fe_{1+δ}Se to > 7 Å in K_xFe_{1-y}Se and to > 9 Å in Li_{1-x}Fe_x(OH)Fe_{1-y}Se. Structure modification is achieved by the shift of the [Fe₂Se₂]-slabs and filling the interlayer space by solvated lithium and iron cations or by large alkaline cations like K.

We report the application of electrochemical approach to modification of Fe_{1+δ}Se superconducting properties. In contrast to chemical way the electrochemical approach allows to insert small amount of non-solvated Li⁺ into Fe_{1+δ}Se structure keeping the native structure and [Fe₂Se₂]-layers arrangement. The amount of intercalated lithium is extremely small (about 0.07 Li⁺ per f.u), however, caused slight change of carrier concentration results in enhancement of T_c up to ~ 44 K. The electrochemical intercalation provides the opportunity to get information about the “T_c vs carrier concentration” relation for this family of superconductors and open new possibilities for T_c-enhancement.

Wednesday, June 14, 2017

Crystal growth and characterization of Fe-based superconductors

*S. Aswartham¹⁾, R. Kappenberger^{1), 2)}, S. Selter¹⁾, F. Scaravaggi¹⁾, Anja U. B. Wolter¹⁾, C. Hess¹⁾, S. Wurmehl^{1), 2)}, B. Büchner^{1), 2), 3)}

¹⁾Leibniz Institute for Solid State and Materials Research, Dresden, Germany. ²⁾Institute for Solid State Physics, TU Dresden, Dresden, Germany. ³⁾Center for Transport and Devices, TU Dresden, Dresden, Germany

*s.aswartham@ifw-dresden.de

Iron-based superconductors are a novel representative of unconventional superconductors besides the famous family of high T_c cuprates [1]. The study of both the magnetic and superconducting state, their interplay and potential nematic order requires the study of single crystals. In this contribution, we will present the important aspects of crystal growth and the influence of chemical substitution in Fe based superconductors. High temperature solution growth technique is one of most powerful and widely used technique to grow single crystals of various materials. Solution growth technique has the potential to control high vapour pressures, given the fact that, in Fe-based superconductors elements with high vapour pressure like As, K, Li and Na have to be handled during the crystal growth procedure. In this scenario high temperature solution growth is the best suitable growth technique to synthesize sizable homogeneous single crystals.

To understand the role of transition metal in superconductivity and magnetism in $BaTM_2As_2$, a thorough investigation with different 3d transition metals is necessary, here we present a comprehensive overview on synthesis and crystal growth of $BaTM_2As_2$ with $TM = 3d$ transition metal [2]. In the $LaOFeAs$ system large crystals of high quality are very difficult to obtain, which greatly hinders scientific progress in this fascinating area. We present our preliminary results on crystal growth of $LaOFeAs$ family [4].

References

- 1) Y. Kamihara et al., J. Am. Chem. Soc. 130, 3296 (2008).
- 2) S. Aswartham, Ph.D. Thesis, TU-Dresden (2012).
- 3) S. Selter et al., In preparation (2017).
- 4) R. Kappenberger et al., In preparation (2017).

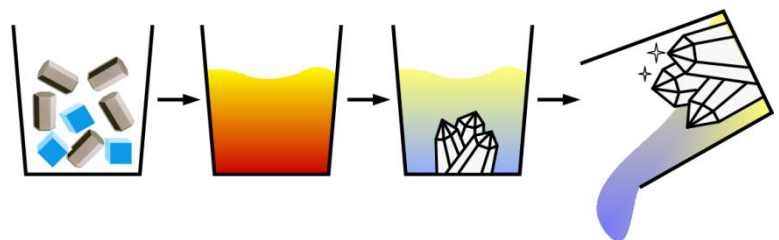


Fig. 1. Schematic diagram of high temperature solution growth technique [2]

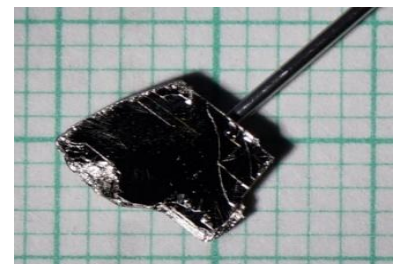


Fig. 2. As grown single crystals of $BaCo_2As_2$ [3]

Wednesday, June 14, 2017

⁵⁷Fe Mössbauer spectroscopy of 11 and 111 iron pnictides

*A. Sobolev, I.Presniakov.

Department of Chemistry, Lomonosov Moscow State University, Moscow, Russia

*alex@radio.chem.msu.ru

Detailed ⁵⁷Fe Mössbauer measurements on FeP_{1-x}As_x (0 ≤ x ≤ 0.5) parent compound and superconducting NaFeAs powder samples have been performed in the range 13 K ≤ T < 300 K, including the points of structural (T_S) and magnetic (T_N) phase transitions. All samples exhibit strongly unusual behavior of hyperfine parameters at temperatures below magnetic ordering.

The analysis of the very complex Zeeman structure for magnetic hyperfine spectra of FeP_{1-x}As_x (0 ≤ x ≤ 0.5) series at low temperatures (T < T_N) is consistent with the double helicoidally modulated magnetic structure, where iron magnetic moments rotate parallel to the (ab) plane with propagation vector along c axis. All series of experimental spectra were analyzed assuming the modulation of the electric hyperfine interactions when the Fe³⁺ magnetic moment rotates with respect to the principal axis of the EFG tensor (V_{zz} || b), and the anisotropy of the magnetic hyperfine field H_{hf}(θ) at the ⁵⁷Fe nuclei (where θ is the angle between the direction of H_{hf} and V_{zz}). The obtained from the fitting a large temperature independent anharmonicity parameter (m ≈ 0.9) of the spiral spin structure, reflecting a bunched spiral within the (ab) plane, results from easy-axis anisotropy in the plane of the iron spin rotation. The angle (φ) of deviation of the hyperfine field H_{hf} from the magnetization direction μ_{Fe} has been estimated (φ ≈ 7 - 13°). Expression for various parameters, that have been used to describe the anisotropic hyperfine field H_{hf}(θ), have been given in terms of the components of the hyperfine coupling tensor (A_{zz} ≠ A_{xx} ≈ A_{yy}) and the dipolar fields (A_{dip}) arising from external iron moments μ_{Fe}. The Bean-Rodbell magnetostriction exchange model has been used to describe the temperature evolution of the reduced hyperfine field. Various mechanisms have been examined in order to interpret the first order magneto-crystalline transition at T_N. From the above observations, we have developed a crystal field model, assuming a stabilization of low spin ferric ions in strong tetragonal crystalline field, which well accounts for the set of observed quadrupolar and magnetic hyperfine parameters.

On the contrary the ⁵⁷Fe spectra of NaFeAs recorded below T_N ≈ 46 K show a continuous distribution of hyperfine fields H_{Fe}. Distribution function p(H_{Fe}) has a bimodal profile emphasizing an inhomogeneous magnetic state of iron cations within the NaFeAs matrix. Analysis of the p(H_{Fe}) function has allowed to evaluate the Neel point, T_N = 46 ± 2K. In the critical range 35 K < T < T_N, the temperature dependence of the <H_{Fe}> value is well described by the power law with the static critical exponent β = 0.16 ± 0.08 indicating that the magnetic transition is essentially two-dimensional in nature. The measurements of the ⁵⁷Fe spectra just above T_N did not reveal any short-range magnetic fluctuations. The obtained from p(H_{Fe}) the low value of the average hyperfine magnetic field <H_{Fe}> ≈ 24 kOe reflects a very low value of a magnetic moments of iron ions in NaFeAs structure.

Unusual shape of the magnetically split Mössbauer spectra at T < T_N was analyzed in term of two models: (i) an incommensurate spin density wave (IC-SDW) modulation of the magnetic structure, (ii) a formation of a microdomain structure or phase separation ("two-site model"). It was shown that the hyperfine parameters obtained using these two models have very similar values over the whole temperature range.

Analysis of the temperature dependence H_{Fe}(T) with the Bean-Rodbell model leads to the structural factor ζ = 1.16 ± 0.05, suggesting that magnetic phase transition is first-order in nature. Our results give almost similar magneto-structural coupling (MSC) effect for NaFeAs and (Sr,Ba)Fe₂As₂ (ζ ≈ 1.08) classes of iron arsenides, but much smaller MSC effect for 1111-type arsenide SrFeAsF (ζ = 0.8), which may be understood as due to different inter-layer properties of these compounds.

A sharp evolution of the V_{zz}(T) and η(T) parameters of the full Hamiltonian of hyperfine interactions near T ≈ (T_N, T_S), were interpreted as a manifestation of an anisotropic electron distribution between the d_{xz}, d_{yz}- and d_{xy}-orbitals of the iron ions.

Wednesday, June 14, 2017

Yanson and Andreev-reflection point-contact spectroscopy of iron-based superconductors

Yu.G.Naidyuk

B.Verkin Institute for Low Temperature Physics and Engineering National Academy of Sciences of Ukraine, Kharkiv, Ukraine
*naidyuk@ilt.kharkov.ua

Yanson point-contact spectroscopy [1] is widely used, versatile tool for the investigation of modern superconductors. In the normal state, Yanson point-contact spectroscopy is a powerful method to study the fundamental processes of conduction electron scattering and their interaction with other quasiparticles and excitations in solids. On the other hand, in the superconducting state, point-contact spectroscopy exploits a phenomenon of Andreev reflection to obtain information about the superconducting order parameter(s). There are expectations that point-contact spectroscopy investigations can vastly contribute to understanding the nature of superconductivity in iron-based superconductors. Here, I will report about the main results that we received in recent years in the study of single crystals and films of several type [1111], [122] and [11] iron-based superconductors [2-7]. Along with the results of the study of some iron-based compounds in the normal state by Yanson point-contact spectroscopy, looking for characteristic bosonic excitations, I will also present recent data of measurements of the superconducting gap in FeSe by Andreev reflection spectroscopy (see examples on Fig.1).

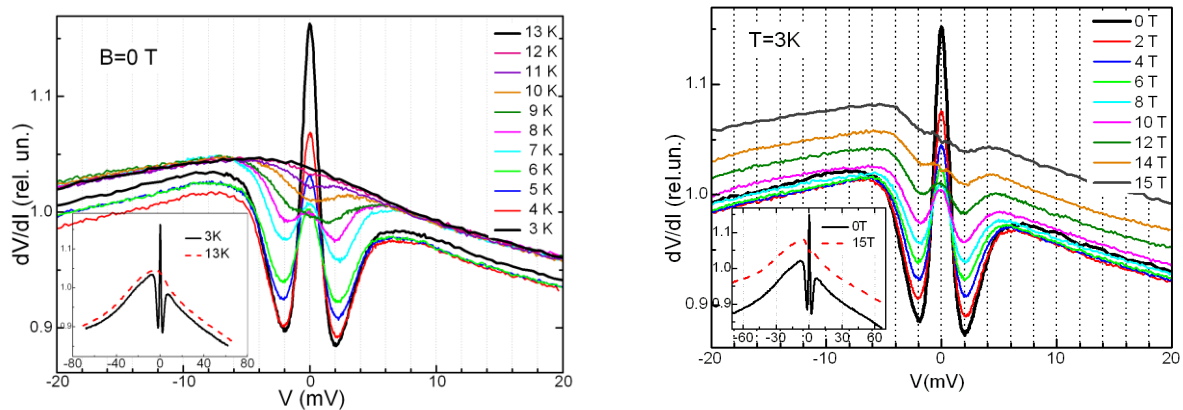


Fig.1 –Examples of dV/dI curves (or Andreev reflection spectra) of a FeSe soft point contact ($R=1.45 \Omega$) with characteristic Andreev reflection double minima structure, measured at different temperatures (left panel) and in magnetic field (right panel). Position of the minima corresponds roughly to the superconducting gap value. Insets show dV/dI curves for point contact from the main panel at the larger bias.

Acknowledgment is given to S. Aswartham, D.L. Bashlakov, L. Boeri, D.A. Chareev, S.-L. Drechsler, D. Efremov, G. Fuchs, N.V. Gamayunova, S. Haindl, O.E. Kvitnitskaya, K. Nenkov, A.N. Vasiliev, S. Wurmehl.

References

- 1) Yu. G. Naidyuk, I. K. Yanson, Point-Contact Spectroscopy (Springer Series in Solid-State Sciences, Vol. 145, New York: Springer, 2005).
- 2) Yu. G. Naidyuk et al., Supercond. Sci. Technol. 24, 065010 (2011).
- 3) Yu. G. Naidyuk et al., Phys. Rev. B 89, 104512 (2014).
- 4) Yu. G. Naidyuk et al., Phys. Rev. B 90, 094505 (2014).
- 5) V. V. Fisun et al., Fiz. Nizk. Temp. 40, 1175 (2014) [Low Temp. Phys. 40, 919 (2014)].
- 6) Yu. G. Naidyuk et al., Fiz. Nizk. Temp., 42, 42 (2016) [Low Temp. Phys. 42, 31 (2016)].
- 7) Yu. G. Naidyuk, G. Fuchs, D.A. Chareev, A.N. Vasiliev, Phys. Rev. B 93, 144515 (2016).

Wednesday, June 14, 2017

Observation of boson resonance in oxypnictide superconductors by means of IMARE spectroscopy

*S. Kuzmichev¹⁾²⁾, T. Kuzmicheva²⁾.

¹⁾M.V. Lomonosov Moscow State University, Department of Low Temperature Physics and Superconductivity, Moscow, Russia ²⁾P.N. Lebedev Physical Institute, Russian Academy of Sciences, Laboratory of Strongly Correlated Systems, Moscow, Russia

*kuzmichev@mig.phys.msu.ru

We studied polycrystalline samples of various 1111-family superconductors: $\text{GdO}_{1-x}\text{F}_x\text{FeAs}$ ($x \approx 0.1$, $T_C = 46\text{--}53$ K), $\text{CeO}_{0.9}\text{F}_{0.1}\text{FeAs}$ ($T_C \approx 41$ K) [1], $\text{Sm}_{1-x}\text{Th}_x\text{OFeAs}$ ($x = 0.08\text{--}0.3$, $T_C = 26\text{--}54$ K) [2], and $\text{LaO}_{1-x}\text{F}_x\text{FeAs}$ ($x \approx 0.1$, $T_C \approx 26$ K) [3].

We used intrinsic multiple Andreev reflection effect (IMARE) spectroscopy realized by a break-junction technique [4]. In natural SnSn-...-S (S — superconductor, n — normal metal) arrays, IMARE causes a subharmonic gap structure (SGS) — a set of dI/dV dips at $eV_n = 2\Delta \cdot m/n$ (m — number of SnS junctions in the array, $n = 1, 2, \dots$). In 1111, we observed two gaps with $2\Delta_L/kT_C = 5.2\text{--}5.7$, and $2\Delta_S/kT_C = 1.2\text{--}1.6$ [5].

During IMARE, electron could emit a boson with energy ε_0 , causing satellite dI/dV dips offset the Δ_L SGS at $eV_n = (2\Delta + k\varepsilon_0) \cdot m/n$ ($k = 1, 2, \dots$ — number of emitted bosons) [6]. We observed a reproducible fine structure of up to $k = 4$ dips which (a) is caused by the bulk rather than surface, (b) holds its position regardless to contact resistance and m , (c) is not caused by a 3rd gap, or k-space Δ_L anisotropy, (d) has a particular T-dependence, proving its electron-boson origin. The directly determined ε_0 scales with T_C together with both gaps within $T_C = 26\text{--}54$ K, with $2\varepsilon_0/kT_C \approx 3.3$ staying close to the expected magnetic resonance energy $\Delta_L \pm \Delta_S$ [7].

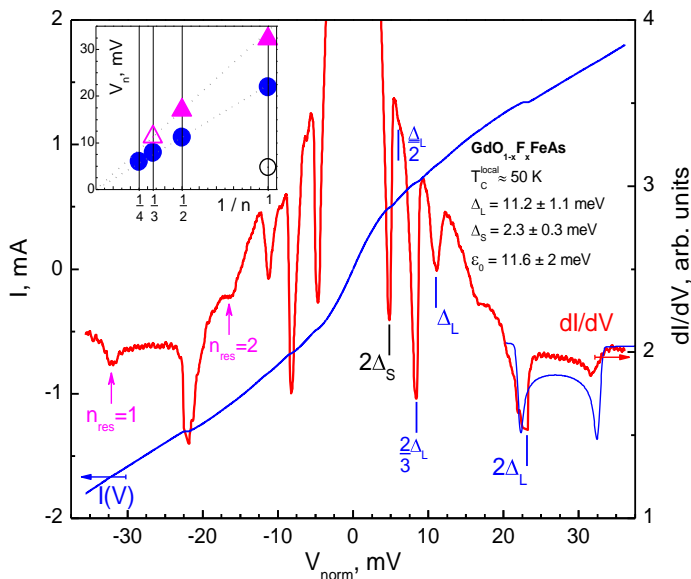


Fig. 1. Normalized current-voltage characteristic $I(V)$ (dark blue line, left vertical scale), and dynamic conductance spectrum (red line, right scale) of SnS-Andreev array formed in Gd-1111 at $T = 4.2$ K. Andreev subharmonics of the large gap correspond to $\Delta_L \approx 11.2$ meV, the $2\Delta_S$ features determine the small gap $\Delta_S \approx 2.3$ meV. The $dI(V)/dV$ features caused by a boson emission are labeled with $n_{\text{res}} = 1, 2$ and arrows, the bosonic energy is $\varepsilon_0 \approx 11.6$ meV. Thin solid line simulates an expected shape of (right side) $n_L = 1$ Andreev feature for the case of anisotropic large gap.

The inset shows the dependence of the positions of Andreev features V_n versus the inverse subharmonic order, $1/n$: for the large gap $V_{L,n} = 2\Delta_L/en$ (blue circles), for the small gap (open circle), and for boson-caused features $V_{\text{res},n} = (2\Delta_L + \varepsilon_0)/en$ (magenta triangles). Dotted lines are guidelines.

References

- 1) E.P. Khlybov, *et al.*, JETP Lett. 90, 387 (2009).
- 2) N.D. Zhigadlo, *et al.*, Phys. Rev. B 82, 064517 (2010).
- 3) A. Kondrat, *et al.*, Eur. Phys. J. B 70, 461 (2009).
- 4) S.A. Kuzmichev, T.E. Kuzmicheva, Low Temp. Phys. 42, 1008 (2016).
- 5) T.E. Kuzmicheva, *et al.*, Physics-Uspexhi 57, 819 (2014).
- 6) U. Zimmermann, K. Keck, Z. Phys. B 101, 555 (1996).
- 7) M.M. Korshunov, *et al.*, Phys. Rev. B 94, 094517 (2016).

Wednesday, June 14, 2017

Iron Incorporation into Layered Nickel-rich Tellurides as a Way to Materials with Controlled Magnetic Anisotropy

A.N. Kuznetsov^{1,2)}, E.A. Stroganova¹⁾, E.Yu. Zakharova¹⁾, A.V. Sobolev¹⁾, D.I. Kirdyankin²⁾¹⁾Department of Chemistry, Lomonosov Moscow State University, Moscow, Russia ²⁾N.S. Kurnakov Institute of General and Inorganic Chemistry, Russian Academy of Sciences, Moscow, Russiaalexei@inorg.chem.msu.ru

Low-dimensional systems of heterometallic bonds are fascinating objects of studies in inorganic and solid state chemistry, their presence often leads to unconventional properties. This talk will be focused on mixed chalcogenides based on the 2D heterometallic fragments, e.g. the recently discovered families of nickel-main group metal tellurides $\text{Ni}_{3-x}\text{MTe}_2$ with x varying from 0 to 1 [1-2]. These compounds are based on the ordered NiAs structure type and, according to the X-ray and HRTEM studies, show different ways of nickel vacancy ordering depending on the type of main group metal they incorporate. For $\text{M}=\text{Ga}$ we have established hitherto unknown superstructure of the NiAs-type arising from the two-dimensional ordering of the vacancies in the ab crystallographic plane. For $\text{M}=\text{Sn}$, a one-dimensional ordering of vacancies is observed, leading to an incommensurate structure. We used these systems as a matrix for incorporating magnetic cations such as iron [3]. Using a high-temperature synthetic approach, we have produced $\text{Ni}_{3-x}\text{Fe}_x\text{MTe}_2$ ($\text{M}=\text{Ga}, \text{Sn}$) samples with x up to 2. Detailed investigation of the samples using X-ray diffraction, ED, and ^{57}Fe and ^{112}Sn Moessbauer spectroscopy demonstrates the ordered nature of iron incorporation, the ordering patterns differ for $\text{M}=\text{Ga}$ and Sn . In the case of the former, it was found that at low iron concentrations, all three nickel positions are partially occupied by iron. However, with an increase in the iron content, the process becomes more that of the vacancy filling, so at the limit of iron incorporation ($x=1$) iron is distributed across those two nickel positions that initially had vacancies (see Figure 1). Iron incorporation into the $\text{Ni}_{3-x}\text{SnTe}_2$, from all the available data, appears to be less ordered. However, it also does not change the structure motif, and no new superstructure arises from substitution.

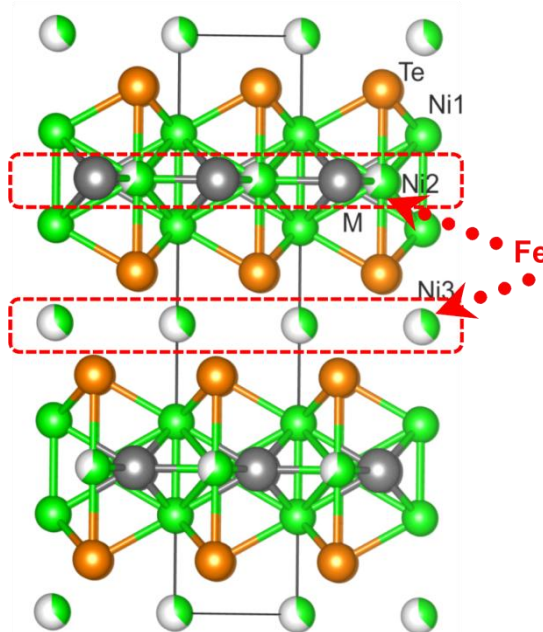


Fig. 1. Preferential sites for iron incorporation in the $\text{Ni}_{3-x}\text{GaTe}_2$ structure.

Magnetic measurements on the gallium-containing compounds show low-temperature ferromagnetic ordering at $x>0.2$, while tin-based ones show an unusual suppression of magnetic signal on the increase of iron content. In both cases, the initial Pauli-like paramagnetic properties of the matrix are modified. More detailed study of the magnetism of the $\text{Ni}_{3-x}\text{Fe}_x\text{GaTe}_2$ series shows that, with an increase in the iron content, the strength of ferromagnetic coupling, as well as the T_c , increases, and while the samples with small x show competing ferro- and ferrimagnetic interactions, diluted in Pauli-like matrix, samples with $x>0.6$ show dominant long-range ferromagnetic ordering at the temperatures below T_c .

This work was supported by Russian Foundation for Basic Research (Grant 15-03-06459) and Russian Academy of Sciences.

References:

- 1) A.A. Isaeva, O.N. Makarevich, A.N. Kuznetsov, T. Doert, A.M. Abakumov, G. Van Tendeloo. *Eur. J. Inorg. Chem.* 2010, 9, 1395–1404.
- 2) O.N. Litvinenko, A.N. Kuznetsov, A.V. Olenov, and B.A. Popovkin. *Russ. Chem. Bull.* 2007, 56, 1945–1947.
- 3) A.N. Kuznetsov, E.A. Stroganova, E.Yu. Zakharova, A.V. Solopchenko, A.V. Sobolev, I.A. Presniakov, D.I. Kirdyankin, V.M. Novotortsev. *J. Solid State Chem.* 2017, 250, 90–99.

Wednesday, June 14, 2017

Selenite and tellurite halides of 3-d metals as possible low-dimensional magnets: synthesis, crystal structures and properties

*P.S. Berdonosov, V.A. Dolgikh.

Department of Chemistry, Lomonosov Moscow State University, Moscow, Russia

*berdonosov@inorg.chem.msu.ru

Magnetism in low-dimensional magnetic systems is a hot topic due to the wide range of physical phenomena exhibited by them. Usually the magnetic subsystem formation is related to the peculiarities of the crystal structure of the substance. Selenite and tellurite compounds are attractive to the search for low-dimensional magnets due to the strong asymmetric surrounding of selenium or tellurium atoms and presence of active pairs of electrons, which act as nonvisible ligand comparable to the oxygen atom in volume. Such electron pairs tend to form cavities, channels or even layers in the crystal structures. As the result, the selenite or tellurite groups also tend to order in the crystal structure. Finally layered (2D) or low-dimensional (1D, 0D) crystal structure may form. The presence of 3d- metal ions in such structure may lead to low-dimensional magnetic subsystem formation and related magnetic properties.

In our work, a number of systems with low-dimensional magnetic behavior were prepared and characterized. Copper (II) ions with $S = 1/2$ compounds $Sr_2M(SeO_3)_2Cl_2$ ($M = Co, Ni, Cu$), $SrCu_2(SeO_3)_2Cl_2$, $CaCu_2(SeO_3)_2Cl_2$, $PbCu_2(XO_3)_2Cl_2$ ($X = Se, Te$) and mineral francisite-like compounds with composition $Cu_3M(SeO_3)_2O_2X$ ($M =$ different Rare Earth Metals; $X = Cl, Br$) possess low-dimensional magnetic properties with different geometry of magnetic subsystems. The iron (III) compound $S = 5/2$ $Bi_2Fe(SeO_3)_2OCl_3$ was found to be quasi one dimensional magnetic. It should be noted, that copper (II) compounds with same formula may crystallize in different crystal structures and exhibit different magnetic properties. For example, $PbCu_2(SeO_3)_2Cl_2$ is isostructural to $SrCu_2(SeO_3)_2Cl_2$, but $PbCu_2(TeO_3)_2Cl_2$ has the same structure as calcium compound $CaCu_2(SeO_3)_2Cl_2$. Magnetic properties of these two types of structures fitted by the different models of spin-spin interactions.

The 1D magnetic subsystem of $Bi_2Fe(SeO_3)_2OCl_3$ is closely related to the crystal structure of this compound where $[BiO_4Cl_3]$ and $[BiO_3Cl_3]$ polyhedrons and bridged SeO_3 groups separate the infinite chains of $[FeO_6]$ apex shared octahedrons. Due to such separation, the magnetic interactions between different chains are very weak.

The comparison to the other known related compounds will be presented.

The work was supported by RFBR project PФФИ 16-03-00463

Thursday, June 15, 2017

Iridates: from Heisenberg antiferromagnets to potential Kitaev spin liquids

* J. van den Brink ¹⁾.

¹⁾ Leibniz Institute IFW Dresden, Germany

* j.van.den.brink@ifw-dresden.de

Relatively recently, more than 40 years after the foundation of modern band structure theory by Kohn and Sham, it was discovered that the electronic bands of simple, noninteracting electron systems have intrinsic topological properties generated by the relativistic spin-orbit coupling (SOC) [1]. The observed richness of topological states on the single-electron level prompts the question what kind of topological phases can develop in more strongly correlated, many-body electron systems.

Correlation effects, in particular intra- and interorbital electron-electron interactions, are very substantial in 3d transition-metal compounds such as the copper oxides, but SOC is weak. In 5d transition-metal compounds such as iridates, the interesting situation arises that the SOC and Coulomb interactions meet on the same energy scale.

The electronic structure of iridates thus depends on a strong competition between the electronic hopping amplitudes, local energy-level splittings, electron-electron interaction strengths, and the SOC of the Ir 5d electrons. The interplay of these ingredients offers the potential to stabilize relatively well-understood states such as a 2D Heisenberg-like antiferromagnet in Sr₂IrO₄, but in principle also far more exotic ones, such as a topological Kitaev quantum spin liquid, in (hyper)honeycomb iridates [2,3].

I will discuss the microscopic electronic structures of these iridates, their proximity to idealized Heisenberg and Kitaev models and our contributions to establishing the physical factors that appear to have preempted the realization of quantum spin liquid phases so far [4-11].

References:

- 1) Kane & Mele, PRL 95, 146802 (2005)
- 2) Jackeli & Khaliullin, PRL 102, 017205 (2009)
- 3) Nussinov & Van den Brink, RMP 87, 1 (2015), arXiv:1303.5922
- 4) Gretarsson et al., PRL 110, 076402 (2013)
- 5) Lupascu et al., PRL 112, 147201 (2014)
- 6) Katukuri et al., NJP 16, 013056 (2014)
- 7) Katukuri et al., PRX 4, 021051 (2014)
- 8) Kim et al., Nature Comm. 5, 4453 (2014)
- 9) Bogdanov et al., Nature Comm. 6, 7306 (2015)
- 10) Nishimoto et al., Nature Comm. 7, 10273 (2016)
- 11) Plotnikova et al., PRL 116, 106401 (2016)

Thursday, June 15, 2017

Constraints on the coupling to low-energy bosons in Fe based superconductors

*S.-L. Drechsler¹⁾, S. Johnston²⁾, S. Borisenko¹⁾, V. Grinenko^{1,3)}, J. Tomczak⁴⁾, and H. Rosner⁵⁾

¹⁾Leibniz Inst. f. Solid State and Materials Research IFW-Dresden, D-01169 Dresden, Germany, ²⁾Dpmt. of Physics & Astronomy, University of Tennessee, Knoxville 37996 USA, ³⁾Dpmt. of Physics, TU Dresden, Germany, ⁴⁾Vienna University of Technology, Vienna, Austria ⁵⁾Max-Planck-Inst. f. Chem. Physics of Solids, Dresden, Germany

*s.l.drechsler@ifw-dresden.de

Although the Fe-based superconductors (FeSC) were discovered ten years ago, there is still no consensus on the relevant microscopic pairing mechanism(s) and main interactions involved. Also a consistent interpretation of their normal state properties is still lacking. Especially the strength of the *el-el* interaction and correlation effects are under debate. Here, we examine several materials and illustrate various problems and concepts that are generic for all FeSC. Based on empirical observations and qualitative insight from DFT, we show that the super-conducting (SC) and normal state properties of the FeSC can be described semi-quantitatively within multiband MIGDAL-ELIASHBERG theory. We account for the large high-energy mass renormalization (MR) phenomenologically and a mode-rate low-energy bosonic MR, in accord with constraints provided by thermodynamic, optical, and ARPES data. When seen in this way, all FeSCs with $T_c < 40\text{-K}$, studied so far, are found to belong to an *intermediate* coupling regime at odds with the strong coupling scenarios suggested in the early period of the FeSC history. The support of SC by intraband *el-ph* coupling or *el-orbital fluctuations* [11] and phonon anomalies [2,3] are briefly addressed, too.

We discuss band shifts [4] as counter parts of the MR measured conveniently by the positions of VAN HOVE singularities (VHS), and the nature of a suggested quantum critical point (QCP) [5] in the *h*-overdoped systems AFe_2As_2 ($A=\text{K, Rb, Cs}$). Using high-precision full relativistic GGA-calculations for the total DOS at E_F , we arrive at a milder MR for Cs122 and the same MR for K122 and Rb122 at variance with other studies. The importance of spin-orbit coupling is supported by GW-calculations [4]. From the calculated mass anisotropies of all Fermi surface sheets, only the ε -pocket near the corner of the BZ is compatible with the observed anisotropy of the upper critical field H_{c2} , pointing to its dominant role in the SC of these three systems. At high fields only that band survives as evidenced by a single-band elliptical angular mass anisotropy [6]. Finally, a general doping phase diagram shown in Fig. 1 is proposed. Thee QCP slightly below 0.5 hole doping is ascribed to the vicinity of an orthorhombic stripe-phase triggered by the d_{xz}/d_{yz} derived VAN HOVE singularity close to E_F (at -14.5 meV for KFe_2As_2 (K122) according to ARPES) in qualitative accord with DMFT and GW calculation and ⁷⁵As NMR data [7]. Its puzzling absence in a STT study for CsFe_2As_2 [8] is ascribed to critical stripe fluctuation causing a local splitting of the tetragonal symmetry and yielding an additional MR seen in the large SOMMERFELD constant γ , but being detrimental for $d_{x^2-y^2}$ pairing in contrast to Sr_2RuO_4 where the VHS approaching E_F strengthens also the SC pairing [9]. Here, it enhances the MR, only, detrimentally for SC and explains the lowest T_c for Cs-122.

References

- 1) S. Johnston, M. Abdel-Hafiez, L. Harnagea, *et al.*, PRB 89, 134507 (2014).
- 2) V. Ivanov, A. Ivanov, *et al.* J. Supercond. Nov. Mat. 29, 3035 (2016).
- 3) Y. Naidyuk *et al.*, PRB 90, 094505 (2014).
- 4) J. Tomczak, *et al.* Phys. Rev. Lett. 109, 237010 (2012).
- 5) F. Eilers, K. Grube, D. Zocco, *et al.*, Phys. Rev. Lett. 116, 237003 (2016).
- 6) T. Terashima, M. Kimata, *et al.* J. Phys. Soc. Jpn. 78, 060504 (2009).
- 7) Z.T. Zhang, D. Dmytrieva, S. Molatta, *et al.*, arXiv:1703.00780 (2017).
- 8) H. Yang *et al.* PRB 93, 224516 (2016).
- 9) A. Stepke, L. Zhao, M.E. Barber *et al.*, Science 355 (6321) eaaf9398 (2017).
- 10) N. Kawaguchi, Fujiwara, S. Iimura, *et al.* PRB 94, 161104 (2016)

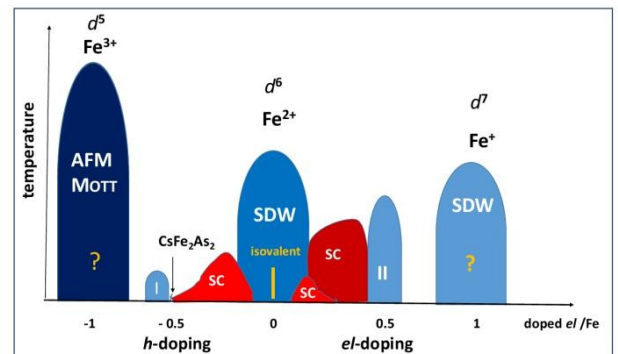


Fig. 1.: Suggested Fe pnictides phase diagram. Blue (red): magnetic (SC) regions, resp.. Phase I - a combined charge, orbital, and spin ordered phase near the QCP responsible for the non-Fermi liquid in Cs122 [7]. Yellow line: isovalent/no doping for such systems as Li(Na)FeAs, P-doped Ba(Sr)-122 and bulk FeSe where the competing magnetic SDW magnetic stripe-phase is absent or strongly suppressed. Phase II - observed but not yet characterized experimentally. The hypothetical SDW phase around Fe+ is our suggestion. Bright (dark red) regions: 122 and H doped La-1111 (under pressure) [10] FeSC, respectively.

Thursday, June 15, 2017

Superconducting State in $\text{LaFe}_{1-x}\text{Co}_x\text{AsO}$ Studied by S - N Point Contacts

*D.Bashlakov¹), S. Aswartham²), S. Wurmehl²), Yu.Naidyuk¹)

¹) B.Verkin Institute for Low Temperature Physics and Engineering, Kharkiv, Ukraine. ²)Leibniz Institute for Solid State and Materials Research, Dresden, Germany.

*bashlakov@ilt.kharkov.ua

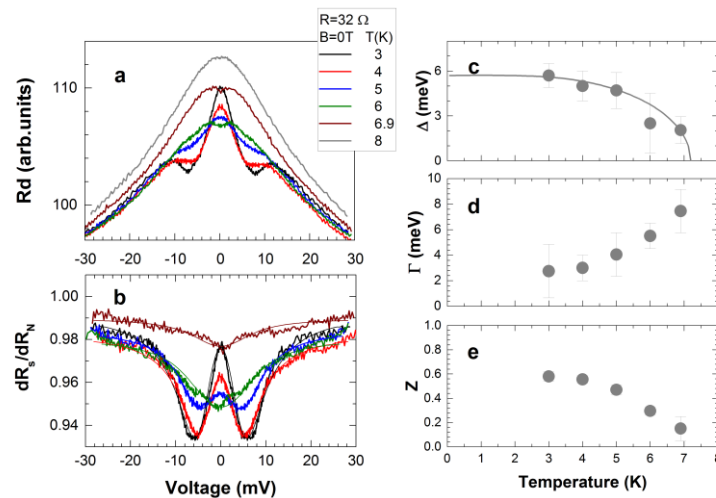


Fig 1. Differential resistance of the $\text{LaFe}_{1-x}\text{Co}_x\text{AsO}$ -Cu point contact showing the Andreev reflection features taken at the various temperatures (a). Normalized to the normal state differential resistance for the same contact along with fitted theoretical curves (thin lines) (b) using fitting parameters superconducting gap Δ , smearing parameter Γ and barrier strength Z (c, d, e).

Conventional needle-anvil type point contacts (PC) [1] as well as a "soft" type point contacts [2] were used to study the superconducting state in the single crystals of $\text{LaFe}_{1-x}\text{Co}_x\text{AsO}$ ($x=0.075$). The single crystal surfaces were found to be nonuniform since the detected superconducting critical temperature T_{cPC} varies for the different contacts in the range from 7 to 11 K. The differential resistance spectra $R_d(V)$ mostly exhibited the single zero-bias minimum, which disappeared above T_{cPC} . This minimum didn't disappear at high magnetic field up to 15 Tesla, what is indicative for the iron-based superconductors due to their high critical field.

The Fig.1a demonstrates rare case of $R_d(V)$ with Andreev-like feature (double-minimum structure) recorded for the S - N contact (superconductor-normal metal contact, where Cu was used as a counter electrode for $\text{LaFe}_{1-x}\text{Co}_x\text{AsO}$). The single gap BTK theory was used to fit experimental data, as shown on Fig.1b. Temperature dependence of the superconducting gap turned out to be close to the BCS curve. Unusual is strong decrease of the barrier strength parameter Z with temperature, what could be due to its semiconducting origin (depleted surface layer) and low barrier height. Received superconducting gap value at low temperature testify strong Cooper pairing in $\text{LaFe}_{1-x}\text{Co}_x\text{AsO}$, judging from the high $2\Delta/kBTC$ ratio of 18 ± 2 , since it largely exceed the BCS value of 3.52.

Acknowledgments are given to D. Efremov, G. Fuchs, N.V. Gamayunova, O.E. Kvitnitskaya, K. Nenkov.

References:

- 1) Yu. G. Naidyuk and I. K.Yanson, Point-Contact Spectroscopy (Springer Series in Solid-State Sciences, Vol. 145, New York: Springer, 2005).
- 2) D. Daghero and R. S. Gonnelli, Probing multiband superconductivity by point-contact spectroscopy, Supercond. Sci. Technol. 23, 043001 (2010).

Thursday, June 15, 2017

Anisotropic superconducting gaps in optimally doped $\text{Ba}_{1-x}\text{K}_x\text{Fe}_2\text{As}_2$ and $\text{BaFe}_{2-x}\text{Ni}_x\text{As}_2$

*T.E. Kuzmicheva¹, S.A. Kuzmichev^{2,1}, A.V. Muratov¹, K.S. Pervakov¹, A.V. Sadakov¹, V.M. Pudalov¹

¹) P.N. Lebedev Physical Institute RAS, Leninsky prospect 53, Moscow 119991, Russia ²) M.V. Lomonosov Moscow State University, Leninskie Gory 1, Moscow 119991, Russia

*kute@sci.lebedev.ru

We studied nearly optimal single crystals of Ba-122 family by intrinsic multiple Andreev reflections effect (IMARE) spectroscopy (“break-junction” technique [1]). The current-voltage characteristics of SnS-Andreev contacts (S — superconductor, n — a ballistic layer of normal metal) showed a pronounced excess current at low bias, and two subharmonic gap structures (SGS) — series of dynamic conductance dips at positions $V_{n,i} = 2\Delta_i/en$ (n is a natural number) corresponding to the large and the small superconducting gaps [2,3]. The doublet-like shape of the SGS dips demonstrated the gap anisotropy in a k-space (extended s-wave symmetry) [4,5].

For nearly optimal potassium-doped $\text{Ba}_{0.65}\text{K}_{0.35}\text{Fe}_2\text{As}_2$ with $T_C \approx 36$ K [6] we determined the large gap $\Delta_L = 6.4\text{--}9.5$ meV (~30 % anisotropy in k-space) and the small gap $\Delta_S \approx 1.8$ meV.

In nickel-doped single crystals $\text{BaFe}_{1.9}\text{Ni}_{0.1}\text{As}_2$ with $T_C \approx 19$ K, we observed two gaps with moderate anisotropy: $\Delta_L = 3.2\text{--}4.4$ meV (~33 % anisotropy in k-space, similarly to $\text{Ba}(\text{K})\text{Fe}_2\text{As}_2$), and $\Delta_S \approx 1.6$ meV.

The directly measured gap temperature dependences $\Delta_{L,S}(T)$ agree well with two-band system of equations by Moskalenko and Suhl [7]. We thank H.-H. Wen, M. Abdel-Hafiez, A.A. Kordyuk, Y.C. Chen for the providing samples and useful discussions.

References:

- 1) J. Moreland and J. W. Ekin, J. Appl. Phys. 58, 3888 (1985).
- 2) M. Octavio et al., Phys. Rev. B 27, 6739 (1983).
- 3) R. Kuemmel et al., Phys. Rev. B 42, 3992 (1990).
- 4) T. P. Devereaux and P. Fulde, Phys. Rev. B 47, 14638(R) (1993).
- 5) A. Poenicke et al., Phys. Rev. B 65, 220510(R) (2002).
- 6) M. Abdel-Hafiez et al., Phys. Rev. B 90, 054524 (2014).
- 7) V.A. Moskalenko, Fiz. Met. Metall. 8, 503 (1959); H. Suhl et al., Phys. Rev. Lett. 3, 552 (1959).

Thursday, June 15, 2017

R&D of 2G HTS wire in joint work of SuperOx Company and MSU

A.Kaul^{1,2)}, A.Molodyk²⁾, S.Samoylenkov²⁾, V.Kalitka²⁾, M.Moyzykh²⁾, A.Mankevich²⁾, A.Markelov²⁾, I.Martynova²⁾, D.Tzymbarenko^{1,2)}, A.Makarevich^{1,2)}, S.Lee³⁾, V.Petrykin³⁾ and V.Chepikov^{1,2)}

¹⁾Department of Chemistry, Lomonosov Moscow State University, Moscow, Russia, ²⁾SuperOx Company, Moscow, Russia, ³⁾SuperOx Japan LLC, Tokyo, Japan.

*arkaul@mail.ru

The development of 2G HTS wire (also named *coated conductors*), the core of which are thin epitaxial REBCO films deposited on textured and buffered metal tapes, is one of most striking achievements of superconducting science and technology. The unique current-carrying capacity of 2G HTS wire (about 500 times higher compared to copper metal), and their appearance at the world market of superconducting materials enable the wide scope of its practical applications.

R&D of 2G HTS wire at Inorganic Chemistry Division (MSU) absorbed a rich experience in HTS study, thin films, and MOCVD of oxide materials. This activity, initially based on the conception of MOCVD of YBCO on RABiTS, made possible the obtaining of few meters long tapes with critical current density of MA/cm² level. Simultaneously a number of related technologies were developed, namely tapes rolling, electropolishing, sputtering, electroplating etc., and the equipment for these roll-to-roll processes was designed and constructed. On this base SuperOx company (www.superox.ru) was registered in 2006 with the aim of 2G HTS wire commercial production and its practical application.

For reliable and reproducible superconducting properties of production 2G HTS wire, it is essential to secure consistent and reproducible composition and microstructure of the HTS layer in the wire architecture, on a daily basis, over years of operation. To meet these requirements the technological paradigm was changed for "PLD on IBAD substrate". Now SuperOx has implemented IBAD and sputtering techniques for fabrication of the substrate with textured buffer layers and the robust pulsed laser deposition method for the HTS layer fabrication.

The great variety of HTS applications dictates fundamentally different modes and conditions of 2G HTS wire operation in corresponding devices: temperature, current, magnetic field, mechanical stress, vibration, electric field density, etc. Therefore, 2G HTS wire intended for a certain application has to meet a specific set of requirements, in other words it must be customized to that application. SuperOx has made deep and thorough customization of 2G HTS wire, it's key differentiation point on the wire market. In this talk, we review the fabrication and quality control processes for SuperOx 2G HTS wire and discuss the superconducting properties of our wire, its customized options and some trends of further development. The participation of SuperOx in current national and European projects aimed to design superconducting equipment with the use of our wire is reviewed with special attention for fault current limiters, which are already nearing commercialization.

Thursday, June 15, 2017

Strong-Coupling Two-Gap Superconductivity in $\text{Mo}_8\text{Ga}_{41}$

*V.Yu. Verchenko¹⁾²⁾, R. Khasanov³⁾, Z. Guguchia³⁾, A.A. Tsirlin⁴⁾, A.V. Shevelkov¹⁾

¹⁾Department of Chemistry, Lomonosov Moscow State University, Moscow, Russia, ²⁾National Institute of Chemical Physics and Biophysics, Tallinn, Estonia, ³⁾Laboratory for Muon Spin Spectroscopy, Paul Scherrer Institute, Villigen, Switzerland, ⁴⁾Experimental Physics VI, Center for Correlations and Magnetism, Institute of Physics, University of Augsburg, Augsburg, Germany

*verchenko@inorg.chem.msu.ru

Recently, W. Xie *et al.* proposed that superconductivity may be favorable in a class of intermetallic compounds featuring endohedral gallium clusters TGa_n (T is transition metal). This compound family includes Rh_2Ga_9 ($T_c = 1.9$ K) and Ir_2Ga_9 (2.2 K), ReGa_5 (2.3 K), $\text{Mo}_8\text{Ga}_{41}$ (9.7 K) and $\text{Mo}_6\text{Ga}_{31}$ (8 K) superconductors. Their crystal structures contain vertex-sharing or edge-sharing TGa_n clusters. We explored one representative of this family, $\text{Mo}_8\text{Ga}_{41}$, which has the highest critical temperature T_c among the whole series. By analyzing properties of the superconducting state, we aim to gain insight into the mechanism of superconductivity in these TGa_n -based compounds.

Here, we report crystal growth, thermodynamic, transport and microscopic properties of $\text{Mo}_8\text{Ga}_{41}$ and its V-substituted analog $\text{Mo}_{8-x}\text{V}_x\text{Ga}_{41}$ ($x < 2$). Electrical resistivity, isothermal magnetization, magnetic susceptibility and heat capacity measurements, and electronic structure calculations were performed to investigate both normal- and superconducting-state properties. Zero-field and transverse-field muon spin rotation and relaxation spectroscopy (μSR) experiments were undertaken to study the order parameter in $\text{Mo}_8\text{Ga}_{41}$ and its evolution upon the V for Mo substitution.

This work is based on the results obtained at the Swiss Muon Source, Paul Scherrer Institute, Villigen, Switzerland. The work has been supported by the Russian Science Foundation, grant #17-13-01033. A.A.T. is grateful for the financial support by the Federal Ministry for Education and Research under the Sofja Kovalevskaya Award of the Alexander von Humboldt Foundation.

References:

1) W Xie, H Luo, BF Phelan, T Klimczuk, FA Cevallos, RJ Cava - PNAS 112, 7048 (2015).

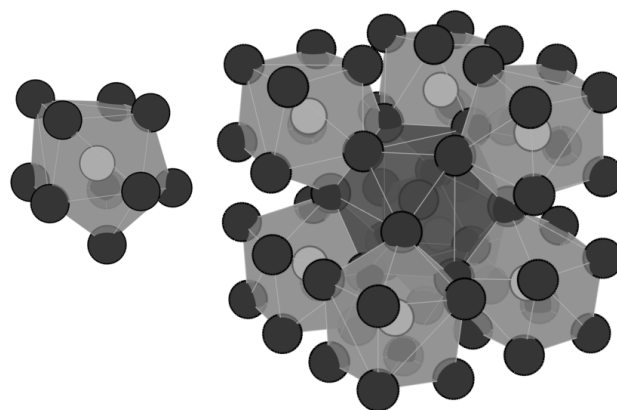


Fig.1. MoGa_{10} clusters forming the cubic arrangement around GaGa_{12} cuboctahedron in the crystal structure of $\text{Mo}_8\text{Ga}_{41}$. Mo atoms are shown in light gray and Ga atoms – in dark gray.

Thursday, June 15, 2017

Evolution of magnetism in Co and Ni substituted FeGa₃ as probed by Ga NQR spectroscopy

* [A.A. Gippius](mailto:gippius@mail.ru)¹⁾²⁾, S.V. Zhurenko¹⁾, C.-S. Lue³⁾, Ben-Li Young⁴⁾, V.Yu. Verchenko⁵⁾, A.V. Shevelkov⁵⁾

¹⁾Department of Physics, Lomonosov Moscow State University, Moscow, Russia ²⁾Shubnikov Institute of Crystallography, Moscow, Russia ³⁾Department of Physics, National Cheng Kung University, Tainan, Taiwan ⁴⁾ Department of Electrophysics, National Chiao Tung University, Hsinchu City, Taiwan ⁵⁾Department of Chemistry, Lomonosov Moscow State University, Moscow, Russia

* gippius@mail.ru (Corresponding author)

The small gap Fe-based semiconductors FeSi, FeSb₂ and FeGa₃ attracted much interest because of their prospective thermoelectric applications and intriguing low-temperature properties. They represent a rare class of non-magnetic and semiconducting Fe-based intermetallic compounds characterized by a small hybridization gap of about 0.5 eV at the Fermi level [1,2]. The formation of the energy gap in these 3*d*-materials is reminiscent of that in strongly correlated 4*f* Kondo-insulators.

Here we present NQR spectroscopy and nuclear spin-lattice relaxation study of electronic and magnetic properties in strongly correlated intermetallic system with gallium Fe_{1-x}M_xGa₃ (M = Co, Ni). In the parent compound FeGa₃ the ^{69,71}Ga spin-lattice relaxation rate 1/T₁(T) reveals an unexpected huge maximum at low T with an essentially magnetic relaxation mechanism indicating the existence of the in-gap states. The other end binary compound, CoGa₃, is a band metal demonstrating metallic Korringa behavior of the spin-lattice relaxation with 1/T₁ ~ T [3]. In the intermediate Fe_{0.5}Co_{0.5}Ga₃ compound 1/T₁(T) is strongly (by ~ 2 orders) enhanced due to antiferromagnetic (AF) spin fluctuations with 1/T₁ ~ T^{1/2} in perfect agreement with Moriya's spin-fluctuation theory [4] for itinerant magnetic systems. Such a 1/T₁(T) behavior is a unique feature of weakly and nearly AF metals.

Special attention is focused on low doping of FeGa₃ by Co (5%) and Ni (2.5%) [5] which are close to the border of metal-insulator transition. It was found that in Fe_{0.95}Co_{0.05}Ga₃ the 1/T₁ is more than one order of magnitude higher and demonstrates different temperature dependence than that in Fe_{0.975}Ni_{0.025}Ga₃ in the entire investigated temperature range of 2 – 300 K. This observation is in contradiction with the simple electronic model predicting equivalence of 5% Co and 2.5% Ni doping for Fe since Ni provides double amount of electrons into conduction band of FeGa₃ in comparison with Co. The obtained result is discussed in terms of paramagnetic centers formed by magnetic moments localized on Fe-Co dumbbells in Fe_{0.95}Co_{0.05}Ga₃ as well as low residual density of in-gap states in Fe_{0.975}Ni_{0.025}Ga₃ providing almost Korringa relaxation mechanism at low temperatures (2 – 10 K) in this compound.

This work was partially supported by the joint Russian-Taiwan Grant RFBR-MOST № 16-53-52012-a.

References

- 1) Z Fisk et al. - Physica B 206-207, 798 (1995).
- 2) G Aepli and Z. Fisk - Comm. Condens. Matter Phys. 16, 155 (1992).
- 3) AA Gippius et al. - Phys. Rev. B 89, 104426 (2014).
- 4) T Moriya - J. Magn. Magn. Mater. 14, 1 (1979).
- 5) MS Likhanov et al. - Journal of Solid State Chemistry 236, 166 (2016).



Thursday, June 15, 2017

Axion electrodynamics of topological insulators-type II superconductor structures

F. Nogueira

Leibniz Institute for Solid State and Materials Research, Dresden, Germany

The electromagnetic response of topological states of matter typically features a so called axion term in the effective Lagrangian, where θ is the fine structure constant and \mathbf{a} is the axion field. This term is a topological invariant and leads to new physically interesting effects in topological insulators, superconductors, and Weyl semimetals. In this talk we will discuss the physical consequences of the axion electrodynamics in heterostructures involving topological insulators and type II superconductors. One interesting specific example that will be discussed is the one of a topological insulator vertical Josephson junction. Due to the axion term a magnetic field applied perpendicular to the junction makes the vortex lines become the source of electric fields, leading in this way to a vortex-driven ac Josephson effect. This yields an example where the vortices become charged, carrying a fractional charge $e/2$. This effect is akin of the so called Witten effect, which predicts that in an axionic system magnetic monopoles acquire a fractional electric charge. This Josephson-Witten effect opens possibilities to electrically manipulate vortices via topological currents, which can in turn be used to create new devices. We briefly discuss the prospects of using these charged vortices as anyons and the possibility of braiding them for quantum computation.

Thursday, June 15, 2017

Fe-based superconductors: complementary research and potential applications

*V.M. Pudalov, Yu.A. Aleshenko, Yu.F. Eltsev, T.E. Kuzmicheva, A.V. Muratov, K.S. Pervakov, A.V. Sadakov, V.A. Vlasenko

Lebedev Physical Institute, RAS, Moscow

*pudalov@lebedev.ru (Corresponding author, 10 point)

Properties of the $\text{BaFe}_{2-x}\text{Ni}_x\text{As}_2$ and $\text{Ba}_{1-x}\text{K}_x\text{Fe}_2\text{As}_2$ single crystals with hole and electron doping, correspondingly, were studied by five complementary techniques: specific heat, lower and upper critical field, infrared reflectivity, and Andreev reflection spectroscopy. Despite the different type of dopants, all compounds demonstrate similar superconducting properties. The specific heat and critical field are the bulk probes, intrinsic Andreev reflection spectroscopy is the local probe, whereas optical spectroscopy and ellipsometry are the surface-sensitive probes. Nonetheless, the results obtained using various techniques are in a good agreement. The major conclusions of our studies are (i) the coexistence of two components of the superconducting condensate with unequal electron-boson interaction; (ii) the two gaps at separate Fermi surface sheets have no nodes in the $k_x k_y$ -plane though possess an extended s-wave symmetry, in agreement with ARPES data; (iii) the two-band model fits satisfactory superconducting properties in these compounds; (iv) the intraband interaction is rather strong and much exceeds the interband one. We fabricated a toy model of the FeSe wire by power-in-tube technique and measured its critical parameters, particularly, T_c equals to 11K, only slightly lower than that for the bulk FeSe.

Thursday, June 15, 2017

Photosensitive semiconductor materials for gas sensors

*M. Rumyantseva¹⁾, A. Chizhov¹⁾, R. Vasiliev¹⁾²⁾, A. Nasriddinov²⁾, E. Pakhova¹⁾, E. Lukovskaya¹⁾, O. Fedorova¹⁾³⁾, A. Gaskov¹⁾.

¹⁾Department of Chemistry, Lomonosov Moscow State University, Moscow, Russia ²⁾Faculty of Materials Science, Lomonosov Moscow State University, Moscow, Russia ³⁾Nesmeyanov Institute of Organoelement Compounds of Russian Academy of Sciences, Moscow, Russia

*roum@inorg.chem.msu.ru

Creation of new materials with gas sensitivity at room temperature (RT) is a key direction in the development of gas sensors technology. The operating principle of semiconductor gas sensors is based on the high sensitivity of the electrical properties of semiconductors surface to the ambient atmosphere composition. However, the "solid – gas" reactions occur on the surface of metal oxide semiconductors (MOS) at rather high temperatures 100-500 °C, which is necessary to increase the concentration of free charge carriers, for the activation of chemical reactions on the surface and for desorption of the reaction products. The need for heating substantially increases power consumption of semiconductor sensors that limits their use in stand-alone and portable devices, especially in communication systems like smartphones. Upon detection of oxidizing gases (NO₂, O₃) sensor signal generation occurs due to adsorption of analyte molecules on the metal oxide surface, which is accompanied by the localization of electrons on the adsorbed species lowering the electrical conductivity (for *n*-type semiconductors). At room temperature, this adsorption process is kinetically irreversible. The role of thermal heating upon NO₂ detection mainly consists in the activation of analyte molecules desorption and recovery of electrophysical properties of the sensitive material to initial state.

We report the realization of a new principle of gas detection using the resistive type sensor operating at RT under a low power visible light source. Bulk MOS are transparent in this spectral range. The solution of this problem becomes possible when sensitive materials are nanocomposites based on nanocrystalline MOS and photosensitizers. The role of photosensitizers consists in shifting the optical sensitivity range of semiconductor oxides towards larger wavelengths. The relative position of the energy bands of MOS and sensitizer must ensure the transfer of photoexcited carriers from the sensitizer to the semiconductor matrix. Selected photosensitizers: CdSe quantum dots (QDS) and organic dyes – Ru(II) complexes with organic ligands, are characterized by absorption in the visible range of the spectrum and have high extinction coefficients.

The role of illumination consists in generation of electrons, which can be transferred into MO_x conduction band, and holes that can recombine with the electrons previously trapped by the chemisorbed acceptor species and thus activate desorption of analyte molecules. Sensor measurements demonstrated that sensitized nanocrystalline MOS can be used for oxidizing gas detection under visible light illumination at RT without any thermal heating.

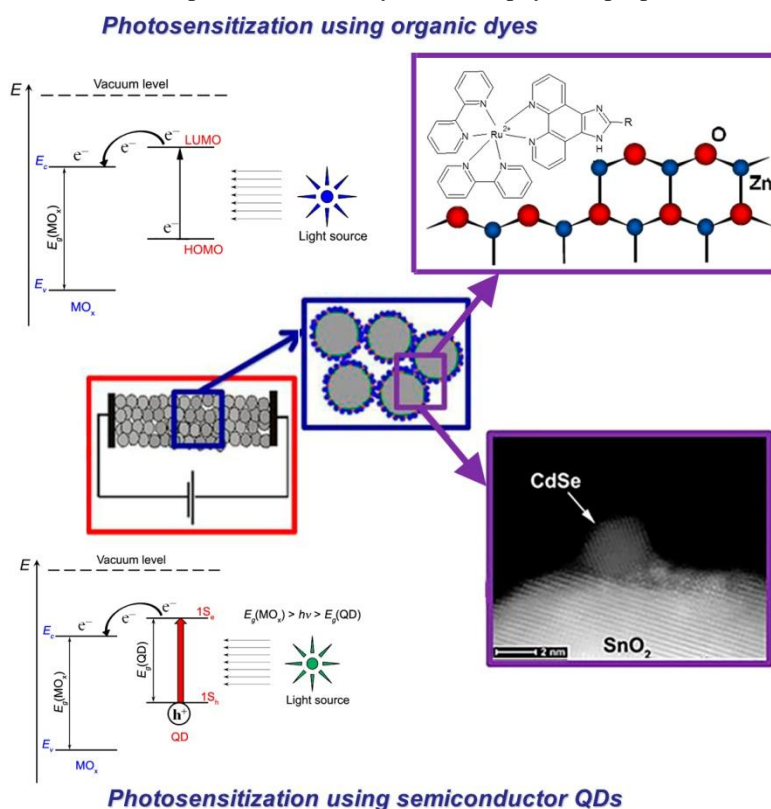


Fig. 1. Scheme of photosensitization

Thursday, June 15, 2017

Alkaline-earth apatites with cobalt ions in the trigonal channels as molecular magnets

*P.E. Kazin¹⁾, M.A. Zykin²⁾, K.A. Babeshkin¹⁾, M. Jansen³⁾

¹⁾Department of Chemistry, Lomonosov Moscow State University, Moscow, Russia ²⁾Department of Materials Science, Lomonosov Moscow State University, Moscow, Russia ³⁾Max-Planck Institute for Solid State Research, Stuttgart, Germany

*kazin@inorg.chem.msu.ru

A single molecule magnet (SMM) is a paramagnetic molecule in which the magnetic moment can be frozen in a certain direction due to a very large magnetic anisotropy. Such molecules exhibit properties both of classical permanent magnets and quantum systems and are perspective components for ultra-high-density magnetic recording, molecular electronics and spintronics. The compounds are mostly represented by d- and f-metal complexes with organic ligands. A magnetic unit includes one metal ion or several exchange-coupled metal ions. The magnetic anisotropy is determined by a strong spin-orbit coupling in combination with a pronounced axial component of the ligand field. To change the magnetization (spin) orientation it is necessary to overcome an energy barrier U_{eff} . This causes the irreversibility of low temperature magnetization determined by blocking temperature T_b and slow relaxation (SR) of magnetization at enhanced temperatures.

Recently we have shown that the Cu-doped apatites may contain separate linear paramagnetic ions $[\text{OCuO}]^{\cdot-}$ which behave like SMMs with U_{eff} ranging from few tens to a hundred of cm^{-1} [1,2]. This encouraged us to perform a study on Co-doped alkaline-earth hydroxyapatites [3,4]. Single phase samples with nominal composition $\text{M}_{10}(\text{PO}_4)_6[\text{Co}_x\text{OH}_{1-2x-d}]_2$, where $\text{M} = \text{Sr}, \text{Ba}$, $x = 0.02 - 0.3$, have been prepared by a high-temperature solid state reaction. All compounds exhibit slow relaxation of magnetization at low temperatures. Three kinds of paramagnetic centers are distinguished in ac-susceptibility measurements. A major fraction of magnetization of strontium compounds shows slow relaxation induced by a magnetic field. It is denoted as normal slow relaxation (NSR) often observed in Co-based SMMs. In strontium compounds with a low Co content, especially after the annealing in oxygen flow, a considerable part of magnetization undergoes to a new very slow relaxation process (VSR) persisting also in the absence of magnetic field. Smaller fraction of magnetization in all the samples shows reversible behavior of up to 1 kHz and is denoted as fast relaxation (FR). In barium compounds a major part of magnetization shows VSR features, and a minor one – FR.

The temperature dependence of the relaxation time τ was approximated with a relaxation model accounting the Orbach, Raman, direct, and tunneling relaxation mechanisms. The NSR process is characterized by $U_{\text{eff}} = 59 \text{ cm}^{-1}$ ($x = 0.02$). The U_{eff} value corresponds well to a zero field splitting energy $2D = -52 \text{ cm}^{-1}$, estimated from the temperature dependence of dc susceptibility. The VSR process is characterized by much higher U_{eff} , reaching 200 and 387 cm^{-1} in barium and strontium compounds respectively. According to the X-ray crystal structure refinement in the strontium and barium apatites, Co situates in the hexagonal channel, statistically shifted from its center so that a bent fragment OCoO forms (with a OCoO angle of $\sim 150^\circ$). Co-K-edge EXAFS data for strontium compound confirm the coordination of Co by two oxygen atoms at a distance of 1.73 \AA . Other oxygen atoms are at non-bonding distances. The NSR and VSR behavior is assigned to an intra-channel Co in the two-fold coordination by oxygen atoms. The modeling of the electronic structure of such atomic group shows that in a linear coordinated Co^{II} , U_{eff} may reach $300 - 500 \text{ cm}^{-1}$. The bending of the complex results in decreasing of U_{eff} , however the high U_{eff} values of $50 - 100 \text{ cm}^{-1}$ persist even at a considerable distortion. The difference in NSR and VSR centers' structure may be connected to a Co coordination peculiarities: a OCoO fragment may constitute a dioxocobaltate(II), oxo-peroxocobaltate(II), or oxo-hydroxocobaltate(II), taking into consideration that the corresponding ligands, O^{2-} , O_2^{2-} , OH^- may be present in the channel of the apatite lattice.

The work was supported by the Russian Science Foundation (RSF) under Grant 16-13-10031.

References

- 1) PE Kazin, MA Zykin, YV Zubavichus, OV Magdysyuk, RE Dinnebier, M Jansen - Chem. Eur. J. 20, 165 (2014)
- 2) PE Kazin, MA Zykin, W Schnelle, C Felser, M Jansen - Chem. Comm. 50, 9325 (2014)
- 3) PE Kazin, MA Zykin, W Schnelle, YV Zubavichus, KA Babeshkin, VA Tafeenko, C Felser, M Jansen - Inorg. Chem. 56, 1232 (2017)
- 4) PE Kazin, MA Zykin, LA Trusov, AA Eliseev, OV Magdysyuk, RE Dinnebier, RK Kremer, C Felser, M Jansen - Chem. Comm. 53, 5416 (2017)

Friday, June 16, 2017

Charge density wave, orbital order and superconductivity in 1T-TaS₂

T. Ritschel¹⁾, G. Garbarino²⁾, M. Hanfland²⁾, M. v. Zimmermann³⁾, H. Berger⁴⁾, B. Büchner^{1),5)}, and J. Geck¹⁾

¹⁾Institute for Solid State and Materials Physics, TU-Dresden, 01062 Dresden, Germany, ²⁾European Synchrotron Radiation Facility (ESRF) Grenoble, France, ³⁾Hamburger Synchrotronstrahlungslabor (HASYLAB) at Deutsches Elektronensynchrotron (DESY), Notkestr. 85, 22603 Hamburg, Germany, ⁴⁾Ecole Polytechnique Federale de Lausanne, Switzerland, ⁵⁾Leibniz Institute for Solid State and Materials Research IFW Dresden, Helmholtzstrasse 20, 01069 Dresden, Germany

*jochen.geck@tu-dresden.de

We present a combined x-ray diffraction, angle-resolved photoemission and density functional theory study of the electronic order in 1T-TaS₂. Our x-ray diffraction studies as a function of temperature and pressure prove that the charge density wave, which we characterize in terms of wave vector, amplitude, and the coherence length, indeed exists in the superconducting region of the phase diagram. The data further imply that the ordered charge density wave structure as a whole becomes superconducting at low temperatures, i.e., superconductivity and density waves coexist on a macroscopic scale in real space. This result is fundamentally different from a previously proposed separation of superconducting and insulating regions in real space and, instead, provides evidence that the superconducting and the charge density wave gap exist in separate regions of reciprocal space [1]. Furthermore, our density functional theory calculations shed new light onto the origin of the various gaps observed for 1T-TaS₂. Most importantly we find that the previous paradigm of a Mott-gap in this system needs to be reconsidered [2]. Instead we find firm evidence that the corresponding gap is due to the hybridization between the TaS₂-layers directly related to the orbital degrees of freedom. The latter is shown to have a dramatic effect on the band structure close to the Fermi level [3].

References:

- 1) T. Ritschel, J. Trinckauf, G. Garbarino, M. Hanfland, M.v. Zimmermann, H. Berger, B. Buechner, and J. Geck; Phys. Rev. B, 87, 125135 (2013).
- 2) B. Sipos, A. F. Kusmartseva, A. Akrap, H. Berger, L. Forró and E. Tuti, Nature Mat. 7, 960 - 965 (2008).
- 3) T. Ritschel, J. Trinckauf, K. Koepf, B. Büchner, M. v. Zimmermann, H. Berger, Y. I. Joe, P. Abbamonte, and J. Geck, Nat. Phys. 11, 328 (2015)

Friday, June 16, 2017

Gap opening in topological surface state

*L.V. Yashina¹⁾, J. Sánchez-Barriga²⁾, O. Rader²⁾

¹⁾Department of Chemistry, Lomonosov Moscow State University, Moscow, Russia ²⁾ Helmholtz-Zentrum Berlin fuer Materialien und Energie

*yashina@inorg.chem.msu.ru

Three-dimensional topological insulators (TIs) are characterized by spin-polarized Dirac-cone surface states that are protected from backscattering by time-reversal symmetry. Within the past few years, TIs have attracted a lot of interest due to their unique electronic structure with spin-polarized topological surface states (TSSs), which may pave the way for these materials to have a great potential in multiple applications. Magnetic doping is expected to open a band gap at the Dirac point of topological insulators by breaking time-reversal symmetry and to enable novel topological phases.

We study the effect of Fe impurities deposited on the surface of the topological insulators Bi_2Se_3 and Bi_2Te_3 by means of core-level and ARPES. We found that the topological surface state is tolerant against magnetic adsorbates. This indicates that topological insulators such as Bi_2Se_3 can be interfaced with a ferromagnet without losing the topological surface state and its unique quasirelativistic dispersion and Dirac point. In order to exhaust possible preparation conditions, room- and low temperature deposition have been compared. They lead to very different behavior, i.e., an opposite doping trend and different chemical environments, but they agree in the dispersion of the topological surface state and its gapless nature. The robustness is the precondition for the exploration and the successful functionalization of interfaces between topological insulators and ferromagnets. This will involve growing a perpendicularly magnetized ferromagnetic film on top of a topological insulator and monitoring the effect of the exchange coupling on the topological surface state underneath [1]. We characterize the atomically precise interface between the 3d transition metal Fe and the TI Bi_2Te_3 at different stages of its formation. Using photoelectron diffraction and holography, we show that after deposition of up to 3 monolayers Fe on Bi_2Te_3 at room temperature, the Fe atoms are ordered at the interface despite the surface disorder revealed by our scanning-tunneling microscopy images. We find that Fe occupies two different sites: a hollow adatom deeply relaxed into the Bi_2Te_3 quintuple layers and an interstitial atom between the third (Te) and fourth (Bi) atomic layers. We further show that upon deposition of Fe up to a thickness of 20 nm, the Fe atoms penetrate deeper into the bulk forming a 2-5 nm FeTe interface layer. In addition, excessive Bi is pushed down into the bulk of Bi_2Te_3 leading to the formation of septuple layers of Bi_3Te_4 within a distance of ~25 nm from the interface. Controlling the magnetic properties of the complex interface structures revealed by our work might turn out to be of critical importance when optimizing the efficiency of spin injection in TI-based devices.

Epitaxial $(\text{Bi}_{1-x}\text{Mn}_x)_2\text{Se}_3$ is a prototypical magnetic topological insulator with a pronounced surface band gap. We show that this gap is neither due to ferromagnetic order in the bulk or at the surface nor to the local magnetic moment of the Mn, making the system unsuitable for realizing the novel phases. We further show that Mn doping does not affect the inverted bulk band gap and the system remains topologically nontrivial. We suggest that strong resonant scattering processes cause the gap at the Dirac point and support this by the observation of in-gap states using resonant photoemission. Our findings establish a mechanism for gap opening in topological surface states which challenges the currently known conditions for topological protection [2].

We have studied quantum phase transition in the $(\text{Bi}_{1-x}\text{In}_x)_2\text{Se}_3$ series of compounds as a function of In composition at room temperature. ARPES data reveal that backscattering channels open up well-before the bulk band gap closes. This is evidenced by the progressive opening of a surface gap at the Dirac node of the TSS with increasing In doping. Our calculations based on the one step-model of photoemission in prototypical TIs reveal that bulk-surface coupling strongly influences the orbital nature of the surface state wave function, and thus the spin polarization of the TSS due to interaction with surface resonances (SR) appearing at the bulk-conduction band edges. The same coupling mechanism is expected to be even more pronounced across the quantum-phase transition.

References

- 1) M. R. Scholz, J. Sánchez-Barriga, D. Marchenko, A. Varykhalov, A. Volykhov, L. V. Yashina, and O. Rader - Physical Review Letters 108, 256810
- 2) J. Sánchez-Barriga, A. Varykhalov, G. Springholz, H. Steiner, R. Kirchschrager, G. Bauer, O. Caha, E. Schierle, E. Weschke, A.A. Unal, S. Valencia, M. Dunst, J. Braun, H. Ebert, J. Minar, E. Golias, L.V. Yashina, A. Ney, V. Holy, O. Rader - Nature Communications 7, 10559

Friday, June 16, 2017

Transport properties of spin-helical Dirac fermions in disordered quantum confined systems

*J. Dufouleur¹⁾, L. Veyrat^{1),3)}, H. Funke¹⁾, B. Dassonneville¹⁾, M. Xypakis²⁾, C. Nowka¹⁾, S. Hampel¹⁾, B. Buchner¹⁾, J. H. Bardarson²⁾ and R. Giraud^{1),4)}

¹⁾IFW Dresden, Helmholtzstraße 20, 01069-Dresden, Germany, ²⁾Max-Planck-Institut für Physik Komplexer Systeme, 01187 Dresden, Germany, ³⁾CNRS, Institut NEEL, F-38042 Grenoble, France, ⁴⁾INAC-SPINTEC, Univ. Grenoble Alpes/CNRS/CEA, 17 Avenue des Martyrs, 38054 Grenoble, France

* j.dufouleur@ifw-dresden.de

Quantum wires of 3D topological insulators offer a serious way to unveil the topological properties of the band structure and are promising systems for the search of robust signatures of topological conductivity and superconductivity in condensed matter. Due to the strong degree of disorder typical for such materials, disorder remains a key limitation for such systems and prevents the emergence of transport properties specific for spin-helical Dirac fermions.

Here, we reveal that the interaction between the static disorder and the quasi-particles of the 3D topological insulator surface states is considerably reduced due to the spin texture of the band structure by investigating the transconductance properties of a Bi₂Se₃ nanoribbon [1]. This result suggests that the ballistic or quasi-ballistic regime could be achieved in narrow structures of 3D topological insulator like nanowires [2,3]. Measurement in a Bi₂Te₃ nanoribbon show that due to this weak coupling of the surface states with the disorder, topological states are quantum confined whereas the massive particles of the bulk do not. This experimental result is supported by theoretical estimation of the transport length [4].

Following our experimental work, transport properties of 3D topological insulators quantum wires are theoretically investigated in the high energy regime usually considered experimentally. We show that the spin-helicity and the linear dispersion of the band structures leads to specific conductance and shot noise properties in this regime. Aharonov-Bohm oscillations and their topological properties are studied in details.

References

- 1) J. Dufouleur *et al.*, Nano Letters 16, 6733-6737 (2016)
- 2) J. Dufouleur *et al.*, Physical Review Letters 110, 186806 (2013)
- 3) J. Dufouleur *et al.*, Scientific Reports 7, Article number: 45276
- 4) J. Dufouleur *et al.*, in prepration

Friday, June 16, 2017

Ultrathin heterostructures based on quasi-2D CdSe and CdTe nanoplatelets: synthesis, structure and optical properties

*R.B.Vasiliev¹⁾²⁾, N.N.Shlenskaya¹⁾, E.P.Lazareva¹⁾, B.M.Saidjonov¹⁾, D.A.Karlova²⁾, A.V.Garshev¹⁾²⁾, A.I.Lebedev³⁾.

¹⁾Department of Materials Science, Lomonosov Moscow State University, Moscow, Russia ²⁾ Department of Chemistry, Lomonosov Moscow State University, Moscow, Russia ³⁾ Department of Physics, Lomonosov Moscow State University, Moscow, Russia

*romvas@inorg.chem.msu.ru

Colloidal quasi-2D nanoplatelets have been attracted considerable interest due to strong quantum confinement effects and electronic properties which are similar to those of epitaxial quantum wells [1-3]. Next step, heterojunction formation, allows to tune the electronic levels, and thus optical properties of semiconductor nanoplatelets using band engineering. To the best of our knowledge, the synthetic approaches for formation of quasi-two-dimensional heterostructures as well as their properties were not well documented yet. In present work CdSe and CdTe nanoplatelets and ultrathin CdSe/CdS and CdTe/CdS heterostructures based on them were prepared by colloidal method. Sizes, morphology, crystal structure and optical properties were analyzed.

Syntheses of CdSe and CdTe nanoplatelets were performed at 120-250°C under argon flow in presence of oleic acid as stabilizer. The quasi-two-dimension morphology is induced by the presence of acetate salt in the reaction medium. Heterostructures were synthesized by ligand exchange with sulphur-containing precursors in *n*-methylformamide at room temperature using phase-transfer method. To vary CdS layer thickness we used successive anionic and cationic layer deposition method.

We report on synthesis of different populations of CdSe and CdTe colloidal nanoplatelets with thicknesses of 1-2 nm and lateral sizes of 100-200 nm. High degree of structural perfection was confirmed by X-ray and electron diffraction studies and zinc-blende structure was found for CdSe and CdTe nanoplatelets as well as for CdSe/CdS and CdTe/CdS heterostructures. High uniformity of nanoplatelet thickness within one population causes extremely narrow peaks in absorption and luminescence spectra with positions fixed for each population. In the case of heterostructure formation we experimentally observed the red shift of absorption and luminescence bands proportionally CdS layer thickness. In the case of CdSe/CdS heterostructures we found strong increase of quantum yield of luminescence.

According TEM study CdSe nanoparticles formed scrolled nanoplatelets and CdTe nanoparticles were found as flat nanoplatelets (Fig.1). After CdSe/CdS heterostructure formation, initially scroll CdSe nanoplatelets unfolded due to thickness increase. However, in the case of CdTe/CdS heterostructures we surprisingly found that nanoplatelets folded in scroll-like structures.

We analyzed the absorption and photoluminescence excitation spectra of CdSe and CdTe nanoplatelets of different thickness and CdSe/CdS and CdTe/CdS heterostructures in the UV region and revealed pronounced and intensive thickness-dependent exciton bands in addition to exciton bands in the visible region. First-principles DFT calculations of the electronic structure and absorption spectra of NPLs shows that these high-energy bands result from transitions at the *X* and *M* points of the 2D Brillouin zone (BZ) of NPLs, which originate from *L* and *X* points of the BZ of bulk crystals. The observation of the UV exciton bands reveals tunable optical properties of cadmium chalcogenide nanoplatelets in UV spectral region, which may be interesting for practical applications.

References:

- 1) S Ithurria, MD Tessier, B Mahler, RPSM Lobo, B Dubertret, ALL Efros - Nat. Mater. 10, 936 (2011).
- 2) NN Shlenskaya, Y Yao, T Mano, T Kuroda, AV Garshev, VF Kozlovskii, AM Gaskov, RB Vasiliev, and K Sakoda - Chem. Mater. 29, 579 (2017).
- 3) RB Vasiliev, AI Lebedev, EP Lazareva, NN Shlenskaya, VB Zaytsev, AG Vitukhnovsky, Y Yao, K Sakoda - Phys. Rev. B 95, 165414 (2017).

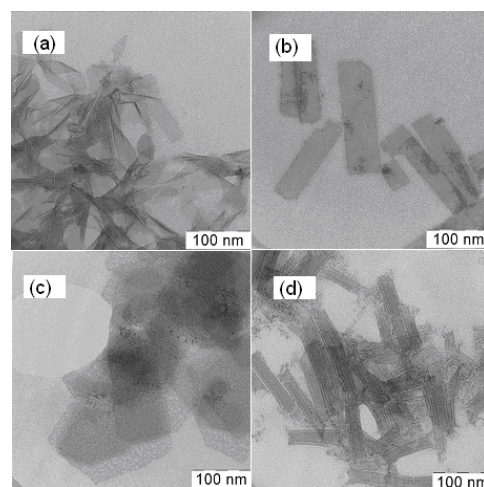


Fig. 1. TEM micrographs of (a) CdSe, (b) CdSe/CdS, (c) CdTe, and (d) CdTe/CdS nanoplatelets

Friday, June 16, 2017

Complex electronic order and time reversal symmetry breaking in Fe-based superconductors studied by nuclear probe spectroscopy

*H.-H. Klauss¹⁾, P. Materne¹⁾, V. Grinenko¹⁾, R. Sarkar¹⁾, S. Kamusella¹⁾, H. Luetkens²⁾, L. Harnagea⁴⁾, S. Wurmehl⁴⁾, B. Büchner⁴⁾, C. H. Lee³⁾, C. Timm⁵⁾, D. V. Efremov⁴⁾, S.-L. Drechsler⁴⁾

¹⁾Institute for Solid State and Materials Physics, TU Dresden, Dresden, Germany ²⁾Laboratory for Muon Spin Spectroscopy, PSI, Villigen, Switzerland ³⁾National Institute of Advanced Industrial Science and Technology (AIST), Tsukuba, Japan

⁴⁾Leibniz Institute for Solid State and Materials Research, Dresden, Germany ⁵⁾Institute for Theoretical Physics, TU Dresden, Dresden, Germany

*henning.klauss@tu-dresden.de

The interplay of itinerant magnetism, electronic nematic order and unconventional superconductivity in Fe based superconductors and other intermetallic systems with complex Fermi surfaces is a fascinating topic in contemporary correlated electron physics.

In my talk I will discuss Mössbauer spectroscopy and muon spin relaxation experiments on several series of hole doped 122 pnictides like $Ba_{1-x}K_xFe_2As_2$ 1,2) and $Ca_{1-x}Na_xFe_2As_2$. The parent compound $BaFe_2As_2$ shows a spin density wave order below $T_N = 165$ K 2). Our microscopic study proves that with increasing Na-substitution level, the magnetic order parameter as well as the magneto-structural phase transition is suppressed. For $x = 0.50$ we find a microscopic coexistence of magnetic and superconducting phases accompanied by a reduction of the magnetic order parameter below the superconducting transition temperature T_c . A systematic comparison with other 122 pnictides reveals a linear correlation between the magnetic order parameter reduction and the ratio of the transition temperatures, T_c/T_N , which can be understood in the framework of a Landau-theory 3). In the optimally doped specimen with $T_c \approx 34$ K, the temperature dependence of the penetration depth and superfluid density were obtained, which proves the presence of two superconducting s-wave gaps.

I will also discuss new evidence for time reversal symmetry breaking in strongly doped $Ba_{1-x}K_xFe_2As_2$ close to a Lifshitz transition at $x = 0.73$ 4). This was predicted e.g. to appear at the crossover between s and s+id superconducting pairing symmetry 5).

References:

- 1) E Wiesenmayer - Phys. Rev. Lett. 107, 237001 (2011)
- 2) T Goltz et al - Phys. Rev. B 89, 144511 (2014)
- 3) P. Materne et al. - Phys. Rev. B 92, 134511 (2015)
- 4) V. Grinenko et al. - arXiv:1705.00656 (2017)
- 5) C Platt et al. - Phys. Rev. B 85, 180502 (2012)

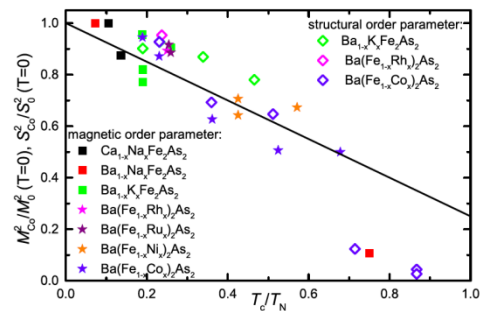


Fig. 1. Universal suppression of magnetic order parameter in 122 Fe based superconductors

Friday, June 16, 2017

Superconductivity vs bound state formation in a two band superconductor

*D. Efremov¹⁾, I. Eremin²⁾, A. Chubukov³⁾

¹⁾ IFW-Dresden, Institute for Solid State Research, D-01171 Dresden, Germany, ²⁾ Institut für Theoretische Physik III, Ruhr-Universität Bochum, D-44801 Bochum, Germany, ³⁾ Department of Physics, University of Minnesota, Minneapolis, Minnesota 55455, USA

*d.efremov@ifw-dresden.de

We discuss the interplay between superconductivity and formation of bound pairs of fermions (BCS-BEC crossover) in a 2D model of interacting fermions with small Fermi energy ϵ_F and a weak attractive interaction, which extends to energies well above ϵ_F . The 2D case is special because a two-particle bound state forms at arbitrary weak interaction, and already at weak coupling, one has to distinguish between the bound-state formation and superconductivity. We briefly review the situation in the one-band model and then consider two different two-band models: one with one hole band and one electron band and another with two hole or two electron bands. At $\epsilon_0/\epsilon_F \ll 1$, where ϵ_0 is the energy of the bound state of two particles in vacuum, the two models behave similarly. But in the opposite case they behave differently: in the model with two hole/two electron bands, the instability temperature of formation of Cooper pairs T_c $\sim \epsilon_0$, and the true superconducting critical temperature T_c^* $\sim \epsilon_0$, like in the one-band model. In between $\epsilon_0/\epsilon_F \sim 1$ and $\epsilon_0/\epsilon_F \gg 1$, the system displays a preformed pair behavior. In the model with one hole and one electron bands, T_c remains of order ϵ_0 , and both remain finite at $\epsilon_0/\epsilon_F \gg 1$ and of the order of ϵ_0 . The preformed pair behavior still does exist in this model because ϵ_0 is numerically smaller than ϵ_F . We apply our results for the model with a hole and an electron band to Fe pnictides and Fe chalcogenides in which a superconducting gap has been detected on the bands that do not cross the Fermi level, and to FeSe, in which the superconducting gap is comparable to the Fermi energy.

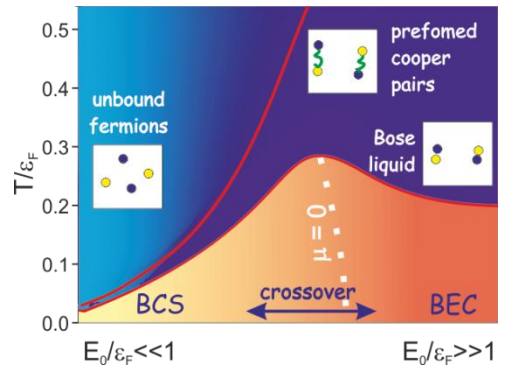


Fig. 1. Magnetization as a function of applied field.

References

1) Andrey V Chubukov, Ilya Eremin, Dmitri V. Efremov, Phys. Rev. B 93, 174516 (2016)



Friday, June 16, 2017

New spin gapped phase above the superconducting state in $\text{Na}_{1-x}\text{Li}_x\text{FeAs}$ single crystals

*S.H. Baek¹⁾, W.H. Nam²⁾, B. Lee²⁾, B. Buchner^{1),3)}, K.H. Kim²⁾

¹⁾IFW Dresden, Helmholtzstr. 20, 01069 Dresden, Germany

²⁾Department of Physics, Seoul National University, Seoul 151-747, Republic of Korea

³⁾Department of Physics, Technische Universität Dresden, 01062 Dresden, Germany

We present a nuclear magnetic resonance (NMR) study of the Li-doped NaFeAs single crystals. The successful incorporation of Li into the parent NaFeAs is evidenced by the progressive evolution of the ^{75}As NMR spectra as a function of doping x . Our NMR data show that the local static and dynamic properties of the system drastically change through a critical doping $x_c \sim 0.03$ above which long-range spin-density-wave (SDW) order disappears and, at the same time, bulk superconductivity emerges abruptly. Strikingly, despite the absence of static moments at $x > x_c$, the spin-lattice relaxation data reveal a clear phase transition occurring at a characteristic temperature T_0 just above the superconducting transition temperature T_c . Based on the fact that the spin excitation spectrum is gapped without involving static magnetism at T_0 , we propose that a charge-density-wave (CDW) instability drives the phase transition at T_0 .

Friday, June 16, 2017

Soliton states in a three-band superconductor with broken time-reversal symmetry

Y. Yerin¹⁾²⁾

¹⁾The Institute for Physics of Microstructures, Nizhny Novgorod, Russia ²⁾B.Verkin Institute for Low Temperature Physics and Engineering

yerin@ipmras.ru

Owing to the emergence of additional degrees of freedom of the order parameter, the nomenclature of topological objects in multiband superconductors is much richer than that in conventional single-band superconductors. Ginzburg-Landau theory describing multiband superconductivity in bulk samples admit topologically stable solutions that can be interpreted as vortices carrying fractional magnetic flux. In the presence of Josephson-type interband coupling, multi-band superconductors generate static solitons of the sine-Gordon type [1,2 and references therein].

Solitons of the interband phase difference can exist by themselves in doubly-connected mesoscopic samples, when the formation of any magnetic vortices in the volume of the superconductor is prohibited energetically. Moreover, soliton states in this case can be induced by an externally applied magnetic field, which makes them a convenient object of the investigation.

Based on the Ginzburg-Landau phenomenological approach, we investigate soliton states in a three-band superconductor with broken time-reversal symmetry (BTRS). In comparison with other similar theoretical studies we consider the creation and characteristics of these solitons induced by external magnetic field for mesoscopic doubly-connected geometry (thin-walled cylinder) of a three-band superconducting system, which corresponds to the real experimental situation.

We demonstrate that due to the degeneration of energy minima of a BTRS three-band superconductor there are different types of solitons. Calculations of the Gibbs free energy of the system show that soliton states in a three-band superconductor with BTRS are thermodynamically metastable and cannot be the ground state for such geometry (fig. 1).

References

- 1) Shi-Zeng Lin, J. Phys.: Condens. Matter 26, 493202 (2014).
- 2) Y. Tanaka, Supercond. Sci. Technol. 28, 034002 (2015).

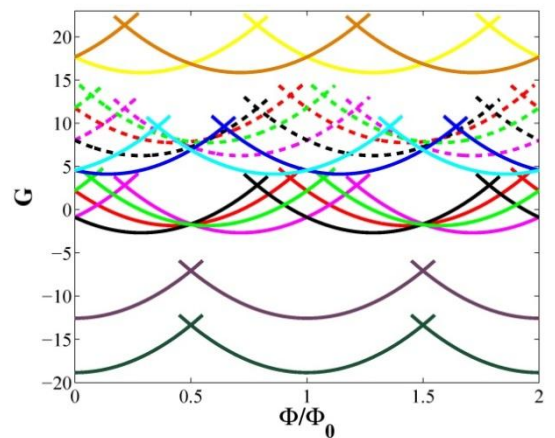


Fig. 1. Gibbs free energy of BTRS ground state (dark green), non-BTRS state (dark purple) and different topological states (N_1, n_2, n_3) for typical ratios of the effective masses $k_2 = 4, k_3 = 2$. Here red (solid and dashed) lines denote topological state with $(N_1, 1, 0)$, magenta (solid and dashed) – $(N_1, 0, 1)$, blue – $(N_1, 1, 1)$, yellow – $(N_1, -1, 1)$, brown – $(N_1, 1, -1)$, cyan – $(N_1, -1, -1)$, black (solid and dashed) – $(N_1, 0, -1)$ and green (solid and dashed) – $(N_1, -1, 0)$.

Poster session



MSU-IFW-ILTPE
Joint Workshop



VolkswagenStiftung

| | | | |
|------------|------------------|------------|------------------|
| <i>P1</i> | M.N. Andreev | <i>P18</i> | E. Kuznetsova |
| <i>P2</i> | S. Bubenov | <i>P19</i> | M.A. Lizunova |
| <i>P3</i> | V. Chepikov | <i>P20</i> | A. Merkulova |
| <i>P4</i> | G. Chernysheva | <i>P21</i> | K.V. Mitsen |
| <i>P5</i> | D. Davydova | <i>P22</i> | E. M. Paerschke |
| <i>P6</i> | E.R. Fatula | <i>P23</i> | A. Pavlov |
| <i>P7</i> | A.A. Fedorova | <i>P24</i> | B. R. Piening |
| <i>P8</i> | R. Gashigullin | <i>P25</i> | I. V. Plokhikh |
| <i>P9</i> | A.A. Gippius | <i>P26</i> | N. Ryzhkov |
| <i>P10</i> | V.E. Goncharenko | <i>P27</i> | G. Shipunov |
| <i>P11</i> | R. Kappenberger | <i>P28</i> | A.E. Sleptsova |
| <i>P12</i> | V. Khudoleeva | <i>P29</i> | A.V.Troitskii |
| <i>P13</i> | Yu.V. Kislinskii | <i>P30</i> | M.D.Tsymlyakov |
| <i>P14</i> | E.S. Klimashina | <i>P31</i> | V. Utochnikova |
| <i>P15</i> | N.N.Kononov | <i>P32</i> | V.V. Utochnikova |
| <i>P16</i> | I.Korsakov | <i>P33</i> | V.V. Utochnikova |
| <i>P17</i> | P.A. Kotin | <i>P34</i> | S.V. Zhurenko |

Thursday, June 15, 2017

P1

The microstructure and optical properties of the Licurgus cup glass

*M.N. Andreev¹⁾, S.O. Klimonsky²⁾, D.I. Petukhov¹⁾, S.I. Bezzubov¹⁾, B.A. Abdusatorov²⁾, D.V. Kuznetsov¹⁾, A.A. Drozdov¹⁾, V.K. Karandashev³⁾

¹⁾Department of Chemistry, Lomonosov Moscow State University, Moscow, Russia; ²⁾Department of Materials Science, Lomonosov Moscow State University, Moscow, Russia; ³⁾Institute of Microelectronics Technology and High-Purity Materials, Chernogolovka, Russia

*maksandreev@inbox.ru

Licurgus cup probably made in Alexandria in the IVth century is one of the most prominent artifacts of the Roman glass. It is a diatreta cut from an elaborately pressed blank of typical NCS glass with a low magnesium and potassium content. The glass is dichroic, appearing jade green in reflected daylight and wine red in transmitted light. The dichroism of the Licurgus cup glass is usually derived from the presence of mixed Ag-Au nanoparticles (AuAgNPs). To study the optical properties of Licurgus cup the glass was prepared starting from the batch calculated using the glass composition published [1]. The glass was molten at 1500°C in alundum crucible in an electric furnace with MoSi₂ heating elements. The melt was poured and quenched into 7-10 mm thick disks with further annealing in a muffle furnace. The material obtained is a transparent green glass without visible dichroism and phase separation. The colour is caused by the Fe(+2) and Fe(+3) ions in its composition (total Fe content 1,14%, ICP MS). During striking initially at 550 - 560°C the glass at first changes colour to yellowish-green and then becomes dichroic and semiopaque. It is well-known that gold and silver nanoparticles exhibit unusual optical properties such as resonant absorption and scattering of light. This fact was used to explain the unique dichroic character of the Licurgus cup glass. However, this contradicts the fact that the gold ruby glass also containing gold particles of similar form and size is not dichroic, being pink-rose in both transmitted and reflected light. The reason for the Licurgus glass to be dichroic derives from its microstructure. As it was shown in [1] and confirmed by our studies, during striking the process of secondary phase separation occurs. The resulted multiphase structure (Fig. 1) consists of discrete pseudo-spherical particles of phosphate glass in a continuous silicate matrix. The prolonged heat-treatment of the sample results in devitrification of a phosphate phase that crystallizes giving ferric-sodium ortho-diphosphate Na₇(FeP₂O₄)₄PO₄ (P-42(1)c, confirmed XRD). This fact proves the importance of iron as a glass micro component. The experiments to obtain dichroic glass starting from glass batch free of iron failed. The iron-free glass of the same composition as glass of Licurgus cup during striking becomes yellowish-red due to the presence of AuAgNP. The light reflection under different angles was studied. At small glancing angles (large angles of incidence) the penetration depth of light diminishes. The number of AuAgNPs that absorb light declines but the light scattering on the surfaces of iron-phosphate glass droplets enhances. Both AuAgNPs and phosphate glass reflect green light but the amount of light scattered by the former is negligible with respect to that of the latter. To summarize, the red colour of the Licurgus cup glass in transmitted light is due to the light absorption of AuAgNPs while the green colour in reflected light is caused by scattering on sodium-iron-phosphate glass droplets.

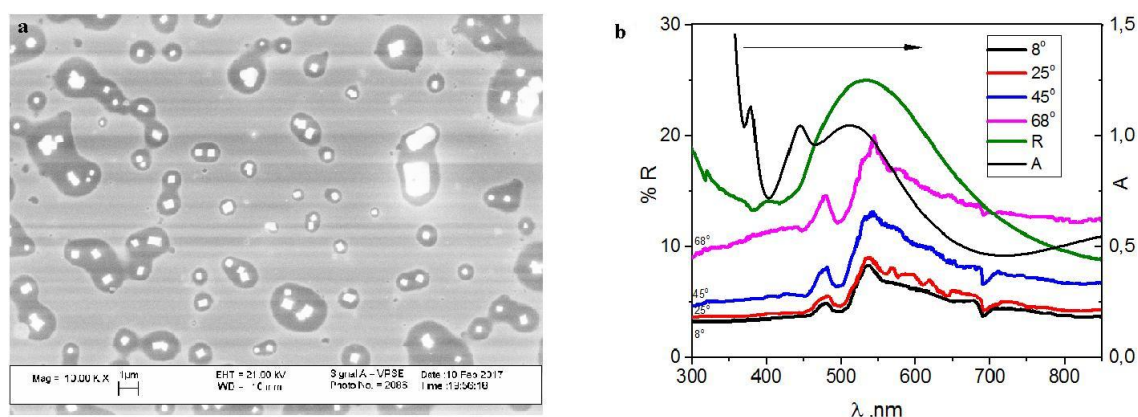


Fig.1. (a) The microstructure of the Licurgus cup glass after prolonged heating (SEM image), (b) Optical absorption (A), reflection spectra of the Licurgus cup glass under different angles (°) of incidence and diffuse reflection (R) spectrum

References:

1) D.J. Barber, I.C. Freestone - *Archeometry*. 32, 33 (1990)

Thursday, June 15, 2017

P2

Diffusion doping route to plasmonic silicon nanocrystals

*S. Bubenov¹⁾, S. Dorofeev¹⁾, N. Kononov²⁾, N. Mordvinova¹⁾³⁾, T. Kuznetsova¹⁾

¹⁾Department of Chemistry, Lomonosov Moscow State University, Moscow, Russia ²⁾A.M. Prokhorov General Physics Institute

³⁾Laboratoire CRISMAT, UMR6508, CNRS-ENSICAEN

*s.bubenov@gmail.com

Semiconductor nanocrystals are a valuable asset for the design of materials and devices, as their electronic structure can be tailored by control of the size and shape composition as well as by intrinsic and extrinsic doping. Specifically, semiconductor nanocrystals may greatly facilitate integration of plasmonics and electronics, as they exhibit localized surface plasmon resonance (LSPR) band in the near-IR region, the position of the band being a function of carrier concentration. Silicon is an abundant and non-toxic material with a variety of surface passivation options: native oxide, silicon nitride, silicon carbide, numerous organic groups. Doping of silicon nanocrystals has been realized via different methods, however, phosphorus doping has so far been associated with impurity segregation at surface and low activation efficiency.

Here we report on oxide shell -mediated diffusion doping of silicon nanocrystals with boron and phosphorus. Diborane and phosphorus were employed as gaseous precursors of the impurities. The syntheses proceeded at 900°C so as to avoid sintering, the annealing time was estimated from diffusivity of the studied impurities in bulk silicon. The obtained nanocrystals are plasmonic when doping level exceeds ~0.1% at., as evidenced by IR absorption studies (Fig.1). The concentration of free carriers obtained from the position of LSPR coincides well with the impurity content in nanocrystalline cores (Fig.2). This indicates high impurity activation efficiency of ~1 for phosphorus and 0.3-0.5 for boron. The radial distribution of dopants was studied during a step-etch process and was found to be rather uniform. The diffusion doping proves to be a prospective way to introduce boron and phosphorus in silicon nanocrystals, potentially hindered only by the solubility of impurities at nanoscale.

This work was supported by Russian Foundation of Basic Research (project no. 17-03-01269).

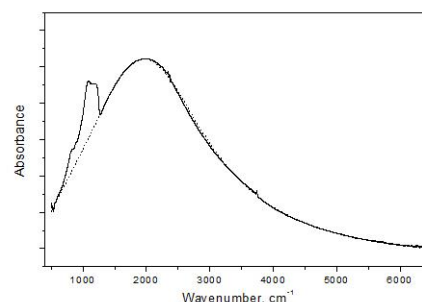


Fig.1. IR-spectrum of P-doped silicon nanocrystals with doping level ~0.2%; dashed line shows a fit under assumption of Drude-like behaviour.

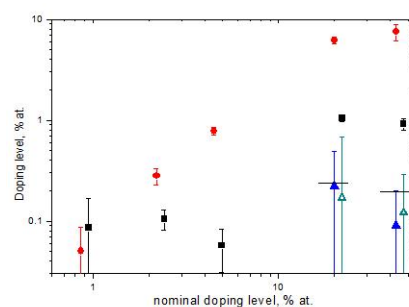


Fig.2. Doping level in the samples: ● - as-produced powders, ■ - aqueous zols, ▲ - after 1 step of HF etch, △ - after 2 steps of HF etch; some points are slightly shifted so as to avoid superimposition of error bars; solid horizontal lines indicate doping levels calculated from LSPR under assumption of activation efficiency of 1.



Thursday, June 15, 2017

P3

High rate PLD and superconducting properties of 2G coated conductors with artificial pinning centers

A. Kaul^{1,2)}, A. Molodyk²⁾, P. Degtyarenko²⁾, S. Lee³⁾, S. Samoilenkov²⁾, *V. Chepikov^{1,2)}, V. Petrykin³⁾

¹⁾Department of Chemistry, Lomonosov Moscow State University, Moscow, Russia ²⁾SuperOx LLC, Moscow, Russia

³⁾SuperOx-Japan LLC, Tokyo, Japan

*sev1990@yandex.ru

An industrial R&D program is ongoing at SuperOx, aimed at improving 2G HTS wire performance in magnetic field. We introduce perovskite artificial pinning centers into the HTS layer matrix. In contrast to most studies described in the literature, we use the high rate production processing parameters and PLD equipment at SuperOx Japan. This paper reports the results of Phase 1 of this program. We fabricated 2G HTS wires using GdBCO PLD targets with 0-7% (wt.) BaZrO₃ or BaSnO₃ at 100, 150 and 200 Hz frequency. The crystal structure and texture parameters of the HTS layer and perovskite inclusions were characterized with XRD. The HTS layer microstructure and morphology were studied with TEM. The angular dependencies of the critical current of the samples were measured by 4-probe transport technique at 77 and 65 K in 1 T magnetic field and derived from magnetic hysteresis curves measured in PPMS in the 4.2-77 K temperature range and 0-9 T magnetic field range. BaZrO₃ and BaSnO₃ formed column-shaped semi-coherent nano-inclusions in the GdBCO film matrix. The typical transverse size of the nano-columns was about 5 nm, and their volume density correlated with the dopant concentration. All doped samples exhibited much lower angular anisotropy of in-field critical current and higher lift factors than non-doped samples. Doped samples demonstrated higher minimum critical current or all field orientations than non-doped samples at 65 K and at lower temperatures. These results are an encouraging start of our program, as they show a positive impact of artificial pinning centers introduced into 2G HTS wires fabricated at production throughput. Future work will be focused on the optimization of PLD growth parameters, in order to maximize the improvements in specific temperature and field conditions, as well as on the verification of reproducibility of the improvements in production wires.

Thursday, June 15, 2017

P4

Optical properties of Ag-doped InP quantum dots prepared by phosphine synthetic route*G. Chernysheva¹⁾, A. Vinokurov¹⁾, N. Mordvinova¹⁾²⁾, S. Dorofeev¹⁾.¹⁾Department of Chemistry, Lomonosov Moscow State University, Moscow, Russia ²⁾Laboratoire CRISMAT UMR6508 CNRS-ENSICAEN-Normandie Université, 14050 Caen, France*chgala@yandex.ru

Quantum dots (QDs) – nano-sized particles, based on semiconductors, which sizes are less than double Bohr radius. This limit leads to quantum-size effects: optical properties of QDs directly depend on QD's sizes and magnitude of band gap (E_g). Among the QDs based on III–V materials InP colloidal QDs have gained the attention due to their stability, low toxicity and the intensive luminescence in the visible and near-IR spectral regions. Recently developed approach to producing InP-based QDs by using phosphine (PH_3) as a source of phosphorus and indium carboxylates as a source of indium with various carbonic acids as surfactants in nonpolar solvents is the simplest nowadays and leads to relatively narrow particle size distributions, high crystallinity of the nanoparticles and the temporal stability of the optical properties. Nanoparticle's doping results in changing of their optical properties. The aim of this work was to dope InP QDs with silver and to determine its effect on nanoparticles optical properties.

It was established, that silver dopes InP QDs and gives new energy levels in the band gap. This process leads to the appearance of luminescence locating approximate to 800 nm. Inverse relationship between the magnitude of excitonic peak intensity and quantity of introduced admixture was identified (fig. 1). It was determined, that increasing of introduced silver quantity relative to the basic component (In) up to 5% results in excitonic luminescence extinction, while further increasing of this magnitude up to 20% results in complete extinction of luminescence in visible and IR-area.

In the case of the sample, doped by 0,5% of silver, it was established, that each subsequent fraction of InP QDs contains smaller particles, while real quantity of silver is decreasing. That fact may be explained by competition of bigger radical of oleic acid and silver for the potential location on the surface of nanocrystal.

Investigation of samples with various silver concentration by TEM showed, that silver quantity increasing gives rise to nanoparticles size decreasing. It may be accounted for the presence of more centers of crystallization in the samples, synthesized with more quantity of silver.

This work was supported by Russian Foundation for Basic Research Grant No. 16-33-00074 mol-a.

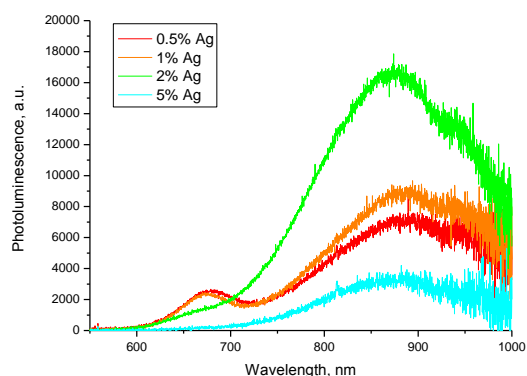


Fig. 1. Concentration dependency of photoluminescence of Ag-doped InP QDs.

Thursday, June 15, 2017

P5

Low-density nanosilicon films deposited from sols

*D. Davydova¹⁾, S. Dorofeev²⁾, N. Kononov³⁾, S. Bubenov²⁾

¹⁾ Faculty of Materials Science, Lomonosov Moscow State University, Moscow, Russia ²⁾ Department of Chemistry, Lomonosov Moscow State University, Moscow, Russia ³⁾ Institute of General Physics. A.M. Prokhorov, Moscow, Russia
*darya.davydova.94@mail.ru

The ability to easily obtain complex patterns of semiconductor material by inkjet printing using nanoparticle sols opens up wide prospects for the use of nanosilicon (nc-Si). The disadvantage of nc-Si films obtained from sols is their low conductivity. There are several reasons for the low conductivity of nc-Si films: low concentration of free carriers in nanoparticles, Coulomb blockade, low density of films, traps on the surface of nanoparticles, barriers on the boundaries between Si nanoparticles.

The purpose of the study is to determine the density of films obtained by different methods from the nc-Si sols for further investigation of the influence of film density on their transport properties.

In our work we used nc-Si, obtained by laser pyrolysis of silane. Sol was prepared by sonication of nc-Si powder in ethanol. From the nc-Si sol, films on glass substrates were prepared by the following methods: drop-casting, ultrasonic assisted drop-casting, spin-coating, deposition of the nc-Si on a substrate in a centrifugal field. The thickness of the films was determined by step-profilometry, and SEM, the surface density of the nc-Si in the films was determined by spectrophotometry. From the data obtained, the bulk density of the films was calculated.

The resulting films have a density of 2-10 times less than theoretically possible for the closest packing of spheres of silicon (fig.1). Step-profilometry gives a film thickness that is underestimated by a factor of 1.3-3 as compared to the SEM data. A thin layer of titanium was deposited on top of the film to obtain correct data by step-profilometry. The image of the cleavage of such structures is shown in figure 2.

This work was supported by Russian Foundation for Basic Research grant № 17-03-01269.

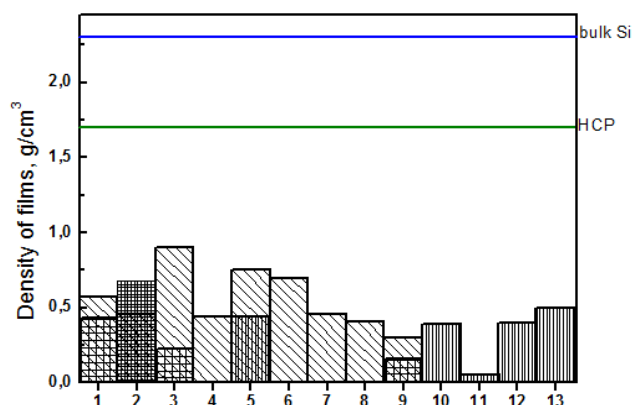


Fig. 1. Dependence of the density of films on the method of their production.

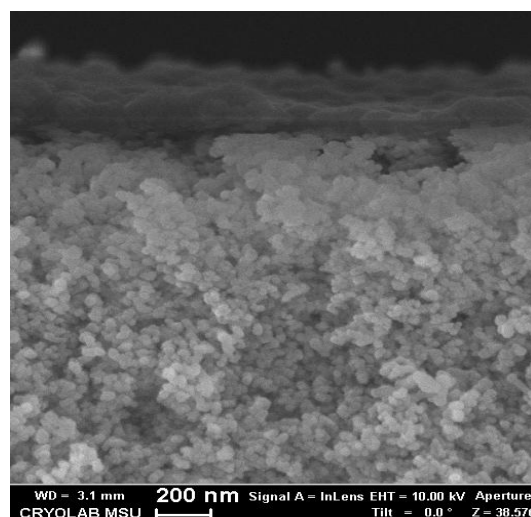


Fig. 2. The silicon film cleavage SEM image.

Thursday, June 15, 2017

P6

The synthesis of MF_2 ($\text{M} = \text{Mg}, \text{Ca}, \text{Sr}, \text{Ba}$) and solid solutions $\text{M}_{1-x}\text{Yb}_x\text{F}_{2+x}$ ($\text{M} = \text{Ca}, \text{Sr}, \text{Ba}$) using beta-cyclodextrin

A.A. Fedorova, *E.R. Fatula, Morozov I.V.

Department of Chemistry, Lomonosov Moscow State University, Moscow, Russia

*uji-f@yandex.ru

In this work a new synthetic approach to obtaining metal fluorides MF_2 ($\text{M} = \text{Ca}, \text{Sr}, \text{Ba}$) and fluorite-type solid solutions $\text{M}_{1-x}\text{Yb}_x\text{F}_{2+x}$ ($\text{M} = \text{Ca}, \text{Sr}, \text{Ba}$) with beta-cyclodextrin is proposed. The synthesis was carried out by thermal decomposition of the metal trifluoroacetate hydrates with beta-cyclodextrin. This method has some important advantages: the simplicity of the process and low synthesis temperature.

The preparation of simple metal fluorides MF_2 ($\text{M} = \text{Mg}, \text{Ca}, \text{Sr}, \text{Ba}$) shows that the addition of beta-cyclodextrin into the reaction mixture leads to the formation of high dispersive metal fluorides [1] that have relatively large surface area (Fig. 1). This fact opens the opportunities to use these materials as catalysts or the supports for catalysts. Also it is interesting to mention that there is a specific content of beta-cyclodextrin in the reaction mixture and its value is various for different metal fluorides. The optimal conditions for obtaining pure samples for each metal fluoride with the large surface area are given in the study.

Also it was shown that the use of beta-cyclodextrin is very effective for the preparation of fluorite-type solid solutions $\text{M}_{1-x}\text{Yb}_x\text{F}_{2+x}$ ($\text{M} = \text{Ca}, \text{Sr}, \text{Ba}$) [2]. It should be emphasized that the decomposition of the metal trifluoroacetates hydrates without beta-cyclodextrin does not lead to the formation of these solid solutions. Moreover, the increase of the synthesis temperature or the synthesis time does not result in obtaining these substances if the reaction mixture does not contain beta-cyclodextrin. However, the using of beta-cyclodextrin allows to obtain pure fluorite-type solid solutions with homogeneous distribution of elements under mild temperature conditions.

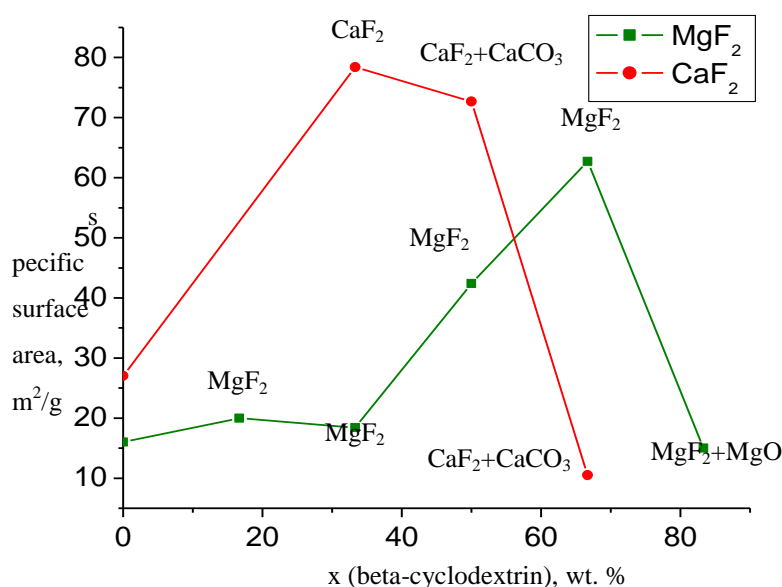


Fig. 1. The specific surface area of MF_2 ($\text{M} = \text{Mg}, \text{Ca}$) obtained with different amount of beta-cyclodextrin.

The authors acknowledge partial support from Lomonosov Moscow State University Program of Development.

References:

- 1) Arkhipenko S.Yu, Fedorova A.A., Morozov I.V., Shaporev A.S. - Mendeleev Communications. 22, 25 (2012)
- 2) A.A. Fedorova, S.Yu. Arkhipenko, E.R. Fatula, N.P. Chikov, N.M. Sorokina, I.V. Morozov. - Procedia Chemistry. 11, 20 (2014)

Thursday, June 15, 2017

P7

Synthesis of NaLuF_4 via thermal decomposition of precursors using β -cyclodextrin

* N.R. Yarenikov, A.A. Fedorova, I.V. Morozov

Department of Chemistry, Lomonosov Moscow State University, Moscow, Russia

*kit-yar@mail.ru

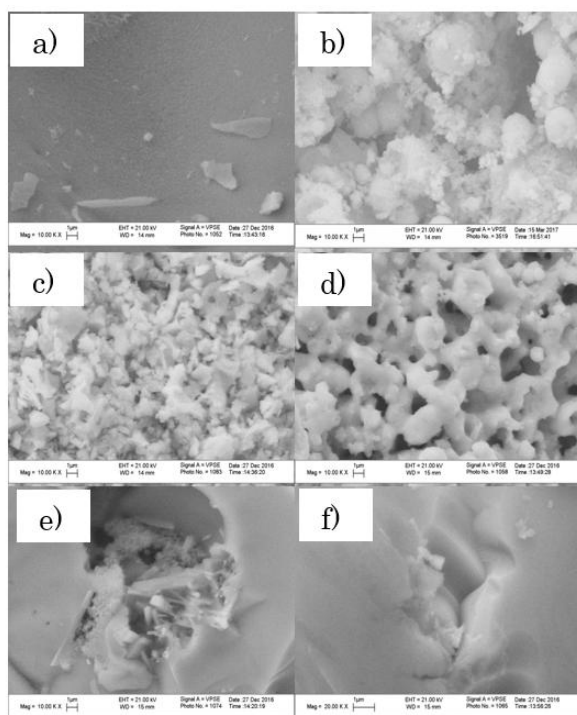


Fig. 1. The temperature's influence on the morphology of products of decomposition at a) 400°C with addition of β -cyclodextrin, b) 400°C, c) 600°C with addition of β -cyclodextrin, d) 600°C, e) 700°C with addition of β -cyclodextrin, f) 700°C.

After analyzing the morphology of substances using SEM it was found that the addition of β -cyclodextrin influences on the shape of the particles of substances obtained. Samples prepared without β -cyclodextrin consist of particles with roundish shape. At the same time samples synthesized with an addition of β -cyclodextrin have particles with more angulate form. The increase of the calcination temperature from 400 to 700°C leads to decreasing the difference between samples prepared with and without addition of β -cyclodextrin (Fig. 1). At the same time the increasing time of calcination at temperature 400°C does not leads to significant changes in samples morphology (Fig. 2) although this leads to change of samples phase composition according XRD data.

References:

1) B.P. Sobolev. The Rare Earth Trifluorides. Part 1. Institut d'Estudis Catalans. Barcelona. 520 p. (2000)

Samples of NaLuF_4 were synthesized via thermal decomposition of lutecium trifluoroacetate hydrate and sodium trifluoroacetate with and without an addition of β -cyclodextrin. Heating was carried out in 5 different modes (2, 25, 170 hours at the temperature of 400°C, 2 hours at the temperature of 600°C and 2 hours at the temperature of 700°C).

At the temperature of 400°C products contained low-temperature hexagonal phase with some impurities of cubic phase were obtained. However the increase of calcination time leads to formation monophasic samples of low-temperature hexagonal phase both for samples prepared with and without an addition of β -cyclodextrin.

At the temperature of 600°C pure high-temperature hexagonal phase was obtained.

When the temperature rises up to 700°C products obtained contain cubic phase with small amount of low-temperature hexagonal phase. By calcination time increase products contained almost pure cubic phase of NaLuF_4 were obtained.

All these results are in agreement with the stability of different crystal modifications of NaLuF_4 [1].

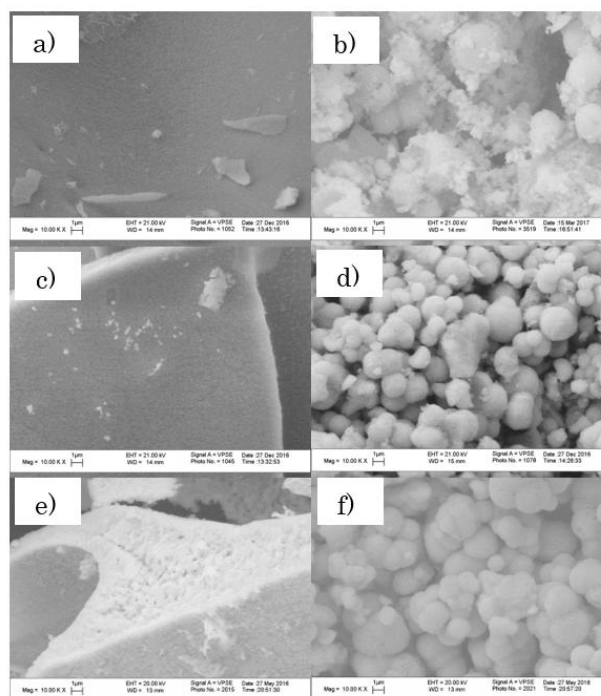


Fig. 2. The time's influence on the morphology of products of decomposition at the temperature of 400°C: a) 2 hours with addition of β -cyclodextrin, b) 2 hours, c) 25 hours with addition of β -cyclodextrin, d) 25 hours, e) 170 hours with addition of β -cyclodextrin, f) 170 hours.

Thursday, June 15, 2017

P8

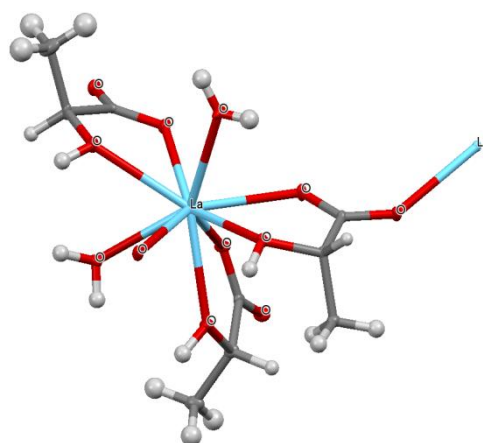
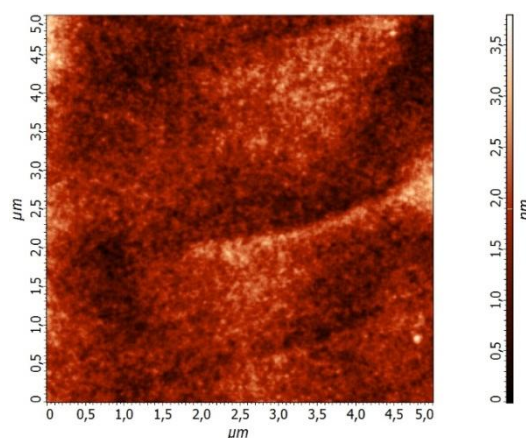
Chemical solution deposition of rare earth and transition metal oxide thin filmsR. Gashigullin¹⁾, M. Kendin¹⁾, V. Shegolev²⁾, I. Martynova²⁾,* D.Tsybarenko²⁾, N. Kuzmina²⁾¹⁾ Department of Material Science, Lomonosov Moscow State University, Moscow, Russia ²⁾ Department of Chemistry, Lomonosov Moscow State University, Moscow, Russia*tsybarenko@gmail.com

Currently, the application of many kinds of emergent functional materials (e.g. superconductors, topological insulators, MIT layers, high-K materials, etc.) in a form of thin films is of high interest due to large surface area, unique chemical and physical properties and economic reasons. The development of simple, cost effective, easy scalable and universal technique of thin films production remains an important task for material sciences. Nowadays the Metal-Organic Chemical Solution Deposition (MOCSD) technique seems to be one of the most perspective, scalable and flexible method for deposition of functional material thin films. MOCSD allows easy and precise control of thin film stoichiometry that is especially important for complex oxides materials, but it requires the initial precursor solutions.

Here, we proposed the metal carboxylates (lactates, pivalates, isovalerates) as initial compounds for MOCSD, because of their low cost, environmental safety and the ability to form strong complexes with cations of heavy metals. We developed synthesis and studied structure, solubility and thermal behavior of the aforementioned compounds of Al, Y, La, Ce-Lu, as well as Mn, Fe and Ni lactates and Zr acetylacetonate. In crystalline state rare-earth iso-valerates were found to be isolated molecules, pivalates had 1D polymeric chain structure and lactates had both bi-nuclear and polymeric structure (fig.1). Designed compounds demonstrated limited solubility in organic solvents that was increased by formation of mixed ligand complexes with ancillary N-donor ligands – monoethanolamine (mea) and diethylenetriamine (deta). Molecular structure and thermal stability of carboxylates and mixed ligand complexes were studied by DFT calculations, XRD and mass spectrometry. As a result clear solutions with concentration as high as 0.3M and proper viscosity of 2-5 mPa·s were prepared. Solution precursors were used for MOCSD preparation of La₂O₃, Y₂O₃, Al₂O₃, ZrO₂ thin films on single crystalline and long length metallic substrates. Obtained films had good homogeneity and smooth surface with average roughness lower 0.8 nm (fig. 2).

Compatibility of these solutions in different bi- and three-component combinations was studied. This allowed us to prepare the thin films of complex oxide materials LaAlO₃, LaNiO₃, LaMnO₃, LuFeO₃.

This work was partially supported by Russian Foundation for Basic Research (11-03-01208). Theoretical calculations were performed using facilities of the Supercomputer Center of the Moscow State University.

Fig. 1. Structure of [La(lact)₃(H₂O)₂]_{inf}.Fig. 2. AFM of La₂O₃ thin film.

Thursday, June 15, 2017

P9

Ab-initio calculations and Ga NQR spectroscopy of intermetallic system $\text{Cr}_{1-x}\text{Mn}_x\text{Ga}_4$

*A.A. Gippius¹⁾²⁾, S.V. Zhurenko¹⁾, K.S. Okhotnikov¹⁾, V.Yu. Verchenko³⁾, A.V. Shevelkov³⁾

¹⁾Department of Physics, Lomonosov Moscow State University, Moscow, Russia ²⁾Shubnikov Institute of Crystallography, Moscow, Russia ³⁾Department of Chemistry, Lomonosov Moscow State University, Moscow, Russia (10 point)

*gippius@mail.ru

Intermetallic compounds with the cubic crystal structure of the PtHg_4 type reveal very different ground state properties depending on their chemical content. While solid solution $\text{Cr}_{1-x}\text{Mn}_x\text{Ga}_4$ ($0 \leq x \leq 0.18$) possesses weakly temperature-dependent properties: diamagnetic response and bad metallic behavior, binary MnGa_4 exhibits typical metallic properties and is ordered antiferromagnetically already at room temperature.

In this work we report on the ^{69}Ga NQR spectroscopy study of intermetallic system $\text{Cr}_{1-x}\text{Mn}_x\text{Ga}_4$ with $x = 0$ and 0.15 based on *ab-initio* calculations of electronic density spatial distribution [1].

NQR experiments on $^{69,71}\text{Ga}$ nuclei were performed using phase-coherent pulsed NQR spectrometer by means of frequency step spin echo technique at 4.2 K. Experimental ^{69}Ga NQR spectra of CrGa_4 and $\text{Cr}_{0.85}\text{Mn}_{0.15}\text{Ga}_4$ measured at 4.2 K are shown in Fig.1. Surprisingly, ^{69}Ga spectrum in CrGa_4 demonstrates complex satellite structure indicating deviation of the local Ga symmetry from stoichiometric cubic one. A possible reason might be either Cr shift from (0,0,0) position caused by removing of the orbital degeneracy similar to the Jahn-Teller distortion or an anti-site effect. Our *ab-initio* calculations show that the non-correlated shift of the Cr atoms is unable to explain satisfactory the observed structure of the Ga NQR spectrum in CrGa_4 .

Substitution of 15% Mn for Cr seems to suppress this non-stoichiometric effect. The observed ^{69}Ga NQR spectra of $\text{Cr}_{0.85}\text{Mn}_{0.15}\text{Ga}_4$ (Fig.1) is discussed in terms of M–Ga–M (M = Cr, Mn) dumbbells formation in the first coordination sphere of Ga atom.

This work was supported by the joint Russian-Taiwan Grant RFBR-MOST № 16-53-52012-a.

References

1)P Blaha et al., WIEN2k, TU Wien, Austria, 2001.

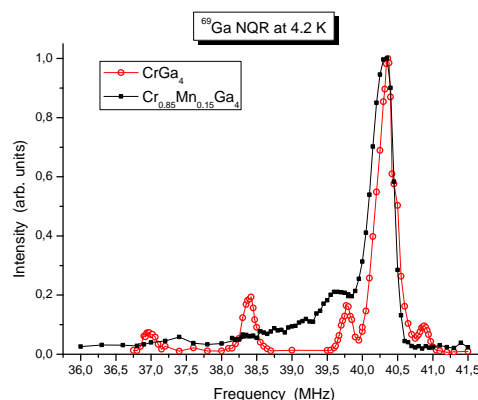


Fig.1. Experimental ^{69}Ga NQR spectra of CrGa_4 and $\text{Cr}_{0.85}\text{Mn}_{0.15}\text{Ga}_4$ measured at 4.2 K.

Thursday, June 15, 2017

P10

Solvothermal synthesis of nanocrystalline titanium dioxide with high surface area

A.M. Lunyov¹⁾, Yu.A. Belousov*¹⁾, V.E. Goncharenko¹⁾, V.D. Dolzhenko¹⁾

¹⁾Department of Chemistry, Lomonosov Moscow State University, Moscow, Russia

*belousov@gmail.com

Nanocrystalline titanium dioxide is a wide-band semiconductor, possesses high sorption activity and chemical stability. These properties ensure its broad use as a semiconductor and photocatalyst. Modern methods of synthesis allow to obtain products of different morphology from nanocrystals to nanotubes and mesoporous spheres.

High surface area titanium dioxide has been synthesized and the relation between conditions of solvothermal method and the material properties has been studied in the current work. Titanium isopropoxide was mixed with ethylene glycol and then was subjected to acetone with water. Resulting amorphous precipitate was treated solvothermal with water-ethanol mixture, then annealed at 300°C. Duration of solvothermal treatment, amount of water in acetone solution and initial concentration of titanium isopropoxide was varied as synthesis conditions.

According to the results of x-ray diffraction, all samples are nanocrystals of anatase with minor admixtures of brookite. Its coherent scattering area is about 10 nm. SEM data shows that right spherical particles of size between 400 and 1500 nm are forming.

The concentration of titanium isopropoxide has an optimum (34 mmol/l) that leads to a high surface area. Its highest value (185 m²/g) corresponds to these synthesis conditions: Ti(OiPr)₄ concentration of 34 mmol/l, 3% of molar water relative to amount of Ti and 12 hours of solvothermal treatment. Reduction of initial concentration below 34 mmol/l leads to decrease of surface area followed by increase of spherical aggregate from 400-500 nm at 78 mmol/l to 1500 nm at 34 mmol/l and more irregularity.

Influence of duration of solvothermal treatment appear at brightest in samples with less concentration: time increase from 6 to 24 hours leads to decrease of surface area in twice from 185 m²/g to 93 m²/g.

The amount of water admixture influences most on samples with less initial concentration: its increase leads to surface area growth with weak influence on product morphology at the same time.

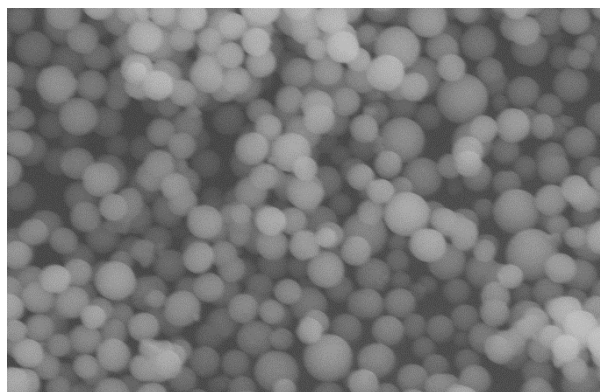


Fig. 1. SEM image of titanium dioxide with surface area value 185 m²/g.

Thursday, June 15, 2017

P11

Tuning magnetism in 122 parent compounds of Fe-based superconductors

*R. Kappenberger^{1),2)}, I. Vinçon^{1), 2)}, Anja U. B. Wolter¹⁾, L. Harnagea¹⁾, F. Cagliaris¹⁾, C. Hess^{1),3)}, H.-J. Grafe¹⁾, S. Aswartham¹⁾, S. Wurmehl^{1),2)}, B. Büchner^{1),2),3)}

¹⁾ Leibniz Institute for Solid State and Materials Research, Dresden, Germany

²⁾ Institute for Solid State Physics, TU Dresden, Dresden, Germany

³⁾ Center for Transport and Devices, TU Dresden, Dresden, Germany

*r.kappenberger@ifw-dresden.de

An important aspect of iron based superconductors is the transition from magnetically ordered to a superconducting state by doping with various elements. Here, we present two different ways of tuning the magnetism of parent compounds in Fe-based superconductors. One way of tuning is a novel type of doping, partial removal of arsenic from $\text{La}(\text{O}_{1-F})\text{FeAs}_1$ [1] which has been shown to slightly increase the transition temperature while simultaneously creating local magnetic moments.

We present an extended analysis of arsenic deficient $\text{BaFe}_2\text{As}_{2-}$ aiming to understand this unexpected behavior. The impact of a variable arsenic deficiency on the spin density wave and local moment formation has been studied by means of magnetic susceptibility, resistivity and nuclear magnetic resonance measurements. Systematic structural changes have been determined by powder diffraction data [2].

Another way of tuning has been found in the new $\text{Na}_{0.6}\text{RE}_{0.4}\text{Fe}_2\text{As}_2$ (RE=La [3], Ce) compounds. Where the addition of ~40% of RE^{3+} in the metastable NaFe_2As_2 parent compound leads to superconductivity with a T_c of 26 K and SDW at 115 (Ce) or 125 K (La). Since the highest T_c in the 122 systems has been reached upon complete suppression of the SDW, this novel family has the potential of reaching even higher T_c . Unfortunately, the Na: RE ratio cannot easily be changed using flux growth, however, additional charge doping with Co on the Fe position is possible, which leads to a drastic increase of the superconducting volume fraction.

References:

- 1) V. Grinenko et al., Phys. Rev. B 84, 134516 (2011)
- 2) I. Vinçon, et al., in preparation (2017)
- 3) J.-Q. Yan et al., Phys. Rev. B 91, 024501 (2015)
- 4) R. K. et al., in preparation (2017)

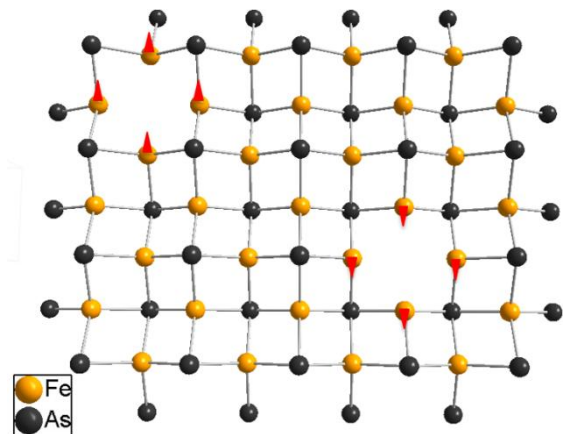


Fig.1. Microscopic model for created magnetic centers by As vacancies. [1]

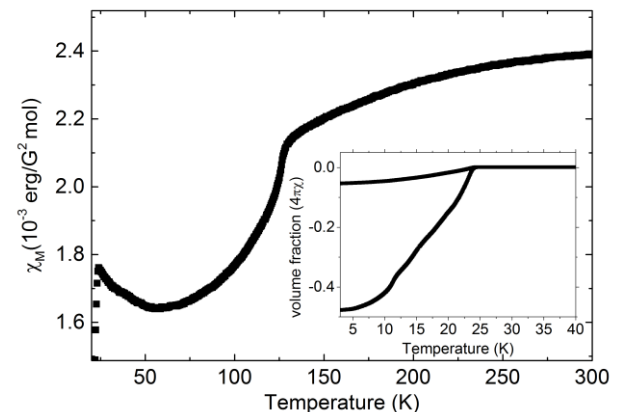


Fig. 2. SDW and superconducting transition in $\text{Na}_{0.6}\text{La}_{0.4}\text{Fe}_2\text{As}_2$ [4]

Thursday, June 15, 2017

P12

Approaches to improve lanthanide NIR luminescent features

*V. Khudoleeva¹⁾, A. Kovalenko¹⁾, P. Rublev²⁾, V. Utochnikova²⁾³⁾¹⁾Faculty of Materials Science, Lomonosov Moscow State University, Moscow, Russia. ²⁾Department of Chemistry, Lomonosov Moscow State University, Moscow, Russia ³⁾P.N. Lebedev Physical Institute of the Russian Academy of Sciences, Moscow, Russia

*vladislava.kh@list.ru

Lanthanide compounds are considered to be the promising class of luminescent materials due to their unique optical properties, including long lifetime of the excited state and large Stokes shift. Among them, near infrared (NIR) emitting compounds are of particular interest as compounds for medical and telecommunication applications because of the transparency windows of biological tissues and fiber optic materials. However, nowadays such materials still have a low NIR luminescence intensity and quantum yields do not exceed a 1%. In addition, the main characteristic of materials for practical applications is the luminosity (B), which is determined not only by the internal quantum yield (QY^{Ln}), but also by the ligand absorption coefficient (ϵ) and the efficiency of the ligand-to-metal energy transfer (η_{sens}): $B = \epsilon \cdot \eta_{sens} \cdot QY^{Ln}$.

The promising NIR-emitting Ln-based compounds are divided into two main classes: 1) coordination compounds with organic ligands, which have large absorption coefficients values, and 2) ligand lanthanide inorganic salts, which surface is modified with organic ligand, i.e. lanthanide fluorides, which have high internal quantum yields. However, the sensitization efficiency is still low today, therefore the task to increase this value is a very actual task.

In order to obtain the compound with high-luminosity NIR luminescence, a complex approach is used in this work, which includes both the search for ligands with high absorption coefficient and sensitization efficiency, and an internal quantum yield increasing.

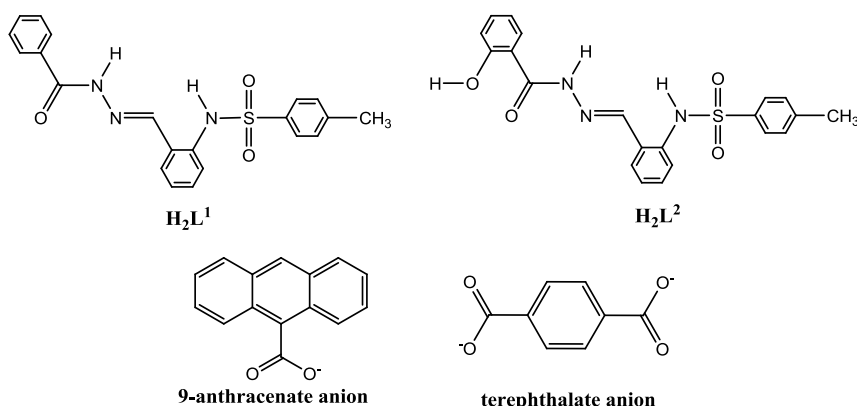


Fig. 1. Structural formulas of used ligands

Thus, ytterbium complexes with anionic polydentate Schiff bases exhibit high quantum yields up to 1.5%, while the sensitization efficiency is 25% (H_2L^1). Such high values can be explained by the formation of charge transfer state. At the same time, the addition of the hydroxyl group in the ligand structure (H_2L^2) leads to the twofold decrease in the quantum yield, which is due to the quenching of the NIR luminescence by the -OH bonds vibrations. Despite the fact, that the internal quantum yields do not exceed 6%, such complex compounds have high brightness values.

Herewith we synthesized the lanthanide fluorides, where the QY^{Ln} value is mainly determined by the efficiency of the concentration quenching processes. The minimization of quenching is possible by increasing the metal-metal distance, therefore bimetallic fluorides $Yb_xLa_{1-x}F_3$ were obtained, which leads to the increase of QY^{Ln} up to 30% in the case of $Yb_{0.05}La_{0.95}F_3$. The surface modification with aromatic carboxylate ligand, for example, 9-anthracenate anion (L) with a sensitizing efficiency of the ytterbium ion of 25% allows to achieve luminosity values of $L@Yb_{0.05}La_{0.95}F_3$ nanoparticles comparable to ytterbium complex compounds.

The ligand selection process can be simplified by using the dysprosium ion as an NIR emitter, whose resonant level (20400 cm^{-1}) a small energy gap with the triplet states of most has known ligands. Despite the greater concentration quenching efficiency than that of the ytterbium, the combination of the metal-to-metal distance increasing approach and the surface modification with terephthalate anion it was possible to obtain a compound with a bright NIR luminescence. In addition, the Dy^{3+} ion has transitions not only in the NIR region, but also in the visible region, which makes its compounds promising as sensor materials.

Thursday, June 15, 2017

P13

Synthesis and characterization of Sr_2IrO_4 and SrIrO_3 thin films.

*Yu.V. Kisilinskii¹⁾, G. Cristiani²⁾, A.M. Petrzhik¹⁾, N.V. Andreev³⁾, A.E. Pestun³⁾, I.N Diuzhikov¹⁾, G. Logvenov²⁾, and G.A. Ovsyannikov¹⁾

¹⁾Kotel'nikov IRE of RAS, Moscow, Russia. ²⁾Max Planck Institute for Solid State Research, Stuttgart, Germany. ³⁾National University of Science and Technology MISiS, Moscow, Russia.

*yulii@hitech.cplire.ru

Strontium iridates are the materials with strong spin-orbit coupling (SOC), where a lot of interesting physics is observed. According a theoretical work [1], compounds with Hubbard energy U less than 2 eV are nonmagnetic metals like SrIrO_3 . In case of $U > 2$ eV the iridates are ferromagnetic insulators due to large SOC with it energy is in order of U , for example Sr_2IrO_4 . For SrIrO_4 a high value of negative magnetoresistance was observed [2]. For SrIrO_3 thin films a metal – insulator transition takes place due to mechanical strain during the films grown [3].

The resistivity of epitaxial thin films of SrIrO_3 ($\rho(300) \approx 0.5 \text{ m}\Omega \text{ cm}$) has not monotonic temperature dependence [4].

The resistivity of Sr_2IrO_4 epitaxial thin films deposited by laser ablation [5] has a semiconductor-like temperature dependence $\rho = \rho_0 \cdot \exp[\Delta E / (2kT)]$ with a slope of $\Delta E \approx 200 \text{ meV}$ in 100 – 150 K temperature range (Fig. 1). The similar behavior was observed for Sr_2IrO_4 epitaxial films in [2]. The semiconductor dependences were observed for films deposited on SrTiO_3 and $\text{LaAlO}_3 + \text{Sr}_2\text{AlTaO}_6$ (LSAT) substrates. Sr_2IrO_4 films on LaAlO_3 substrates have 2 - dimensional variable range hopping (VRH) dependency $\rho = \rho_{2D} \cdot \exp[(T_{2D}/T)^{1/3}]$ with constants T_{2D} of 10^6 K (Fig. 1). Sr_2IrO_4 films have lattice parameters $a = 0.397 \text{ nm}$ which is large than the parameter of LaAlO_3 $a = 0.38 \text{ nm}$ and the films experienced a compressive strain. Probably the compression influences on the $\rho(T)$ dependency.

At high temperatures, $T > 150 \text{ K}$, $\rho(T)$ curves of Sr_2IrO_4 films are close to 3 - dimensional Mott VRH dependences $\rho = \rho_{3D} \cdot \exp[(T_{3D}/T)^{1/4}]$ with constants T_{3D} of 10^8 K . From experimental T_{3D} and T_{2D} values we have estimated localization radii a 1 nm and density of states at Fermi level N_F $10^{18} \text{ eV}^{-1} \text{ cm}^{-3}$ by method of Knotek, et al [6]. In our samples we have observed larger constants $T_{3D} 1/(a^3 N_F)$ than were calculated for Sr_2IrO_4 by other authors [7]. It points on lower density of localized states N_F in our thin films compare to ones was obtained in [7].

To distinguish between the semiconductor conductivity mechanism and the variable range hopping one a spectral measurement were performed. The information about electric transport properties of our strontium iridate thin films and about deposition condition of the films will be presented.

The work is partially supported by Scientific School grant NSH-8168.2016.2, Russ. Acad. Sci “Corr” project.

References:

- 1) MA Zeb, H-Y Kee - Phys. Rev. B 86, 085149 (2012)
- 2) M Ge, TF Qi, OB Korneta, et al. - Phys. Rev. B 84, 100402 (2011)
- 3) A Biswas, K-S Kim, YH Jeong - Journal of Appl. Phys. 116, 213704 (2014)
- 4) YuV Kisilinskii, GA Ovsyannikov, AM Petrzhik, et al. - Phys. of the Sol. State 57, 2519 (2015)
- 5) AM Perzhik, G Cristiani, G Logvenov, et al. – Technical Physics Lett. to be published (June 2017)
- 6) ML Knotek, M Pollak, TM Donovan - Phys.Rev. Lett. 30, 853 (1975)
- 7) Chengliang Lu, A Quindeau, H Deniz, et al. - Appl. Phys. Lett. 105, 082407 (2014)

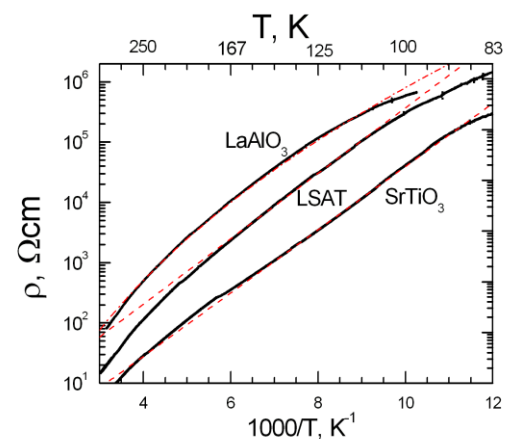


Fig.1. Resistivity versus $1/T$ dependences for Sr_2IrO_4 films of 30 nm in thickness. Substrates on which the films were deposited are: LaAlO_3 , LSAT, SrTiO_3 . Semiconductor – like dependences are dashed straight lines and 2D hopping dependence is dash-dot curve.

Thursday, June 15, 2017

P14

Highly permeable 3D printed polylactide/calcium phosphate biocomposites with carbonated hydroxyapatite modified surface

*E.S. Klimashina^{1,2)}, P.V. Evdokimov¹⁾, D.M. Zuev²⁾, V.I. Putlayev^{1,2)}

¹⁾Department of Chemistry, Lomonosov Moscow State University, Moscow, Russia. ²⁾Department of Materials Science, Lomonosov Moscow State University, Moscow, Russia

*klimashina@inorg.chem.msu.ru

The fundamental task of creating a new generation of highly permeable biocomposites for bone tissue regeneration on the basis of biodegradable polymers (polylactide, PLA) filled with resorbable calcium phosphates and possessing the support of specific proteins that induce osteosynthesis was solved. The main purpose of such materials is fabrication on their basis of tissue engineering constructions by filling them with osteoinductive substances. At the same time, such biocomposite should have: a) strength characteristics sufficient for manipulation during their surgical installation at the site of the bone defect, b) have a certain arrangement of macropores - an architecture that provides osteoconductivity - germination of the bone tissue inside the implant, c) be hydrophilic and provide support (adsorption) of specific proteins, d) shows the ability to biodegrade the polymer phase and resorption of the mineral phase of the filler [1]. In the process of exploitation in the body such material will play the role of the original supporting and guiding element, and in the future - slowly dissolves in the interstitial fluid of the organism, promoting the new bone tissue growth.

To achieve the above, the 3D printed filled polylactide models were additionally treated in solutions of the artificial interstitial fluid SBF, polyvinyl alcohol, increasing the adhesion properties of material surface.

Prototypes of implants with developed modified carbonated hydroxyapatite (Fig. 1) were obtained with improved roughness and wettability, capable of actively supporting proteins in example of albumin.

Also processing of three-dimensional models of the cementing reaction was carried out to form a resorbable brushite phase to establish the hydrophilic coating and improving the mechanical characteristics.

This work was supported by Moscow City Government with RFBR № 15-38-70047; RFBR № 15-08-99597 and with the financial support of the RF President Grant, project MK-8668.2016.8.

References:

1) V.M. Ievlev et al., J. Inorganic Materials. 51, 1297-1315 (2015).

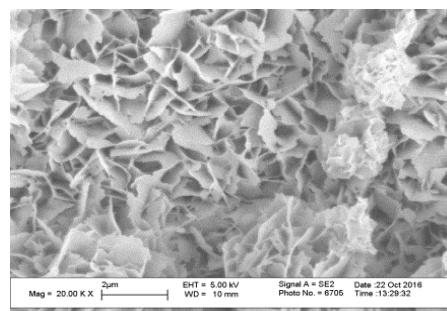


Fig.1. Microstructure of modified surface of 3D structures of PLA samples after processing in SBF for 7 days

Thursday, June 15, 2017

P15

Thin nanosilicon films as elements of flexible, ultrathin power sources

*N.N.Kononov², S.G.Dorofeev¹, S. S. Bubenov¹, A. N. Zolotykh¹, D. V. Grigoriev¹

¹)Department of Chemistry, Lomonosov Moscow State University, Moscow, Russia

²)A.M. Prokhorov General Physics Institute, RAS, Moscow, Russia

*nnk@kapella.gpi.ru

The intensive development of the technology of manufacturing miniature electronic devices requires the creation of miniature power sources and energy storage devices for them.

In these theses we report new class of an ultrathin batteries based on a films consisting of silicon nanoparticles (nc-Si film) and bounded by two flat metal electrodes with the upper electrode being nanoporous and capable of passing the molecules of water and oxygen.

The total thickness of such a battery is 2 μm , which makes it an ideal candidate (using a flexible substrate) as a flexible power source, which for example can be embedded in electronic paper or used in next-generation smart cards. Also, such sources can be organized directly on the surface of silicon chips. The value of the detected electro-motion force (EMF) depends on the temperature of the sample, as well as on the humidity of atmosphere surrounding the sample and on the presence of oxygen in it, but the main factor leading to generation of the EMF in sample is the presence of the water vapor in the environment. The maximum emf value obtained in the nc-Si thin-film structure was 1.5V. The power released by the structure to an external matched load in the temperature range from 20 to 150° C reaches values 10^{-2} to $5 \cdot 10^{-1}$ W / g.

A typical dependence of the EMF of the structure Al/nc-Si/M film/Al (or Ni) on the humidity of the ambient air is shown in Figure 1.

In Figure 2 EMF generated by sample Al/nc-Si/ITO in air is shown as a function of reciprocal temperature (semi-log plot). To quantitatively account for this EMF behavior we propose the model shown in the inset of Figure 2. In the model, it is assumed that in the sample simultaneously with the spontaneously generated EMF(ε), there is some parallel process of transport of electric charges, which shunts it. We propose that shunting resistance is largely independent of temperature in the studied temperature interval and the series resistance with EMF is of activation character.

From the analysis of the process of generation of EMF by the structures into which a Nafion membrane was introduced, and also from the analysis of impedance spectra, it was established that the main role in the separation of charges inside the structure is determined by ion transport, namely by the proton conductivity.

We propose that EMF generation in Al/nc-Si/M structures is initiated by diffusion of water vapor through porous contact leading to oxidation of nc-Si and the diffusion of H^+ ions from top electrode to the bottom one.

This work was supported by Russian Foundation for Basic Research grant № 15-02-09135.

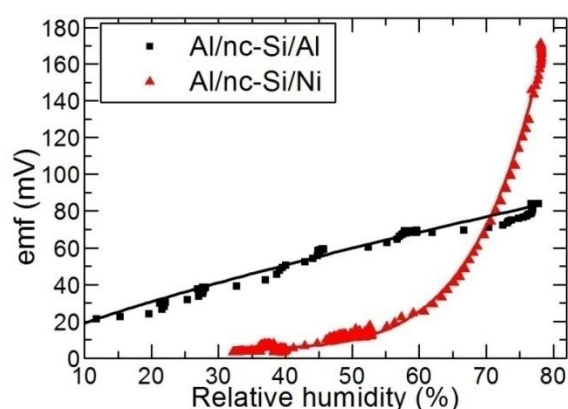


Fig 1. Dependences of EMF of Al/nc-Si/M structures on relative humidity of surrounding atmosphere at $T = 27^\circ\text{C}$: (■) – $M = \text{Al}$, (▲) – $M = \text{Ni}$; (solid lines) – power law fits of the dependences.

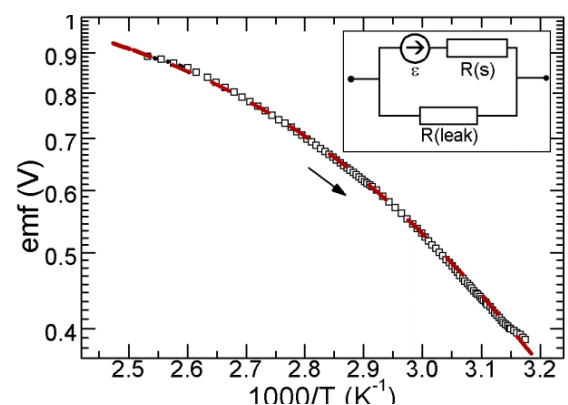


Fig. 2. Dependence of EMF generated by Al/nc-Si/ITO structure on reciprocal temperature, semi-log plot; (dashed line) – approximation of the dependence to the model of shunted EMF source discussed in the main text; (inset) – equivalent scheme of the model

Thursday, June 15, 2017

P16

p-type TCO: $\text{CuCr}_{1-x}\text{Mg}_x\text{O}_2$ ceramics and epitaxial thin films

*I.Korsakov¹, V.Kytin², V.Kulbachinsky², D.Kondratieva², D.Kohan², V.Zaytsev², A.Pavlikov², E.Konstantinova², A.Grigoriev¹, L.Bourova¹, A.Mankevich¹, Ju.Shakirova¹, A.Putilova¹

¹)Department of Chemistry, Lomonosov Moscow State University, Moscow, Russia ²)Department of Physics, Lomonosov Moscow State University, Moscow, Russia

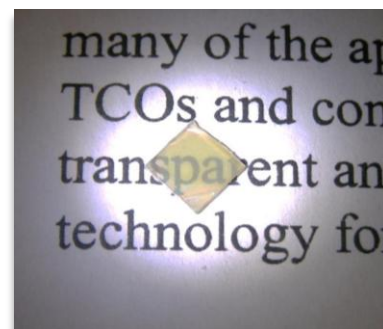
*korsakov@inorg.chem.msu.ru

Transparent conducting oxides (TCOs) are wide bandgap (>3.0 eV) semiconductors combining visible-range transparency and electrical conductivity in a single material. TCOs are used as transparent electrodes in optoelectronic devices such as photovoltaic cells, light emitting diodes, flat panel displays.

The most popular TCOs currently used are of n-type (F-doped SnO_2 (FTO) and Sn-doped In_2O_3 (ITO), Al-doped ZnO), but there are no p-type TCOs with comparable characteristics. Electrical conductivity of p-type materials is some orders of magnitude lower than that of n-type materials. This limits the development of transparent electronic components such as p-n junction diodes. Currently, research of p-type TCOs is focused on Cu- or Ag-based delafossite compounds, such as CuMO_2 or AgMO_2 ($M=\text{Al, Fe, Cr, Sc, In, Ga, Y}$ etc.). To date, Mg-doped CuCrO_2 thin films show the record high conductivity among the delafossite oxides, however, their visible-range transparency is limited. Mechanisms of conductivity and properties of charge carriers in this material are still not clear, also multiferroic properties have been reported.

In our work $\text{CuCr}_{1-x}\text{Mg}_x\text{O}_2$ solid solutions with magnesium content $0 < x < 0,03$ were synthesized in forms of polycrystalline ceramics and thin films. To achieve the uniform distribution of Mg-doping element in the samples, a chemical solution synthesis was performed and single phase ceramics was sintered in an argon atmosphere at 1000°C . Epitaxial thin films were deposited by MOCVD on various single crystalline substrates.

XRD characterization, optical, Raman and ESR spectroscopy, as well as electrical measurements were performed. The Raman spectra contained peaks corresponding to E_g and A_{1g} vibrational modes of CuCrO_2 , they were shifted to higher frequencies by Mg-doping. The band gap value was determined from diffuse light scattering spectra. The positive sign of Seebeck coefficient confirmed p-type of electrical conductivity. The resistivity of the samples was decreased by more than 5 orders of magnitude with increasing magnesium content from 0 to 3 at .% and amounted to 0.6 Ohms.cm at room temperature. The activation energy of electrical conductivity in the samples doped with Mg was 4-5 times less than in the samples without Mg, which confirms the different nature of the acceptor levels in undoped and doped samples.



Support of the Russian Foundation for Basic Research is kindly acknowledged (RFBR 15-03-07408a).

Thursday, June 15, 2017

P17

AgCl and AgBr doped CdSe quantum dots

*P.A. Kotin, S.G. Dorofeev, T.A. Kuznetsova

Department of Chemistry, Lomonosov Moscow State University, Moscow, Russia

*kotin-pa@mail.ru

Semiconductor quantum dots (QDs) are zero-dimensional objects, which deserved a particular attention due to their unique optical properties, high stability to the environment and high surface-to-volume ratio [1]. The equally important factor is the possibility of the direct modification of QDs electronic and optical properties, using doping [2].

Despite a large number of publications devoted to CdSe QDs, special attention is still focused on the doping problem [3,4]. Here, we propose novel precursors – AgCl and AgBr. It is known from literature, that halide ions lead to obtaining anisotropic quantum dots [5], but the authors didn't observe their optical properties. Silver is not widely used as dopant and only in a few publications silver nitrate is used as a doping agent for CdSe QDs in cation-exchange reactions [6].

In contrast to previous publications we realized doping directly during the colloidal synthesis of nanoparticles. As a precursor of Cd we used cadmium oleate, a precursor of selenium was tri-n-octylphosphine selenide (TOPSe) and silver halides were diluted in TOP to get solutions with different concentrations. Oleic acid serves as a stabilizer for colloidal synthesis.

We found that a gradual increase of the amount of silver halides in synthesis makes it possible to obtain tetrapods (TPs) with different leg length and large ellipsoidal nanoparticles (NPs) possessing an intensive near IR photoluminescence. To investigate a process of NPs formation we proposed a sampling during colloidal synthesis. We also investigated NPs structure and optical properties.

Each of the two ensembles of particles (TPs and EPs) possesses its unique optical spectrum, but both share intensive defect bands. The sample, which contains the largest ellipsoidal particles, has a strong infrared photoluminescence ranging up to 0.9 eV (~1400 nm). This feature is unusual for undoped CdSe quantum dots due to the bulk band gap energy of this semiconductor – 1,74 eV.

References:

- 1) ML Landry et al. - J. Chem. Educ. 91, 274 (2014)
- 2) DJ Norris, AL Efros, SC Erwin – Science 319, 1776 (2008)
- 3) JZ Zhang, JK Cooper, S Gul - J. Phys. Chem. Lett. 5, 3694 (2014)
- 4) V Chikan - J. Phys. Chem. Lett., 2, 2783 (2011)
- 5) J Lim et al. - Chem. Mater. 25, 1443 (2013)
- 6) A Sahu et al. - Nano Lett. 12, 2587 (2012)

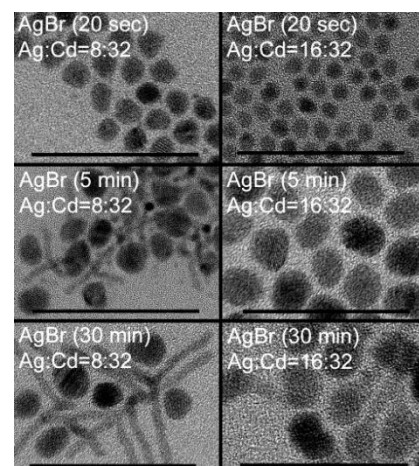


Fig. 1. Transmission electron microscopy of AgBr doped CdSe QDs with different AgBr amount in synthesis and different growth time. Scale bar is 50 nm.

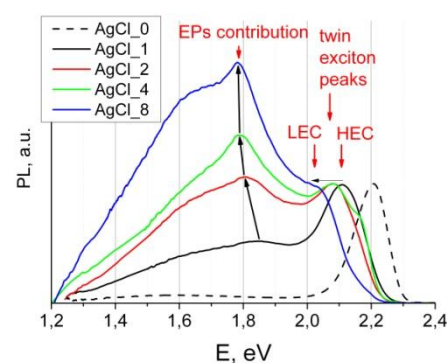


Fig. 2. Photoluminescence spectra of AgCl doped CdSe quantum dots with different AgCl amount in synthesis.

Thursday, June 15, 2017

P18

Complex selenite-halides with low-dimensional magnetic systems

*E.Kuznetsova¹⁾, P. Berdonosov¹⁾, V. Dolgikh¹⁾, O. Gajtko²⁾, K. Zakharov³⁾, M. Markina³⁾, E. Zvereva³⁾, O. Volkova³⁾, A. Vasiliev³⁾

¹⁾Department of Chemistry, Lomonosov Moscow State University, Moscow, Russia ²⁾Kurnakov Institute of General and Inorganic Chemistry of the Russian Academy of Sciences, Moscow, Russia ³⁾Department of Physics, Lomonosov Moscow State University, Moscow, Russia

e.kuznetsova@inorg.chem.msu.ru

Transition metal oxohalide compounds containing also so-called lone pair elements with stereochemically active lone electron pairs have proved to be a family of compounds with a rich variability of low-dimensional arrangements of the transition metal ions [1]. The lone pair elements and the halogens act as “chemical scissors” reducing the dimensionality of crystal structure, thus leading to a high probability for forming low-dimensional magnetic subsystems (e.g. spin layers or spin chains) based on transition metal ions. From this point of view, the class of selenite halides seems promising for the search for potential low-dimensional magnets.

The most explored systems contain Cu^{2+} and Ni^{2+} , due to the interest in spin 1/2 or 1 lattices or to the formation of different coupling regimes. Mineral francisite $\text{Cu}_3\text{Bi}(\text{SeO}_3)_2\text{O}_2\text{Cl}$ is characterized by the rare combination of chemical elements met in this mineral only. It was shown that Bi can be substituted by Y or lanthanide [2, 3], thus resulting in the formation of a family of isostructural compounds with quasi-2D magnetic properties. This family of compounds is a good example of a situation where correlations between composition, crystal structure and physical properties can be observed and evaluated experimentally.

Less studied are classical quasi-one-dimensional magnetic systems based on ions with high spin values, e.g., $S = 5/2$. There are only two iron selenite-halides described in literature [4, 5], so the search for new compounds is an actual problem.

In this study synthesis, crystal structure and magnetic properties of $\text{Cu}_3\text{M}(\text{SeO}_3)_2\text{O}_2\text{Cl}$ ($\text{M} = \text{Y}, \text{La}, \text{Pr}, \text{Nd}, \text{Sm}, \text{Eu}, \text{Gd}, \text{Tb}, \text{Dy}, \text{Ho}, \text{Er}, \text{Tm}, \text{Yb}, \text{Lu}$) and $\text{Bi}_2\text{Fe}(\text{SeO}_3)_2\text{OCl}_3$ are presented. Interrelation between chemical composition, crystal structure and magnetic behavior of francisite-like compounds is discussed.

Polycrystalline samples of francisite-like compounds were obtained by solid-state reaction in evacuated quartz tubes. CuO , CuCl_2 , SeO_2 , M_2O_3 ($\text{M} = \text{Y}, \text{La}, \text{Nd}, \text{Sm}, \text{Eu}, \text{Gd}, \text{Dy}, \text{Ho}, \text{Er}, \text{Tm}, \text{Yb}, \text{Lu}$), TbOCl and PrOCl were used as starting compounds. Preliminary characterization by powder X-ray diffraction confirmed phase purity according to the previously suggested structural model. Structure refinement was performed by Rietveld method on powder samples using JANA 2006 software. As the initial model, the structural data for $\text{Cu}_3\text{Bi}(\text{SeO}_3)_2\text{O}_2\text{Cl}$ were used. The magnetization and susceptibility data were taken over the temperature range 2–400 K in applied field strengths up to 7 T.

All compounds obtained crystallize in orthorhombic $Pmmn$ space group. A nearly linear dependence of the unit cell parameters of lanthanide selenite oxohalides with a francisite-type structure on the ionic radius of Ln^{3+} ($\text{CN} = 8$) is observed. It was shown that all compounds of francisite family reach long-range ordered antiferromagnetic state at low temperatures and exhibit field-induced metamagnetic transition prior to full saturation in moderate magnetic field.

Originally single crystals of the new bismuth-iron selenite-oxochloride $\text{Bi}_2\text{Fe}(\text{SeO}_3)_2\text{OCl}_3$ were found in the reaction mixture of chemically pure BiOCl , FeOCl and anhydrous SeO_2 . After a structure determination the composition of the compound was confirmed by directed synthesis from a mixture of chemically pure Bi_2O_3 , SeO_2 , and FeCl_3 . The powder XRD pattern was indexed in the monoclinic space group $P2_1/m$ with cell constants $a = 8.575(5) \text{ \AA}$, $b = 7.133(4) \text{ \AA}$, $c = 8.603(6) \text{ \AA}$, and $\beta = 107.04(3)^\circ$. These values are in good agreement with single-crystal experimental results. The new compound shows quasi-1D magnetic behavior due to the presence of a reasonably isolated set of spin $S = 5/2$ zigzag chains of corner sharing FeO_6 octahedra in its structure.

This study was supported by RFBR grant №16-03-00463a.

References:

- 1) Becker R., Johnsson M., Solid State Sciences, 7, 375-380 (2005).
- 2) P.S. Berdonosov, V.A. Dolgikh, Russ. J. Inorg. Chem., 53, 1353-1358 (2008).
- 3) R. Berrigan, B.M. Gatehouse, Acta Cryst., C52, 496-497 (1996).
- 4) Hu, S.; Johnsson, M. Dalton Trans., 42, 7859–7862 (2013).
- 5) Hu, S.; Johnsson, M.; Law, J. M.; Bettis, J. L., Jr.; Whangbo, M.-H.; Kremer, R. K. Inorg. Chem., 53, 4250–4256 (2014).

Thursday, June 15, 2017

P19

Mobility Edge wave functions in Charge density waves

*M.A. Lizunova^{1) 2)}, J. van Wezel²⁾, C. de Morais Smith¹⁾.

¹⁾ Institute for Theoretical Physics, Utrecht University, Utrecht, The Netherlands ²⁾ Institute for Theoretical Physics, University of Amsterdam, Amsterdam, The Netherlands

*m.a.lizunova@uu.nl

It is well known the Harper equation describing the integer quantum Hall effect in two dimensions, also gives a mean-field description of charge density wave materials in one dimension. In particular, the quantized adiabatic transport (Thouless pumping) in charge ordered systems corresponds directly to topological transport between edge states upon insertion of a flux quantum in a quantum hall cylinder (Laughling's gauge argument).

Here, we show that the existence of a mobility edge, thought to be responsible for connecting edge states in the quantum Hall setup, is not necessary for realizing topological transport in a sliding charge density wave. We use the absence of gauge invariance in the charge ordered chain to explicitly construct the evolution of wave functions across the mobility edge, and compare it to the situation in the integer quantum hall effect to clarify the nature of the transport in both.

References

1) F Flicker, J van Wezel - EPL 111, 37008 (2015)

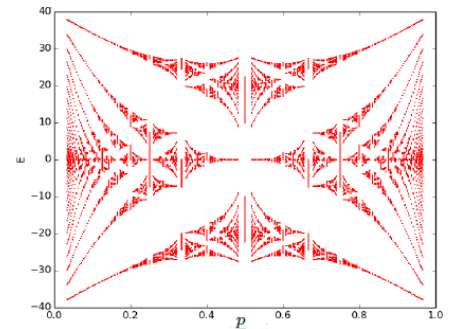


Fig.1. Hofstadter's butterfly, all possible energies E versus the filling factor ν .

Thursday, June 15, 2017

P20

When chemistry meets physics: unconventional synthetic approach and peculiar magnetic states in CuOHF and Cu₃(OH)₂F₄

*A. Merkulova¹⁾, I. Danilovich¹⁾, C. Balz²⁾, I. Morozov¹⁾, A. Vasiliev¹⁾, A. Polovkova¹⁾, E. Zvereva¹⁾, Y. Ovchenkov¹⁾, B. Rahaman³⁾, T. Saha-Dasgupta⁴⁾, H. Luetkens⁵⁾, O. Volkova¹⁾, A. Shakin⁶⁾

¹⁾ Lomonosov Moscow State University, Moscow, Russia, ²⁾ Quantum Condensed Matter Division, Oak Ridge National Laboratory, Oak Ridge, Tennessee 37830, USA, ³⁾ Aliah University, Kolkata 700156, India, ⁴⁾ S.N. Bose National Centre for Basic Sciences, Kolkata 700098, India, ⁵⁾ Laboratory for Muon-Spin Spectroscopy, Paul Scherrer Institute, 5232 Villigen, Switzerland, ⁶⁾ National University of Science and Technology "MISIS", Moscow 119049, Russia

*anna.merkulova@mail.ru

Copper hydroxyhalids present great interest for crystal chemistry research as well as for physics of strongly correlated electron systems [1, 2]. These compounds usually form coordinated polymers. Thus, they are promising candidates in search for low dimensional and geometrically frustrated magnetic systems. To date, only copper hydroxychlorides have been thoroughly studied. Here, we present the synthesis and magnetic properties of two copper hydroxyfluorides: CuOHF and Cu₃(OH)₂F₄.

CuOHF, light olive powder, was obtained by boiling the saturated CuF₂ solution in accordance with the reaction CuF₂ + H₂O = CuOHF + HF. This compound has a layered structure, formed by copper(II) octahedra with joint edges. The octahedra are arranged in a triangular motif. Being isostructural to CuOHCl, copper hydroxyfluoride was expected to demonstrate similar magnetic interactions, described by the Shastry-Sutherland model [2]. Surprisingly, slight difference in bond lengths yielded a quite different magnetic structure (Fig. 1). Physical measurements and first principles calculations indicate that CuOHF experiences a transition into static but magnetically short range antiferromagnetic state at T_N = 9,5 – 11,5 K [3].

Crystal structure of Cu₃(OH)₂F₄ was first established in [5], but our goal was to develop a synthetic approach to obtain single phase samples. Single phase sample of Cu₃(OH)₂F₄ is an olive green powder synthesized by heating the solid mixture of CuF₂·2H₂O and Cu(OH)F in a sealed Teflon autoclave for two days at 200 °C. Measurements of thermodynamics and resonance properties suggest canted antiferromagnetic ground state at T_C = 12.5 K [4].

References:

- 1) M. Hagihala, X.G. Zheng, T. Toriyi, T. Kawae, Journal of Physics: Condensed Matter, 19: 145281, 2007
- 2) T. Pungas, Master's Thesis, Tartu 2014
- 3) I. Danilovich, A. Merkulova, A. Polovkova, et al. Vehement Competition of Multiple Superexchange Interactions and Peculiar Magnetically Disordered State in Cu(OH)F, Journal of the Physical Society of Japan 85: 024709, 2016
- 4) G. Giester, E. Libowitzky Crystal structures and Raman spectra of Cu(OH)F and Cu₃(OH)₂F₄, Z. Kristallogr. 218: 351–356, 2003

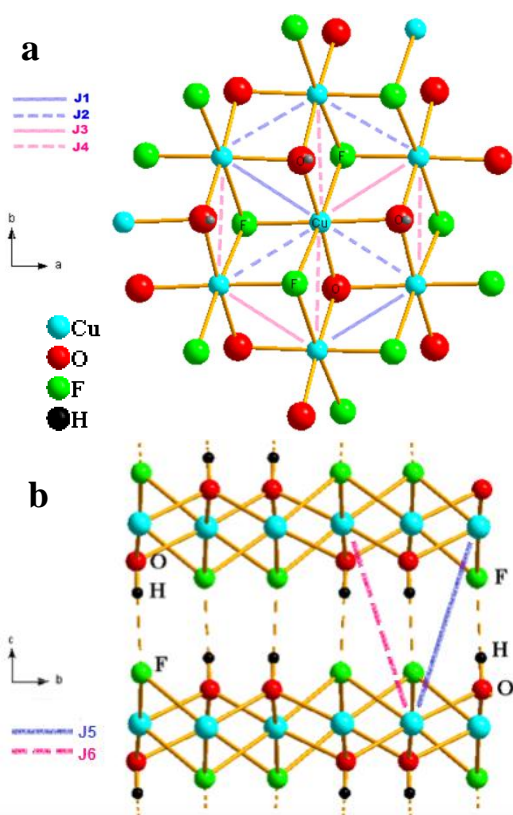


Fig.1. Antiferromagnetic (AFM) and ferromagnetic (FM) interactions in CuOHF [3].

a, intra-layer interactions: J1, J2 – AFM, J3, J4 – FM

b, inter-layer interactions: J5 – AFM, J6 – FM



Thursday, June 15, 2017

P21

Self-localization of doped carriers and superconducting phase diagrams of cuprates and pnictides

*K.V. Mitsen, O.M. Ivanenko

Lebedev Physical Institute, Moscow, Russia

*mitsen@sci.lebedev.ru

We propose a model of heterovalent doping of HTSC (both cuprates and pnictides) based on the view of the self-localization of doped carriers due to the formation of trion complexes in the basal planes [1]. Such trion complex is a bound state of a doped carrier and charge transfer (CT) excitons that are generated in certain cells in its vicinity. The arrangement of such cells containing CT excitons (CT plaquettes) in the basal plane of the crystal is determined by its crystal structure and type of dopant so that the dopant concentration range corresponding to the existence of a percolation cluster of CT plaquettes can be readily calculated for each particular compound. We demonstrate that these dopant concentration ranges coincide to good accuracy with the experimental ranges of superconducting domes on the phase diagrams of the HTSC compounds considered. The fact that the proposed method of constructing phase diagrams proved similarly successful both for cuprates and pnictides is a serious argument in favour of the common nature of the superconducting state in these classes of HTSCs.

Thus the superconductivity takes place only in the cluster of CT plaquettes that includes a continuous network of adjacent cations (in cuprates) or anions (in pnictides) that are the centres of CT plaquettes. In this phase electron states are a superposition of band and exciton states. We suppose that a percolation cluster of CT plaquettes in doped cuprates and pnictides can be considered as one more type of structures (in addition to one-dimensional Little chains [2] and Ginzburg sandwiches [3]), where the exciton mechanism of superconductivity can be realized.

In elaboration of the model, we introduce views of the formation of Heitler–London (HL) centres – pairs of CT plaquettes centred on pairs of adjacent Cu cations (in cuprates) or As anions (in pnictides) – in such a system. At HL centre, two electrons and two holes can form a bound biexciton state owing to the possibility of two holes (in cuprates) or two electrons (in pnictides) in singlet state to be in space between the central ions and be attracted simultaneously to two electrons (holes) on these ions. The existence of such HL centres makes it possible to explain the generation of additional free carriers in the normal state and the emergence of superconducting pairing as results of the interaction of band electrons with HL centres.

References:

- 1) KV Mitsen, OM Ivanenko - Phys. Usp. 60 (4) (2017).
- 2) WA Little - Phys. Rev. A134, 6 (1964).
- 3) VL Ginzburg - Sov. Phys. JETP 20, 1549 (1965).

Thursday, June 15, 2017

P22

Correlation induced electron-hole asymmetry in quasi-2D iridates

*E. M. Paerschke¹, K. Wohlfeld², K. Foyevtsova³, J. van den Brink^{1,4}

¹Leibniz Institute for Solid State and Materials Research, Dresden, Germany ²Institute of Theoretical Physics, University of Warsaw, Poland ³University of British Columbia, Vancouver, Canada ⁴Institute for Theoretical Physics, TU Dresden, Dresden, Germany

*ekaterina.plotnikova@phystech.edu

We determine the motion of a charge (hole *or* electron) added to the Mott insulating antiferromagnetic (AF) ground-state of quasi-2D iridates such as Ba_2IrO_4 or Sr_2IrO_4 [1,2].

We show that correlation effects, calculated within the self-consistent Born approximation, render the hole and electron case very different. An added electron forms a spin-polaron, which closely resembles the well-known cuprates, but the situation of a removed electron is far more complex. Many-body $5d^4$ configurations form a state which can be singlet and triplets of total angular momentum J and strongly affect the hole motion between AF sublattices.

This not only has important ramifications for the interpretation of (inverse-)photoemission experiments of quasi-2D iridates but also demonstrates that the correlation physics in electron- and hole-doped iridates is fundamentally different.

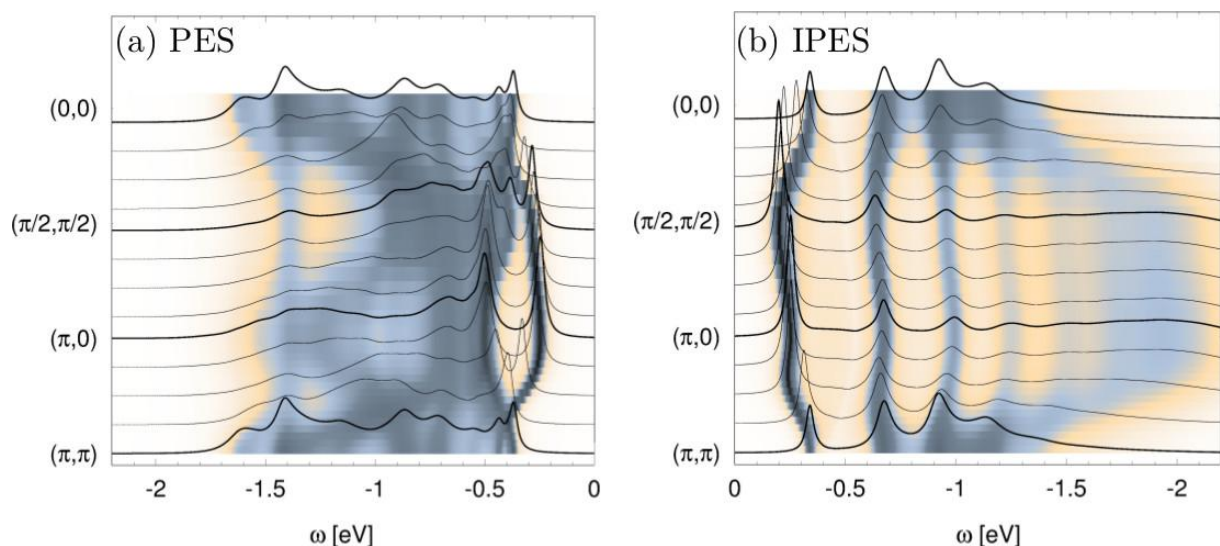


Fig. 1. Calculated (a) photoemission (PES) and (b) inverse-photoemission (IPES) spectral functions for quasi-2D iridates.

References :

- 1) NA Bogdanov, VM Katukuri, J Romhányi, V Yushankhai, V Kataev, Bernd Buechner, J van den Brink, L Hozoi - Nature Comm. 6, 7306 (2015)
- 2) EM Plotnikova, M Daghofer, J van den Brink, K Wohlfeld - Phys. Rev. Lett. 116, 106401 (2016)



Thursday, June 15, 2017

P23

Spectral function of a single hole in an anisotropic ferromagnet in a magnetic field

*A. Pavlov¹⁾, J.van den Brink¹⁾²⁾, D.Efremov¹⁾.

¹⁾ Institute for Theoretical Solid State Physics, IFW Dresden, 01069 Dresden, Germany. ²⁾ Institute for Theoretical Physics, TU Dresden, 01069 Dresden, Germany

*a.pavlov@ifw-dresden.de

We study the spectral function of a single hole in a quantum easy plane ferromagnet in a magnetic field. We show in a self-consistent perturbation theory that the hole spectrum is strongly renormalized by spin flip processes due to spin-orbit interaction. The renormalization strongly depends on the magnetic field. For low and high magnetic fields the hole is characterized by the quasiparticle spectral function with strong damping. At the saturation field the quasiparticle peak disappears and the spectral function is completely incoherent.

Thursday, June 15, 2017

P24

Theoretical prediction and experimental realization of Weyl- and Dirac semimetals

*B. R. Piening¹⁾, I. O. Cherniavskii¹⁾³⁾, G. Shipunov¹⁾³⁾, I. V. Morozov¹⁾³⁾, D. Efremov¹⁾, J. Van den Brink¹⁾, M. Gillig¹⁾, C. Hess¹⁾, S. Aswartham¹⁾, B. Büchner¹⁾²⁾

¹⁾ Leibniz Institute for Solid State and Materials Research, Dresden, Germany. ²⁾ Institute for Solid State Physics, TU Dresden, Dresden, Germany. ³⁾ Department of Chemistry, Lomonosov Moscow State University, Moscow, Russia

*b.r.piening@ifw-dresden.de

Until now only few materials are known as 3D Dirac and Weyl semimetals are compounds with strong spin-orbit coupling and broken either time reversal or inversion symmetry which protects band crossings. Angle-resolved photoemission spectroscopy has indeed observed Weyl points and fermi arcs which connect the Weyl points as one characteristic of this exotic state²⁾.

There are two types of Weyl semimetals: type-I Weyl semimetals are characterized by a point like fermi surface and the type-II Weyl semimetals appear at the contact of electron and hole pockets³⁾. A significant difference between type-I and type-II Weyl semimetal is a tilted Dirac cone in type-II⁴⁾, which has been established experimentally by several angle resolved photoemission spectroscopy studies⁵⁾.

WTe₂, MoTe₂ are two of the very few materials which were identified as Weyl semimetals of type-II, this work maps out the phase diagram of W_{1-x}Mo_xTe₂. The aim is to explore the novel physical properties in a type-II topological Weyl semimetal like the extreme large magnetoresistance (XMR)⁶⁾ in WTe₂ and ideally shift the Weyl points closer to the Fermi energy by chemical doping.

The synthesis of the W_{1-x}Mo_xTe₂ single crystals was done by Te flux, followed by a hot centrifugation to separate the crystals from the Te-flux. The needle-like single crystals (Fig.1) were investigated in terms of structure, transport properties (Fig.2) and angle-resolved photoemission spectroscopy. Except of the pure MoTe₂ which shows the well-known⁷⁾ first-order structural phase transition (around 250 K) from the monoclinic β-phase to the orthorhombic T_d phase, all other compositions already grew in the T_d phase (orthorhombic Pmn21), which is necessary for the observed type-II protected Weyl states.

References:

- 1) S-M. Huang et al. - Nature Communications | 6:7373 | DOI: 10.1038/ncomms8373
- 2) S. Borisenko et al. - arXiv:1507.04847 (2015)
- 3) A. A. Soluyanov et al. - Nature 527, 495-498 (2015)
- 4) Y. Sun, Y., S.-C. Wu, M. N. Ali, C. Felser, B. H. Yan - Phys. Rev. B. 92, 161107(R) (2015).
- 5) Deng, K. et al. - Nat. Phys. 12, 1105–1110 (2016).
- 6) M. N. Ali et al. - Nature. 514 205-208 (2014)
- 7) H. P. Hughes, R. H. Friend - J. Phy. C: Solid State Phys. 11, L103-05 (1978)

semimetals¹⁾. In general

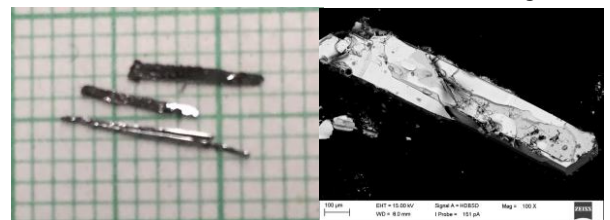


Fig. 1. Left: needle-like W_{1-x}Mo_xTe₂ single crystals from Te-flux growth, right: SEM-picture of W_{0.95}Mo_{0.05}Te₂ single crystal with 100x magnification.

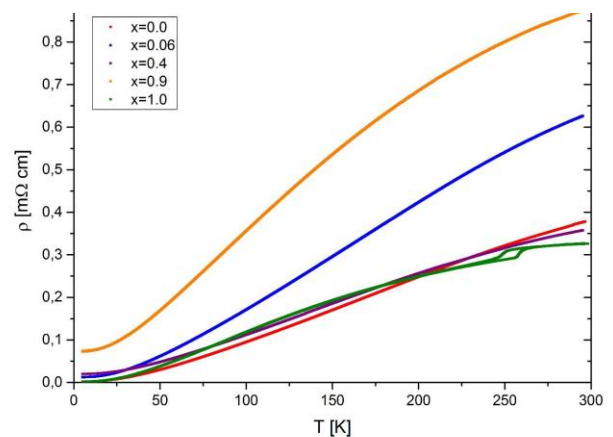


Fig. 2. Resistivity data of W_{1-x}Mo_xTe₂: All crystals show the semi-metallic nature and MoTe₂ has a structural phase transition around 250 K.

Thursday, June 15, 2017

P25

On the Substitution in the Anionic Sublattice of Iron-Based Superconductors, BaFe_2As_2 and BaNi_2As_2

*I. V. Plokhikh, D. O. Charkin, K. E. Gurianov, S. M. Kazakov.

Department of Chemistry, Lomonosov Moscow State University, Moscow, Russia

*igor.plohih@gmail.com

The “iron-arsenide” family of layered pnictide and chalcogenide superconductors, discovered about a decade ago, hosts now hundreds of representatives. The most abundant is ThCr_2Si_2 structure type, which houses the famous archetypes pnictides, BaNi_2As_2 and BaFe_2As_2 . A necessary condition of superconductivity in these and other compounds is slight electron or hole doping into the $[\text{Fe}_2\text{Pn}_2]^{2-}$ ($\text{Pn} = \text{P}$ or As) layers. Superconductivity in BaFe_2As_2 can also be induced by so-called “chemical pressure”, *e.g.* in $\text{BaFe}_2(\text{As}_{2-x}\text{P}_x)_2$ solid solutions [1]. While various substitutions at the both Ba and Fe Wyckoff sites were studied thoroughly, substitution at the As position is almost untouched, except the above mentioned isovalent option. One could expect that aliovalent doping with the elements of 14 (S, Se, Te) and 16 (Si, Ge, Sn) groups may induce superconductivity both by changing the average oxidation state of iron and via the chemical pressure.

Our studies demonstrate that Group 16 elements do not substitute into the structures of BaFe_2As_2 and BaNi_2As_2 , probably due to the high stability of barium chalcogenides formed instead. In contrast, relatively wide solid solutions with Si, Ge and Sn exist. In BaFe_2As_2 , up to 10% of As can be substituted with Si and Ge but not Sn, as shown by precise cell parameters determination and energy dispersive X-ray analysis. In BaNi_2As_2 the pattern is slightly different. The solid solution with Si was not observed, while for Ge and Sn corresponding maximal substitution degree is about 20% and 10%, respectively. We observe, probably for the first time, incorporation of at least 5% of Pb into the BaNi_2As_2 structure resulting in a considerable shift of lattice parameters.

The key to the understanding such behavior is that in all cases, a decrease of c cell parameter is observed, despite Tt^{4+} anions are characterized by larger radii compared to As^{3-} . The overall pattern can be explained assuming formation of interlayer dumbbells, *i.e.* Tt_2^{6-} “bridges”, the Si_2^{6-} being too small but Ge_2^{6-} or Sn_2^{6-} fitting the matrix BaT_2As_2 structure much better (Fig. 1). Such mechanism of charge compensation also implies retention of iron oxidation state and absence of superconductivity. Indeed, according to magnetic susceptibility measurements, all studied samples were not superconducting.

This work was supported by Russian Science Foundation (Grant № 14-13-00738).

References

1) S. Jiang, H. Xing, G. Xuan et al. - J. Phys.: Condens. Matter. 21, 382203 (2009).

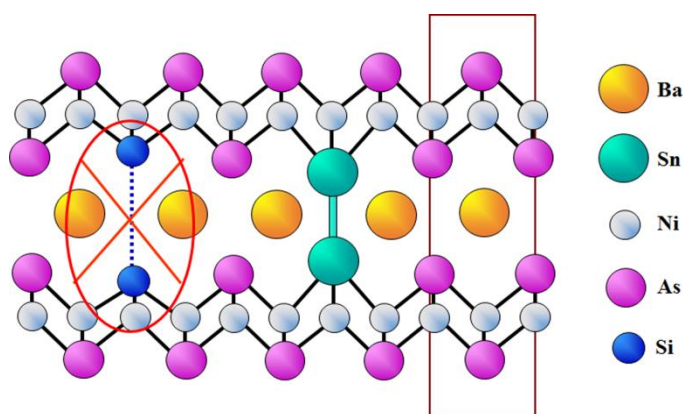


Fig.1. The scheme of interlayer dumbbells formation in the structures of BaNi_2As_2 and BaFe_2As_2 .

Thursday, June 15, 2017

P26

Metal-organic chemical solution deposition of inorganic fluoride thin films

*N. Ryzhkov¹⁾, D. Grebenyuk¹⁾, A. Anosov²⁾, S. Loskutova¹⁾, D. Tsybarenko¹⁾

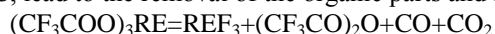
¹⁾Department of Chemistry, Lomonosov Moscow State University, Moscow, Russia ²⁾Department of Material Science, Lomonosov Moscow State University, Moscow, Russia

*nrzhkv@gmail.com

Low refractive indices, high transparency in range from UV to IR and low phonon energy make inorganic fluorides to be important optical materials. Nowadays there is increasing interest to complex fluorides as functionalized materials. Hexagonal β -NaYF₄ for example is considered to be one of the most promising host materials for up-conversion phosphors.

Development of easy and cost effective approaches to fluoride thin films deposition is a problem of strategic importance nowadays. One of the most perspective ways to obtain high-quality thin films is metal organic chemical solution deposition (MOCS) where the solutions of metal carboxylates are used as precursors.

In our work rare earth, alkaline earth and alkaline elements trifluoroacetates and pentafluoropropionates were applied as starting materials for preparation of fluoride films by MOCS. Pyrolysis of precursors at low temperatures, typically 300 – 600°C, lead to the removal of the organic parts and formation of fluorides:



Because of their polymeric or oligomeric crystal structure, the rare earth carboxylates are poorly soluble in organic solvents. This problem can be solved by preparation of precursor solutions in alcohols, with addition of ancillary ligands, such as polyglymes and polyamines, — diglyme, monoethanolamine (mea), diethylenetriamine (deta), etc. — to increase the solubility of the carboxylates by formation of mixed-ligand complexes with lower nuclearity, as the donor ligand saturates the metal ion coordination sphere.

Mixed-ligand heavy rare earth complexes of trifluoroacetates with diethylenetriamine (deta) of general formula Ln(tfa)₃(deta)₂ (Ln = Y, Dy-Lu) were synthesized and characterized by elemental analysis, NMR, FT-IR spectroscopy, TG-DTA analysis and single crystal and powder X-ray diffraction.

Effectiveness of the trifluoroacetate complexes [Y(tfa)₂(deta)₂](tfa) and [Na(tfa)(Htfa)] as fluoride precursors was demonstrated by the example of NaYF₄ powder syntheses and thin film depositions. The as deposited films were amorphous/nanocrystalline and required high-temperature annealing in Ar+HF atmosphere to suppress the pyrohydrolysis.

Both α - and β -NaYF₄ in various quantitative ratios depending on annealing temperature and composition of precursor solution were obtained (Fig. 1). Surface morphology of thin films was studied by SEM and AFM. Carbon and oxygen impurities (presence and quantitative estimation) were characterized by FT-IR spectroscopy (diffuse reflectance measurements), Raman spectroscopy and EDX analysis. NaYF₄ thin films codoped with Yb³⁺ and Tm³⁺ were characterized as up-conversion phosphors.

The financial support from Russian Foundation for Basic Research (16-03-00923) is acknowledged.

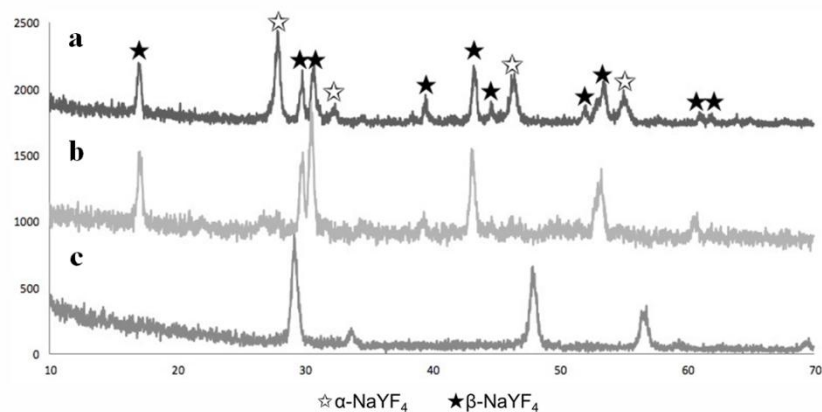


Fig. 1. GIXRD patterns of NaYF₄ thin films deposited from solutions (a) Y(tfa)₃+Na(tfa)+deta, (b) 0.7Y(tfa)₃+Na(tfa)+0.3Gd(tfa)₃+mea, (c) Y(tfa)₃+Na(tfa)+mea

Thursday, June 15, 2017

P27

Synthesis and crystal structure investigation of $\text{Cd}_3(\text{As}_{1-x}\text{P}_x)_2$ *G. Shipunov¹⁾, A. Maksutova¹⁾, K. A. Ivshin²⁾, O. N. Kataeva²⁾, I. O. Chernyavsky¹⁾, K. N. Denisova³⁾, I. V. Morozov¹⁾¹⁾Department of Chemistry, Lomonosov Moscow State University, Moscow, Russia ²⁾A. E. Arbutov Institute of Organic and Physical Chemistry ³⁾Department of Physics, Lomonosov Moscow State University*ship@inorg.chem.msu.ru

The structure of Cd_3As_2 can be described as a distorted structure of the antifluorite type in which one quarter of cadmium positions are vacant. This compound exists in several polymorphic forms, which have different vacancy ordering[1]. Low temperature modification (LT, space group $I4_1/acd$) is known for its interesting properties: It is three-dimensional electronic analogue of graphene and it shows giant magnetoresistance[2,3]. At this point we decided to investigate possibility of arsenic substitution to phosphorous in LT and to examine crystallographic features of substituted compound.

Single crystals of different substitution levels were obtained via two methods: by sublimation and by growth from cadmium flux (self-flux). Growth by sublimation technique was carried out by mixing elements powders, putting reaction mixture into evacuated sealed quartz tube which then was put in two-zone furnace in 800°C-600°C temperature gradient. Growth from cadmium flux was performed by sealing mixture of arsenic and phosphorous powders with excess of cadmium metal shavings in evacuated quartz tube, crystals were obtained by slowly cooling the mixture from 800°C to 400°C with further separation from cadmium flux by centrifuging at 400°C.

Crystals' composition was studied by SEM-EDX. Samples obtained via sublimation show significant difference between nominal composition and composition of a crystal, which can be explained by difference in saturated vapor pressure of Cd_3As_2 and Cd_3P_2 resulting in vapor composition shift during synthesis. For batch grown by self-flux real composition was closer to nominal.

For self-flux sample with $x=0.2$ and $x=0$ X-Ray powder diffraction was performed, which showed that substituted sample is 2-phase mixture of target (LT) and intermediate temperature modification (IT, space group $P4_2/nmc$). Self-flux sample of unsubstituted Cd_3As_2 is in LT modification and has small admixture of metallic cadmium, which is due to incomplete separation during centrifuging.

For four crystals with different substitution level, single-crystal X-ray diffraction (SC XRD) was performed. Only one of these showed target modification (sublimation, nominal $x=0.1$, according to SC XRD $x=0.028$), other three were obtained in IT. In all cases, phosphorous is distributed between various positions unequally (fig. 1): positions with coordination type 4+2 are favored by phosphorous, while position with coordination number 6 is showing less atoms of phosphorus. This can be explained by smaller size of P^{3-} compared to As^{3-} and preference for lower coordination number in case of P^{3-} .

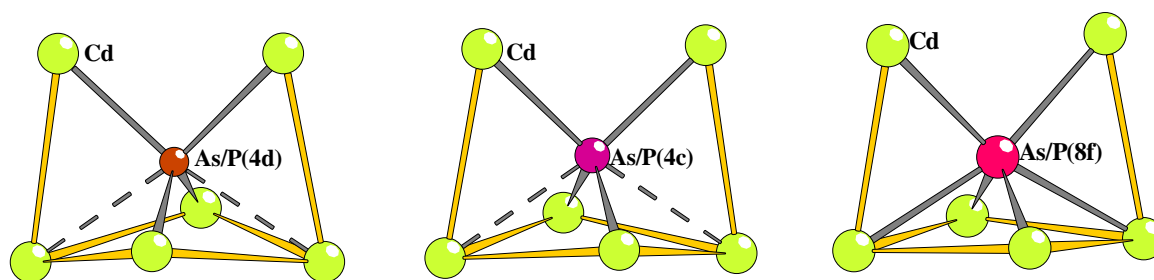


Figure 1: Different arsenic positions in IT modification (space group $P4_2/nmc$). In positions 4d (a) and 4c (b) two cadmium atoms out of six are significantly further away from arsenic atom (coordination type 4+2), while in position 8f (c) bond lengths are more consistent (resulting in coordination number 6). All bond lengths are in ångström.

References:

- 1) M. N. Ali et al – Inorg. Chem., 53, 4062-4067 (2014)
- 2) T. Liang et al – Nat. Mater., 14, 280-284 (2015)
- 3) S. Borysenko et al – Phys. Rev. Lett., 113, 027603-5, (2014)

Thursday, June 15, 2017

P28

Ferrites with the highest coercivities among metal oxides materials

A.E. Sleptsova¹⁾, L.A. Trusov¹⁾, E.A. Gorbachev¹⁾, E.S. Mitrofanova¹⁾, I.V. Roslyakov¹⁾, V.A. Lebedev¹⁾, A.V. Vasiliev¹⁾, D.D. Zaytsev¹⁾, B.P. Gorshunov²⁾, P.E. Kazin¹⁾, R.E. Dinnebier³⁾, M. Jansen³⁾

¹⁾ Moscow State University, Moscow, Russia, ²⁾ Moscow Institute of Physics and Technology, Dolgoprudny, Russia, ³⁾ Max Planck Institute for Solid State Research, Stuttgart, Germany

sleptsovaanastasia@gmail.com

Magnetic materials with large coercivity have broad applications ranging from permanent magnets and data storage media to high-frequency electromagnetic wave isolators. The only known ferrite material exhibiting coercivity over 20 kOe (also considered as “giant coercive force”) at room temperatures is ϵ -Fe₂O₃ [1]. Also it shows millimeter wave absorption up to 210 GHz [2-3]. However, ϵ -Fe₂O₃ is a rare iron oxide and its production as pure phase is quite complex. Hard magnetic ferrites (MFe₁₂O₁₉, M = Ba, Sr, Pb) also possess high magnetocrystalline anisotropy but their coercivity is significantly lower and rarely exceeds 6 kOe for pure phase. The doping by aluminum could lead to coercivity rise up to 18 kOe, however the magnetization in this case is significantly lower than of ϵ -Fe₂O₃ [4].

Here we report a simple synthesis of Ca-Al double substituted strontium hexaferrite Sr_{1-x/12}Ca_{x/12}Fe_{12-x}Al_xO₁₉. The rise of the substitution ratio x leads to decrease of magnetization, but significant increase of coercivity. At $x = 4$ the sample coercivity is 21.3 kOe, which is higher than for ϵ -Fe₂O₃ with the same magnetization of 15 emu/g. At $x = 5.5$ the coercivity reaches 36 kOe, which is the highest value known for ferrite materials. However, further increasing the substitution degree doesn't lead to improve coercivity (H_C of $x = 6$ is 21 kOe). Nevertheless, the coercivity could be further enlarged by alignment of the hexaferrite particles dispersed in a polymer by the external magnetic field. Such oriented composites possess nearly square hysteresis loops with coercivity up to 40 kOe for $x = 5.5$ compound while magnetized in alignment direction. Materials with gigantic coercivity values have potential in future high-density magnetic recording media as their particle size can be considerable reduced while maintaining hard magnetic properties. Also we have studied the millimeter wave absorption properties of the samples. The high anisotropy fields result in very high natural ferromagnetic resonance frequencies. The FMR frequency increases with substitution ratio and reaches the record-high values of 180 – 240 GHz for $x = 4 - 5.5$. The present materials should be suitable for high frequency millimeter wave devices (absorbers and rotators) because it can curb electromagnetic interference problems as the FMR frequency corresponds to the highest window of air, which is the anticipated carrier frequency for next-generation millimeter wave wireless communications. Also we have studied the features of the crystalline structure of the samples by high precision synchrotron radiation diffraction and revealed that the presence of calcium results in shrinking of oxygen surroundings in bipyramidal iron position, which could be a reason of the increase of magnetocrystalline anisotropy compared to simple aluminum doping of strontium hexaferrite.

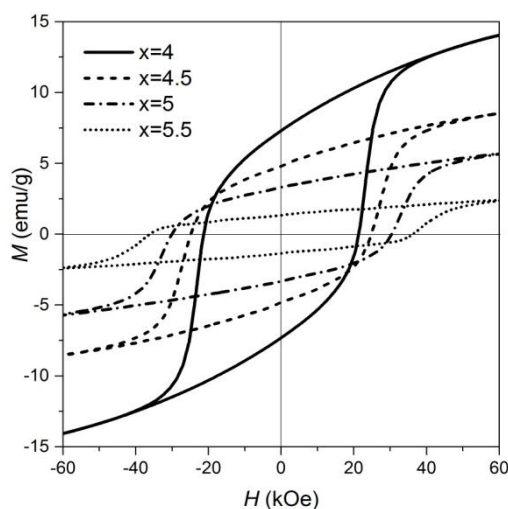


Fig. 1. Hysteresis loops of Sr_{1-x/12}Ca_{x/12}Fe_{12-x}Al_xO₁₉ samples.

Support by RFBR Grant 15-03-04277 is acknowledged.

References:

- 1) J. Tuček, R. Zbořil, A. Namai, S. Ohkoshi, *Chem. Mater.*, 22(2010) 6483.
- 2) A. Namai, et. al., *Nat. Commun.*, 3 (2012) 1035.
- 3) H. Luo, *J. Magn. Magn. Mater.*, 324 (2012) 2602.

Thursday, June 15, 2017

P29

Effects of Structural Ordering in HTS-2G Tapes under the Action of Shock Waves*A.V.Troitskii¹⁾, V.V.Voronov¹⁾, G.N.Mikhailova¹⁾, V.Ya. Nikulin^{2,3)}, P.V.Silin²⁾,¹⁾ Prokhorov General Physics Institute of RAS, Moscow, Russia ²⁾ P.N.Lebedev Physical Institute of RAS, Moscow, Russia ³⁾ National Research Nuclear Center MEPhI, Moscow, Russia

*at@kapella.gpi.ru

The report presents the results of a study of the functional properties of a HTS-2G tape based on $\text{GdBa}_2\text{Cu}_3\text{O}_{7-\delta}$ subjected to shock waves. The purpose of these studies is to find methods to improve the current characteristics of high-temperature superconductors.

Using the method of X-ray diffraction and measurements of superconducting characteristics, a modification of the HTS tape, namely, the parameters of the unit cell of the superconductor and the protective layers of silver and copper, was investigated. Relaxation of stresses in the superconductor layer was detected with a constant parameter **c** of the unit cell. It is shown that under the shock-wave impact regime used, the microstructure of the HTS layer (grain size and microdeformation) improves.

In the work, a composite high-temperature superconductor tape of the second generation of SuperOx production on the basis of $\text{GdBa}_2\text{Cu}_3\text{O}_{7-\delta}$ compound of 4 mm width, obtained by the laser deposition method, was studied. The elementary crystal cell of the superconductor $\text{GdBa}_2\text{Cu}_3\text{O}_{7-\delta}$ is orthorhombic with approximately equal values of the parameters **a** and **b** and a significantly larger value of the parameter **c**. In the samples of the tape we studied, the (**a-b**) plane lies in the plane of the substrate, and the normal to this plane coincides with the direction of action of the shock wave in this experiment.

As a source of shock waves, an electric discharge setup of the plasma focus type (PF-4 of the Tulip complex, FIAN) was used. The installation of this type makes it possible to obtain cumulative plasma jets with an ion density of the order of 10^{18} cm^{-3} . The strong shock wave (SW) emerges when exposed to a plasma jet on the surface of a solid target. SW is then transmitted to the HTS samples installed directly behind the target. PF Installation parameters: the maximum energy stored in the installation's capacitor bank is 4 kJ, the plasma flow energy hitting the target at $\sim 100 \text{ J}$. The time of the action on the target in this case is about 50 ns. The energy flux density on the target was $\sim 10^9 - 10^{10} \text{ W / cm}^2$, and the velocity of the plasma jet is $(1-4) \cdot 10^7 \text{ cm/s}$. The discharge chamber of PF is filled with an inert gas – argon – under pressure of 2 Torr. A 0.2 mm-thick plate of molybdenum protects the surface of the HTS sample from the direct impact of the plasma pulse. Moreover, for the purpose of aligning the SW impact on the surface of the HTS sample, the 2 mm gap between the molybdenum plate and the sample was filled with epoxy resin.

The results of X-ray diffractometry show that for the superconducting layer after the shock-wave impact the width of the reflex decreases, for Ag layer it increases substantially, and for Cu, the width changes can be neglected. Thus, the microstructure of the layer (grain size and microdeformation) of HTS under the action improves. It is interesting to note that an opposite effect is observed for the Ag layer. Estimates show that the block sizes for HTS and Ag more than 150 nm do not contribute to the width of the reflex. When SW impact on the superconducting sample, microdeformations appear $\delta a/a \approx 4 \cdot 10^{-4}$ in the Ag layer, in the HTS layer, microdeformations of $\delta c/c$ decrease by approximately $6 \cdot 10^{-4}$. Both in HTS and in Ag, microdeformation is small.

The positions of the maxima were used to calculate the parameters of the unit cell **c** for HTS $\text{GdBa}_2\text{Cu}_3\text{O}_{7-\delta}$ and **a** for Ag in the initial sample and sample after the impact of the shock wave. The results of the measurements show that the impact of the shock wave has practically no effect on the lattice constant **c** in $\text{GdBa}_2\text{Cu}_3\text{O}_{7-\delta}$ and **a** in Ag.

It is known that the effect of shock waves causes the formation of radiation-induced point defects - collective pairs Frenkel, vacancies and interstitial atoms, and introduction of dislocation loops. These collective Frenkel pairs are formed at the leading edge of the shock wave as they pass through a solid body. In this case, the density of emerging vacancies may exceed by several orders of magnitude the density of thermal vacancies existing in the initial material at the experimental temperature. In superconductors, as a result of annihilation, recombination, and clustering of Frenkel pairs, various radiation effects can arise, such as the generation of additional pinning centers of Abrikosov vortices, and, under certain conditions, amorphization of the material. In the present work, it has also been found that under certain conditions, the microstructure of the superconductor can be improved.

The authors are grateful to S.V. Samoylenkov, A.A. Molodyk and S. Lee for providing HTS samples.

Thursday, June 15, 2017

P30

Synthesis of complex fluorides with weberite-type structure: $\text{Na}_2\text{M}^{\text{II}}\text{M}^{\text{III}}\text{F}_7$ ($\text{M}^{\text{II}} = \text{Ni}, \text{Co}, \text{Mn}$; $\text{M}^{\text{III}} = \text{Fe}, \text{Cr}$)

*M.D.Tsymlyakov¹⁾, A.A.Fedorova¹⁾, O.A.Shlyakhtin¹⁾, I.V. Morozov¹⁾

¹⁾Department of Chemistry, Lomonosov Moscow State University, Moscow, Russia

*tsymmmd@gmail.com

This work is dedicated to the synthesis of metal trifluoroacetate hydrates of several 3d-metals (Ni^{II} , Co^{II} , Mn^{II} , Cr^{III} and Fe^{III}) and the investigation of their thermal decomposition in order to obtain corresponding complex fluorides with the composition $\text{Na}_2\text{M}^{\text{II}}\text{M}^{\text{III}}\text{F}_7$.

Trifluoroacetate hydrates of manganese, cobalt and nickel were obtained by the interaction of basic carbonates of corresponding metals with trifluoroacetic acid; and trifluoroacetate hydrates of chromium and iron – by the reaction of their hydroxides (precipitated by ammonia from the nitrate solution) with trifluoroacetic acid.

Chemical composition of the obtained hydrates was confirmed by the titrimetric method. XRD analysis revealed the identity of their phase content to the literature data [1].

The process of thermal decomposition of the metal trifluoroacetate hydrates was investigated in air and in argon flow by means of thermogravimetric and differential thermal analysis. According to these data, a decomposition process consists of two main stages. The first one is connected with the loss of crystallohydrate water while the second one – with the decomposition of trifluoroacetic group to fluoride one. It is interesting to note that the influence of decomposition atmosphere is negligible for the nickel compound only. However, even in this case, the difference appeared at $T > 500^\circ\text{C}$. This can be attributed to the process of pyrohydrolysis of obtained products.

According to TG-MS analysis of evolved gases, the main gaseous products of these thermal decomposition processes are water vapor, carbon dioxide and various fluorocarbons. The relative amount of these gases gave additional information about the processes occurred during the decomposition. Along with individual metal trifluoroacetate hydrates, a thermal decomposition of their mixtures with and without β -cyclodextrin was also studied.

XRD analysis of thermolysis products demonstrated the absence of oxide phases at $T = 400$ and 700°C almost in all cases. Along with $\text{Na}_2\text{M}^{\text{II}}\text{M}^{\text{III}}\text{F}_7$, these products usually contained $\text{Na}_3\text{M}^{\text{III}}\text{F}_6$, $\text{NaM}^{\text{II}}\text{F}_3$, $\text{M}^{\text{II}}\text{F}_2$ and $\text{M}^{\text{III}}\text{F}_3$. The smallest amount of secondary phases was observed at 400°C for $\text{M}^{\text{III}} = \text{Fe}$ and $\text{M}^{\text{II}} = \text{Ni}, \text{Co}$.

According to previous studies [2, 3], a synthesis of $\text{Na}_2\text{NiFeF}_7$ and $\text{Na}_2\text{CoFeF}_7$ by the solid state method in noble metal ampoules demands a continuous reaction time (4 days at $T = 800^\circ\text{C}$) and is also accompanied by the formation of secondary phases. The present study demonstrated a possibility to obtain these complex fluorides within 4 hours due to the application of the modern soft chemistry synthesis techniques.

References

- 1) Morozov I.V., Karpova E.V., Glazunova T.Yu, Boltalin A.I., Zakharov M.A., Tereshchenko D.S., Fedorova A.A., Troyanov S.I. – Rus. J. of Coord. Chem. 42, 647 (2016)
- 2) M. Welsch, D. Babel - Z. Naturforsch. 47b, 685 (1992)
- 3) R. Haegle, W. Verscharen - J. Solid State Chem. 24, 77 (1978)

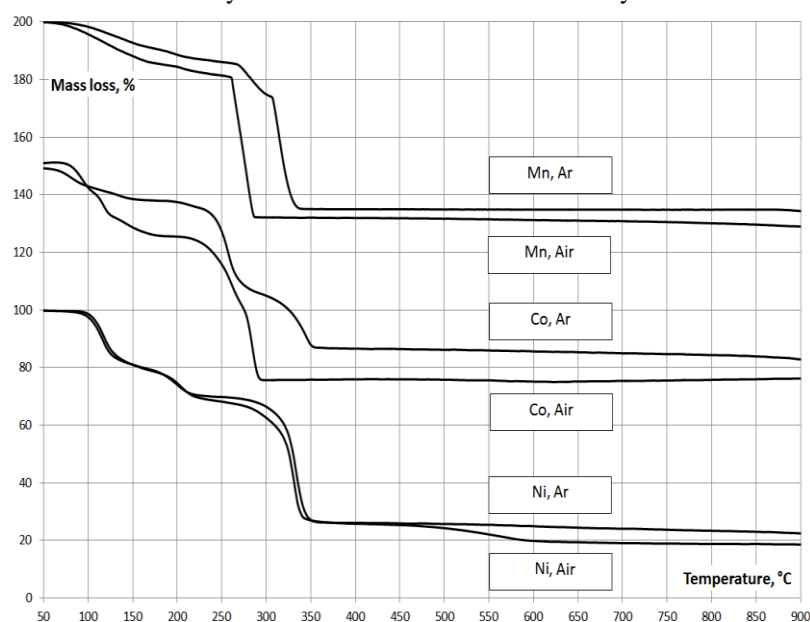


Fig.1. TG curves of the decomposition of metal trifluoroacetate hydrates of Mn, Co and Ni in air and argon flow

Thursday, June 15, 2017

P31

Approaches to increase lanthanide NIR luminescence

A. Kovalenko¹⁾, V. Khudoleeva¹⁾, P. Rublev¹⁾, *V. Utochnikova^{1,2)}

¹⁾ Department of Materials Sciences, Lomonosov Moscow State University, Moscow, Russia ²⁾ Lebedev Physical Institute RAS, Moscow, Russia

Valentina.utochnikova@gmail.com

Due to the special optical properties, such as large Stokes shift and the lifetime of the the excited state, lanthanide compounds are unique luminescent materials. Among them, NIR emitting compounds are of particular interest due to their use in medicine and telecommunications because of the presence of so-called "transparency windows" of biological tissues and fiber optic materials in the NIR range. However, to date, such materials still possess low NIR luminescence intensity, and their quantum yields do not exceed a fraction of a percent. In addition, the main characteristic of photoluminescent materials is the luminosity (B), which is determined not only by the internal quantum yield (Q_{Ln}^{Ln}), but also by the ligand absorption ϵ and the ligand to lanthanide energy transfer efficiency (η_{sens}): $B = \epsilon \cdot \eta_{sens} \cdot Q_{Ln}^{Ln}$.

In the present work lanthanide compounds capable of NIR luminescence were divided into two main classes: coordination compounds with organic ligands, which have large values of absorption coefficients ¹, and lanthanide inorganic salts surface-modified with an organic ligand, especially fluorides, which possess high internal quantum yields ². Thus, the main problem to solve was the increase in the sensitization efficiency η_{sens} , which values are usually low.

To obtain luminophores with high luminosity in NIR range, a comprehensive approach was used in this paper, which included both the search for ligands with high absorption and sensitization efficiency, and an increase in the internal quantum yield.

In lanthanide fluoride nanoparticles the internal quantum yield is mainly determined by the efficiency of the concentration quenching processes. Their minimization by increasing the metal-metal distance in bimetallic fluorides $Yb_xLa_{1-x}F_3$ allows to increase the internal quantum yield up to 30% in the case of $Yb_{0.05}La_{0.95}F_3$. Surface modification with aromatic carboxylates, for example, 9-anthracenate anion (ant⁻) with ytterbium sensitization efficiency of 25% allowed to achieve $B = 80$ for ant@ $Yb_{0.05}La_{0.95}F_3$.

The ligand selection process can be simplified by using the dysprosium ion as NIR emitter, its excited stae energy (20400 cm^{-1}) is high enough to facilitate the energy transfer from common ligands. In spite of the greater efficiency of the concentration quenching than of ytterbium ion, the combination of the metal-to-metal distance enhancement approaches and the surface modification with the terephthalate anion made it possible to obtain a compound with a bright NIR luminescence. In addition, the Dy^{3+} ion has transitions not only in the infrared range, but also in the visible range, which makes its compounds promising for various sensory applications.

Ytterbium complexes with polydentate anionic Schiff bases possessed the internal quantum yields which did not exceed 6% unlike frluorides, and their quantum yields reached 1.5%, which is rather high for NIR emitting lanthanide complexes. It was possible due to rather high sensitization efficiency of 25%. Such high values were reached due to the formation of a charge transfer state, namely, ligand to metal. At the same time, the introduction of the hydroxy-group in the ligand structure leads to a twofold decrease in the quantum yield, which is due to the easy quenching of the IR luminescence on the vibrations of -OH bonds. Despite the low internal quantum yield, these complexes exhibited high brightness values up to $B = 900$ due to high absorption of $\epsilon = 20000 \text{ cm}^{-1}$.

This work was supported by President's grant MK-2810.2017.3.

References:

- 1)Utochnikova, V. V. et al. Lanthanide complexes with 2-(tosylamino)benzylidene-N-benzoylhydrazone, which exhibit high NIR emission. *Dalt. Trans.* 44, 12660–12669 (2015).
- 2)Utochnikova, V. V., Kalyakina, A. S., Lepnev, L. S. & Kuzmina, N. P. Luminescence enhancement of nanosized ytterbium and europium fluorides by surface complex formation with aromatic carboxylates. *J. Lumin.* 170, 633–640 (2015).

Thursday, June 15, 2017

P32

Features of luminescence in heterometallic lanthanide complexes

D.S.Koshelev¹⁾, A.Yu.Grishko¹⁾, A.S.Kalyakina¹⁾, *V.V. Utochnikova^{1,2)}¹⁾ Faculty of Materials Science, Lomonosov Moscow State University ²⁾ Lebedev Physical Institute RAS, Moscow, Russia
Valentina.utochnikova@gmail.com

Luminescent lanthanide coordination compounds (LCC) are nowadays of growing interest due to their unique photophysical properties, i.e. long lifetimes, high brightness and narrow emission bands. One of the methods, which allows altering the luminescent properties of LCCs is the replacement of the luminescent ion by an auxiliary ion in its crystallographic positions.

The following schemes of implementing this method are possible: 1) decrease of concentration quenching, 2) increase of the luminescent quantum yield (QY) due to the increase of the ligand (L)-to-lanthanide (Ln) energy transfer efficiency, 3) the participation of non-luminescent ions in the sensitization of luminescent ion process. In our group all these approaches were used to study photophysical effects in lanthanide aromatic carboxylates.

In the series of compounds $(Yb_xLu_{1-x})(ant)_3$ (Hant – 9-anthracenecarboxylic acid), the scheme 1 was used to find out the optimum value x . We assumed, that this optimum exists due to the presence of two competing processes: the higher x value, the lower the number of luminescent Yb ions and the lower the effect of concentration quenching. This optimal value of x was measured to be 0.2 with QY of 2.5% correspondingly¹.

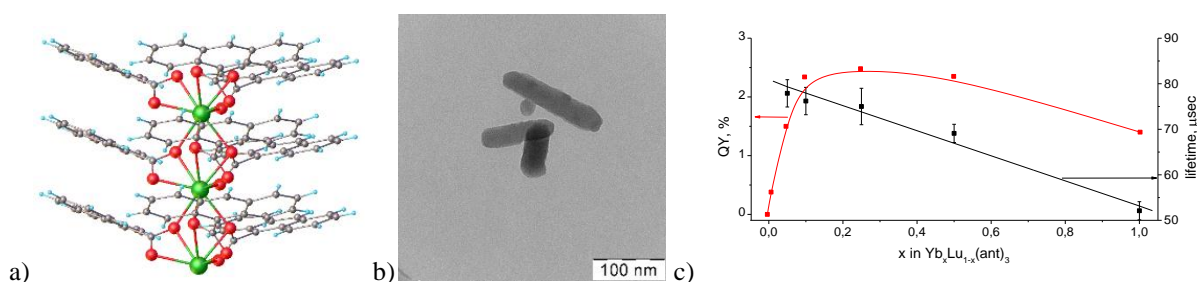


Fig.1. a) Polymeric chain in structure and b) TEM image of $Yb(ant)_3$. c) Lifetimes and QYs of $Yb_xLu_{1-x}(ant)_3$

In order to increase the QY value for lanthanide fluorobenzoates $(Eu_{0.5}Tb_{0.5})(L)_3 \cdot xH_2O$, (HL = fluorobenzoic acid with vary fluorination degree, 10 ligands in total), the scheme 2 was implemented. Therefore, $L \rightarrow Eu$ sensitization scheme was replaced by $L \rightarrow Tb \rightarrow Eu$ scheme to reduce the energy gap between the triplet level of the ligand (22000 cm^{-1}) and the emitting level of Eu^{3+} (17200 cm^{-1}). In some fluorobenzoates, the introduction of Tb^{3+} leads to the increase of QY, while a maximum 2-fold increase from 15% to 30% was achieved for Eu^{3+}/Tb^{3+} pentafluorobenzoate².

Both schemes 2 and 3 were implemented for lanthanide terephthalates $(Eu_xM_{1-x})_2(tph)_3 \cdot 4H_2O$, (M = Y, Gd, Tb, and Htph - terephthalic acid). According to the scheme 2, Tb^{3+} and Gd^{3+} were introduced in order to increase the $L \rightarrow Eu$ energy transfer efficiency and the efficiency of intersystem crossing, respectively. However, such an introduction of auxiliary ions possess no noticeable effect on the luminescence properties. According to the scheme 3, an inspiring effect of multiphotonic relaxation was obtained: the constant QY values in a wide range of luminescent ion concentrations $0.005 > x > 1$. We also formulated the criteria for the manifestation of this effect, as well as the criteria for the appearance of concentration quenching in the lanthanide complexes^{3,4}.

This work was supported by President's grant MK-2810.2017.3.

References:

- 1) Utochnikova, V. V. et al. Lanthanide 9-anthracenate: solution processable emitters for efficient purely NIR emitting host-free OLED. *J Mater Chem C* 4, 9848–9855 (2016).
- 2) Kalyakina, A. S. et al. Highly Luminescent, Water-Soluble Lanthanide Fluorobenzoates: Syntheses, Structures and Photophysics, Part I: Lanthanide Pentafluorobenzoates. *Chem. - A Eur. J.* 21, 17921–17932 (2016).
- 3) Utochnikova, V. V. et al. Lanthanide heterometallic terephthalates: Concentration quenching and the principles of the 'multiphotonic emission'. *Opt. Mater. (Amst)*. 1–8 (2017). doi:10.1016/j.optmat.2017.02.052
- 4) Grishko, A. Y., Utochnikova, V. V., Averin, A. A., Mironov, A. V. & Kuzmina, N. P. Unusual Luminescence Properties of Heterometallic REE Terephthalates. *Eur. J. Inorg. Chem.* 2015, 1660–1664 (2015).

Thursday, June 15, 2017

P33

The peculiarities of lanthanide aromatic carboxylate use in OLEDs

*E. Latipov¹⁾, A. Aslandukov¹⁾, A. Vashchenko²⁾, *V. Utochnikova^{1,2)}.

¹⁾ Department of Materials Sciences, Lomonosov Moscow State University, Moscow, Russia ²⁾ Lebedev Physical Institute RAS, Moscow, Russia

Valentina.utochnikova@gmail.com

Over the past few decades lanthanide coordination compounds (LCC) have found their applications in many areas of research, i.e. as emission layers in organic light-emitting diodes (OLED). Among the many classes of LCCs, aromatic carboxylates are interesting as luminescent materials, due to the effective luminescence and high thermal and UV stability. However, their broad implementation as emission layers is difficult, since they do not possess the intrinsic charge carrier mobility. Because of the special mechanism of LCC luminescence, the use of classical approaches to increasing transport properties results in of the device efficiency decrease.

In order to improve the transport properties of the Ln-based emission layer two approaches were used. The first one is the introduction of a phosphorescent material into the transport material host, which is able to coordinate the lanthanide ion directly and to sensitize its luminescence. The second approach is the increase of the anionic ligand transport properties due to modification of its structure.

In order to implement the first approach, the derivatives of phosphine oxide and phenanthroline have been chosen (Fig. 1), which are electron transport materials and able to coordinate the lanthanide ion. To select among these materials effective sensitizers, the ternary complexes of the composition $\text{LnCl}_3(\text{Host})_n$ ($\text{Ln} = \text{Tb}, \text{Eu}; n = 0,5-2$) were obtained, and their photophysical characteristics (i.e. photoluminescence quantum yields) were measured. Among these materials the effective sensitizers have been selected, where the sensitization efficiency reaches 100%.

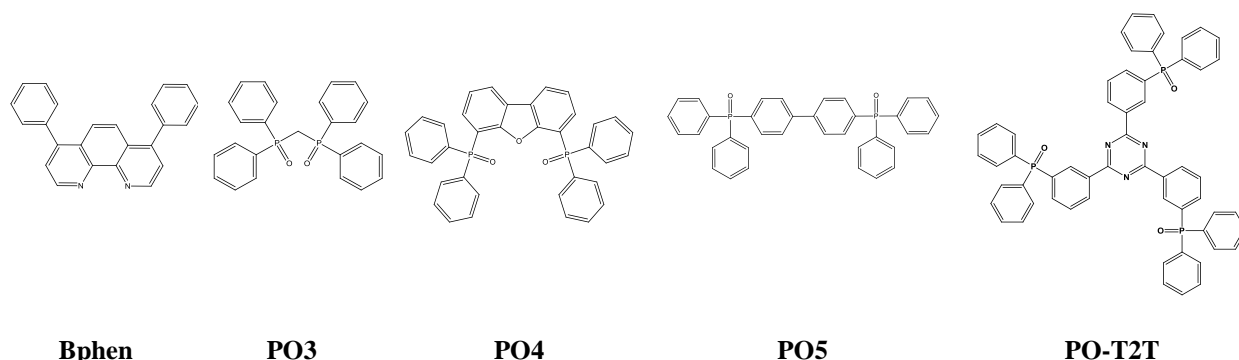


Fig. 1 Some of the sensitizing host materials

In the second approach, heteroaromatic electron-deficient systems, namely aryl-substituted pyrazole-carboxylates, have been chosen to provide electron transport properties (Fig. 2), in which the aryl substituent provides effective electron transport between ligands. Quantum yields of lanthanide complexes with these ligands reached 100% in the case of terbium complexes and 16% in the case of europium complexes.

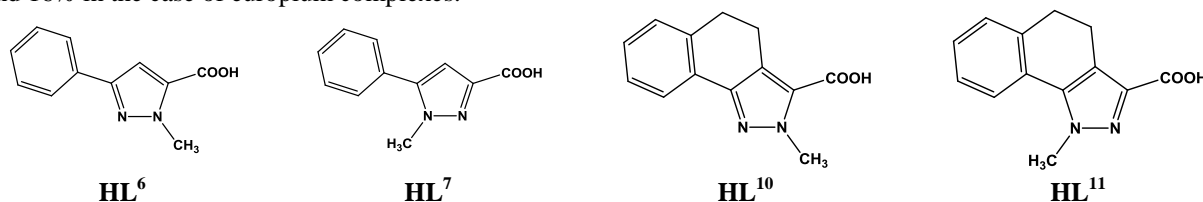


Fig. 2 Some of the electron-transport anionic ligands

Testing in OLED has shown that the use of these two approaches effectively leads to the manufacturing of diodes with pure ionic lanthanide luminescence, whose brightness reaches 350 Cd/m^2 and might be comparable with the brightness of OLED which are nowadays used in OLED devices.

This work was supported by President's grant MK-2810.2017.3 and RFBR (grant Nos 16-29-10755, 16-53-76018).

Thursday, June 15, 2017

P34

NMR and NQR spectroscopy study of binary intermetallic superconductor $\text{Mo}_8\text{Ga}_{41}$

* S.V. Zhurenko¹⁾, A.A. Gippius¹⁾²⁾, K.S. Okhotnikov¹⁾, V.Yu. Verchenko³⁾, A.V. Shevelkov³⁾

¹⁾Department of Physics, Lomonosov Moscow State University, Moscow, Russia ²⁾Shubnikov Institute of Crystallography, Moscow, Russia ³⁾Department of Chemistry, Lomonosov Moscow State University, Moscow, Russia

*zhurenko.sergey@gmail.com

Binary intermetallic compound $\text{Mo}_8\text{Ga}_{41}$ is considered as a non-typical superconductor with $T_c = 9.7$ K. Indeed, the normalized jump of the specific heat at T_c is $\Delta c_p/\gamma T_c = 2.83$ [1]. This value indicates a much stronger electron-phonon coupling in the superconducting state of $\text{Mo}_8\text{Ga}_{41}$ than that in the weak-coupling BCS limit, where $\Delta c_p/\gamma T_c = 1.43$ is expected. $\text{Mo}_8\text{Ga}_{41}$ crystallizes in the V_8Ga_{41} type of crystal structure with a complex network of gallium atoms occupying 9 crystallographic positions where Ga1 position in the center of a GaGa_{12} cuboctahedron with crystallographic position (0;0;0.5) has no contacts with Mo atoms in its first coordination sphere [1].

Here we report NQR and preliminary NMR spectroscopy study of $\text{Mo}_8\text{Ga}_{41}$ based on *ab-initio* calculations of electric field gradient (EFG).

NQR experiments on $^{69,71}\text{Ga}$ nuclei were performed by means of phase-coherent pulsed NQR spectrometer using a frequency step Hahn echo technique at 4.2 K. Experimental $^{69,71}\text{Ga}$ NQR spectrum in $\text{Mo}_8\text{Ga}_{41}$ measured at 4.2 K is shown in Fig.1. It demonstrates a very complex NQR intensity distribution comprising two groups of 8 peaks in each corresponding to ^{71}Ga (14 – 25 MHz) and ^{69}Ga (25 – 38 MHz) isotopes in eight crystallographic sites except Ga1 for which NQR frequency is too low to be detected by our spectrometer. Preliminary $^{69,71}\text{Ga}$ NMR spectra measured on Ga1 atoms with low EFG are discussed.

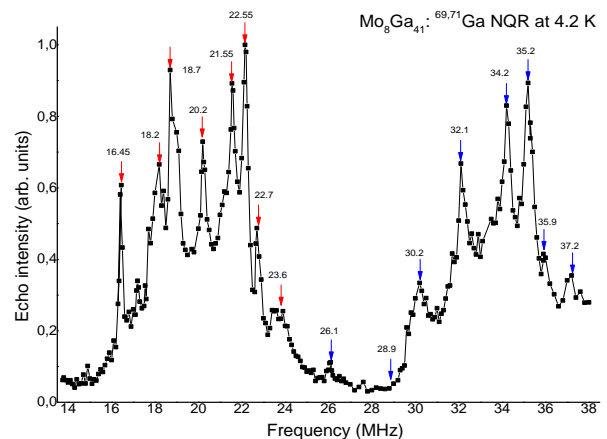


Fig.1. Experimental $^{69,71}\text{Ga}$ NQR spectrum in $\text{Mo}_8\text{Ga}_{41}$ measured at 4.2 K.

This work was supported by the joint Russian-Taiwan Grant RFBR-MOST № 16-53-52012-a.

References

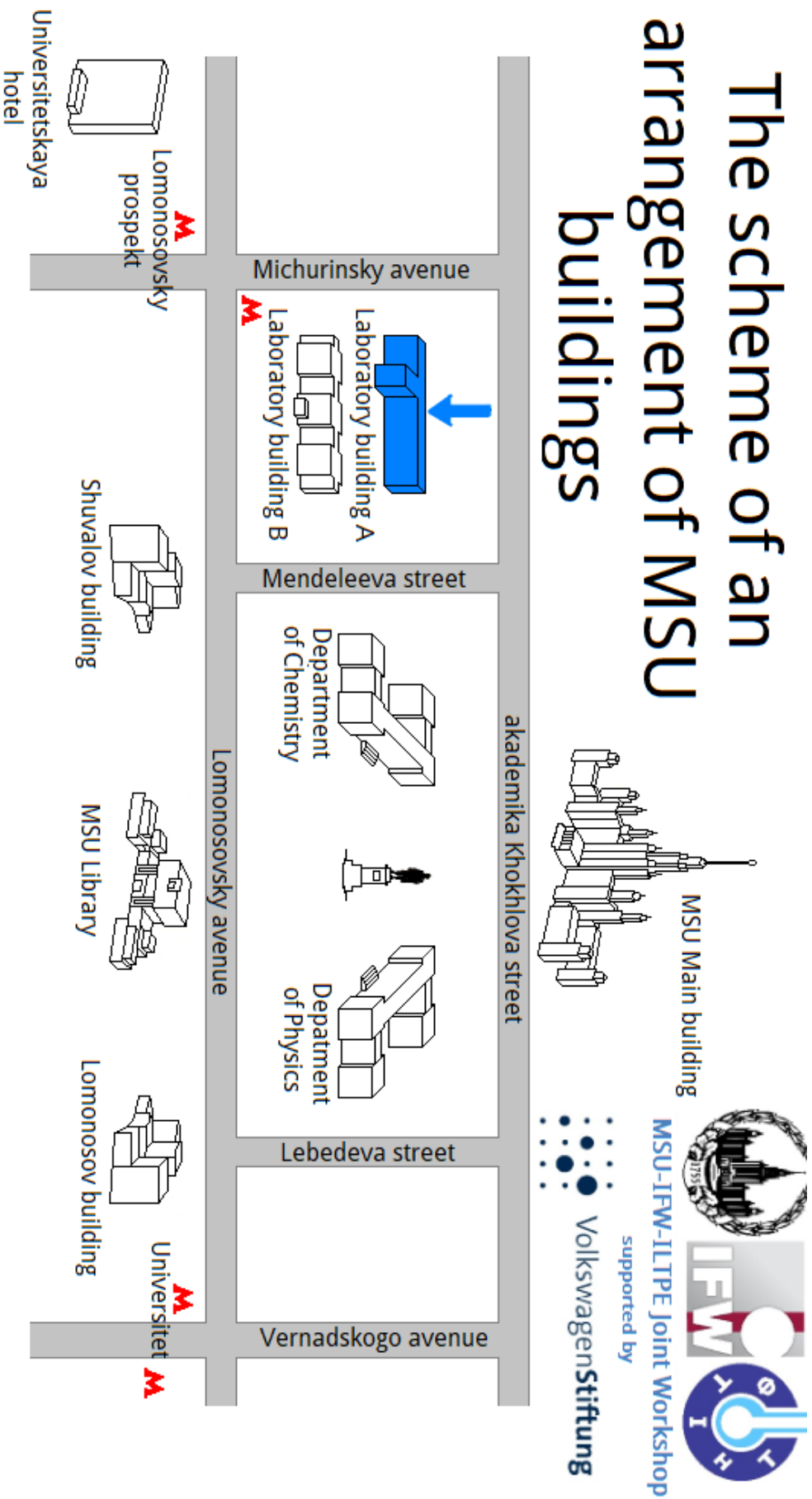
1) V Yu Verchenko et al., Phys. Rev. B 93, 064501 (2016).

For Notes

For Notes

For Notes

The scheme of an arrangement of MSU buildings



Отпечатано в ООО «КЛУБ ПЕЧАТИ»
 127018, Москва, 3-й проезд Марьиной рощи, д. 40, к. 1
 Тел.: +7 (495) 669-50-09
www.club-print.ru